

CHALMERS



[Source:http://www.gepower.com](http://www.gepower.com)

Implementation and Performance Analysis of a Multi Megawatt Variable Speed Wind Turbine using Matlab® and Simulink®

Thesis for the degree of Master of Science in Engineering (MScEng)

ASHOKE KUMAR SEN GUPTA

*Department of Energy & Environment
Division of Electric Power Engineering*
CHALMERS UNIVERSITY OF TECHNOLOGY
Göteborg, Sweden 2007

THESIS FOR THE DEGREE OF MASTER OF SCIENCE IN ENGINEERING (MScEng)

**Implementation and Performance Analysis
of a Multi Megawatt Variable Speed Wind Turbine
using Matlab® and Simulink®**

ASHOKE KUMAR SEN GUPTA

Division of Electric Power Engineering
Department of Energy & Environment
CHALMERS UNIVERSITY OF TECHNOLOGY
Göteborg, Sweden 2007

Performed at: Chalmers University of Technology
Göteborg, Sweden

Examiner:

Dr. Torbjörn Thiringer
Bitr Professor
Division of Electric Power Engineering
Department of Energy & Environment
Chalmers University of Technology
Göteborg, Sweden 2007

Implementation and Performance Analysis of a Multi Megawatt Variable Speed Wind Turbine using Matlab® and Simulink®

ASHOKE KUMAR SEN GUPTA

© Ashoke Kumar Sen Gupta, 2007.

Department of Energy and Environment
Division of Electric Power Engineering
Chalmers University of Technology
SE-412 96 Göteborg
Sweden
TEL: +46 (0)31-772 1000
FAX: +46 (0)31-772 1633
<http://www.chalmers.se/ee/SV/forskning/forskargrupper/elteknik>

Cover page courtesy of GE® Wind Power

উৎসর্গ

আমার মা, স্বর্গীয় বাবা, দিদি, কিশোরদা, দাদা, বৌদি

আমার নবপরিণীতা স্ত্রী "মুক্তা"

এবং

আমার মামা "নিমল কান্তি দাশ গুপ্ত" যঁার জন্যই জীবনে আমি এতদূর আসতে পেরেছি

Implementation and Performance Analysis of a Multi Megawatt Variable Speed Wind Turbine using Matlab® and Simulink®
ASHOKE KUMAR SEN GUPTA
Division of Electric Power Engineering
Department of Energy and Environment
Chalmers University of Technology

Abstract

This thesis implements and investigates the functionality of the GE 3.6 MW Wind Turbine model implemented in Matlab® and Simulink® when exposed to a wind step and a frequency disturbance

The robustness of the Wind Turbine is tested by varying the aerodynamic parameters $C_{p,max}$ and λ_{opt} .

It is found that, the implemented model operate as expected in different wind speed regions under different disturbances e.g. wind speed step, grid-fault. However, while simulating in the low-wind speed region, it is found that, the pitch controller does not work according to the expected behaviour. The pitch-angle tends to change, although it should not be the case for low-wind speed operation.

The frequency response in the low-wind speed region of the investigated WT shows that an external signal added with the torque controller output in the frequency range of 0.4~1 Hz can be reflected unaffected on the electrical power output and when the gain of the torque controller is increased from the base case, the above mentioned frequency range changed to 0.6~1 Hz.

Keywords: variable speed wind turbine, performance co-efficient, tip-speed ratio, frequency response.

Acknowledgements

This work has been carried out at the Division of Electric Power Engineering, Department of Energy and Environment, at Chalmers University of Technology. The financial support provided by the Swedish Institute (SI) as an MKP scholarship during the whole study period in Sweden is gratefully acknowledged.

The author would like to thank his supervisor and examiner Nayeem Rahmat Ullah and Dr. Torbjörn Thiringer for their kind patience, constant guidance, encouraging comments and revising the thesis manuscript to give it a better shape. Many thanks go to Dr. Tuan A. Le, Dr. Stainslaw Gubanaski, Dr. Ola Carlson, Dr. Yuriy Serdyuk, Dr. Jörgen Blennow, Dr. Sonja Lundmark for their lectures, supports and willingness to help with various aspects of problem solving. The author express special thanks go to Robert Carlson for helping in course matters.

The author also express sincere gratitude to all the staff and faculty at the Division of Electric Power Engineering who anyway giving support during thesis work at the department. Thanks to Jan Olov giving IT facilities.

Special thaks go to student colleagues from Chalmers 2006-2007 International Masters Programme in Electric Power Engineering for making last one and half year more interesting.

The author also express sincere appreciation for warm Swedish hospitality and reception during the period in Sweden.

The author also express his sincere grtatitude to the authorities of Chittagong University of Engineering and Technology, Chittagong, Bangladesh, granting study leave to come here in Sweden.

Finally but not the least, the author wish to thank his family members for their special support, love and patience during the period of study at Chalmers University of Technology, Göteborg, Sweden.

Table of contents

Abstract.....	iv
Acknowledgements	v
Table of contents	vi
List of Symbols & Abbreviations.....	viii
1 INTRODUCTION.....	1
1.1 General Background	1
1.2 Previous Work	2
1.3 The Aim of the Thesis.....	2
1.4 Thesis Layout.....	3
2 AN OVERVIEW OF WTG.....	4
2.1 Historical Background	4
2.1.1 Mechanical Power Generation.....	4
2.1.1 Electrical Power Generation	4
2.2 Current status of wind power worldwide.....	5
2.3 Wind properties	6
2.4 Wind Power Turbine.....	7
2.4.1 Power output from a wind turbine	8
2.5 Aerodynamic power control	13
2.5.1 Stall control.....	14
2.5.2 Active stall control.....	14
2.5.3 Pitch control.....	14
2.6 Wind turbine concepts	15
2.6.1 Fixed speed	16
2.6.2 Limited variable speed using external rotor resistance.....	17
2.6.3 Variable speed with small scale frequency converter.....	18
2.6.4 Variable speed with full scale frequency converter.....	19
3 POWER SYSTEM REQUIREMENTS FOR WTG.....	20
3.1 Grid operation of wind turbine	20
3.2 Interaction with the Electricity Network.....	21
3.2.1 Short-circuit power level.....	22
3.2.2 Voltage variations and flicker	23
3.2.3 Harmonics	23
3.2.4 Frequency.....	24
3.2.5 Reactive power.....	25
4 MODEL AND CASE STUDIES.....	27
4.1 Simulation tool used	27
4.2 The GE® WTG	27
4.2.1 GE WTG characteristic curves	30

4.3	Case studies	33
5	SIMULATION RESULTS	34
5.1	GE® base Cases	34
5.1.1	Simulation in the low-wind-speed region	35
5.1.1.1	With pitch-angle controller loop inactive	35
5.1.1.2	Comparison of simulations in low-wind speed region	38
5.1.2	Simulation for transition from low-to-high wind speed region	41
5.1.3	Simulation in the high-wind-speed region	43
5.1.3	Grid-fault simulation in the low-wind-speed region	46
5.1.3.1	Pitch-angle controller loop inactive	46
5.1.3.1	Pitch-angle controller loop active	48
5.1.4	Grid-fault simulation in the high-wind-speed region	50
5.1.5	Grid-fault severity	53
5.2	Effect of $C_p(\lambda)$	56
5.2.1	Case-1: Reducing the maximum value of C_p	58
5.2.1.1	Simulation in the low-wind-speed region	58
5.2.1.1	Simulation in the high-wind-speed region	61
5.2.2	Case-2: Shifting the $C_p(\lambda)$ curve rightward along the λ -axis	63
5.2.2.1	Simulation in the low-wind-speed region	64
5.2.2.2	Simulation in the high-wind-speed region	66
5.2.3	Case-3: Shifting the $C_p(\lambda)$ curve leftward along the λ -axis	68
5.2.3.1	Simulation in the low-wind-speed region	68
5.2.3.2	Simulation in the high-wind-speed region	71
5.2.4	Comarison table	74
5.3	Frequency response in low-wind speed region	75
6	CONCLUSIONS AND FUTURE WORK	77
6.1	Conclusions	77
6.2	Future work	78
	References	79
	Appendix	80
	GE parameters	80
	Sample Matlab® program	83
	Sample Simulink® model	86

List of Symbols & Abbreviations

Symbols

A_r	rotor swept area
C_p	aerodynamic coefficient of performance
ρ	air density
α	angle of attack
β	pitch angle of the blade
λ	tip-speed ratio
ω_r	rotor-speed

Abbreviations

WECS	Wind Energy Conversion System
WTG	Wind Turbine Generator
WS	Wind Speed
DFIG	Doubly Fed Induction Generator
VSWT	Variable Speed Wind Turbine

Chapter 1

Introduction

The world-wide concern about the environment has led to increasing interest in technologies for generation of electricity from renewable sources is to use wind turbines. The wind power as an energy source has been used for a long time. Denmark was the first country to utilize wind energy to produce electricity [1]. Wind electricity generation has been expanding rapidly during recent years, due to largely technological improvements, industry maturation and an increasing concern regarding the emissions associated with burning fossil fuels. Thus the operation of the wind farm and its response to disturbances or other changing conditions on the power system is becoming of increasing concern, especially in cases where the wind farms represent a significant portion of local generation.

1.1 General Background

Wind turbines often do not take part in voltage and frequency control and if a disturbance occurs, the wind turbines are disconnected and reconnected when normal operation has been restored. These power system control services is currently carried out by conventional synchronous generation. Increasing levels of wind generation has resulted in an urgent need for the assessment of their impact on frequency or voltage control of power systems. Wind turbine generators (WTGs) can be divided into two basic categories: Fixed-speed and Variable-speed. A Fixed-speed WTG generally uses a squirrel-cage induction generator to convert the mechanical energy from the wind turbine into electrical energy. A variable-speed wind turbine uses a doubly-fed induction generator (DFIG) and a partial scale frequency converter. The fast controllability of the power electronic converter can be utilized to shape the response of the wind turbine against various network disturbances and thus making the wind turbine to react responsibly.

1.2 Previous Work

In a previous work [2], the capability of providing a short-term excess active power support of a commercial multi megawatt Variable Speed Wind Turbine (VSWT) is quantified and the findings are generalized by considering different effects of WT's parameters like $C_p(\lambda)$, H_{WT} .

1.3 The Aim of the Thesis

The goal of the thesis is to implement an example WT system (GE 3.6 MW of DFIG type) in Matlab® and Simulink® and to test its functionality to be able to use the model for power system study such as frequency control, power oscillation damping, etc.

First, a commercial WT is to be implemented in Matlab® and Simulink® and tested the functionality in low-wind speed, transition from low-to-high wind speed and high-wind speed region by applying a step in wind speed. The functionality is also tested against grid faults of varying severity.

Secondly, the functionality is to be tested by changing the WT's aerodynamic parameters $C_{p,max}$ and λ_{opt} leaving the controller parameters unchanged.

Finally, the frequency response characteristic in the low-wind speed region of the WT is to be plotted (with and without varying the WT control parameters) to be able to determine the frequency range where the WT under investigation can provide a satisfactory contribution towards power system frequency control support and power oscillation damping.

1.4 Thesis Layout

Chapter 2 presents an overview of the most important theories of wind turbine.

Chapter 3 presents brief description of power system requirements of wind turbine.

Chapter 4 presents brief description of modelling of wind turbine and implementation

Chapter 5 simulation results and analysis.

Chapter 6 conclusions and future works

References

Appendix

Chapter 2

An Overview of WTG

The power of the wind has been utilised for at least 3000 years [3]. There are three principle parts of a wind power system: the turbine, nacelle (including the generator and yaw mechanism) and tower. The turbine captures the wind's energy by spinning a generator in the nacelle. The nacelle houses the electric generator, mechanical gearing, speed and wind sensor, control systems and portions of the yaw mechanism that orients the turbine into the wind. The tower containing the electrical conduits and yaw motor (usually) supports the nacelle and provides access to the nacelle for maintenance [3]. Later, some commonly used generator systems for a wind turbine are discussed.

2.1 Historical Background

Until the early twentieth century wind power was used to provide mechanical power to pump water or to grind grain. At the beginning of modern industrialisation, the use of the fluctuating wind energy resource was substituted by fossil fuel fired engines or the electrical grid, which provided a more consistent power source [3].

2.1.1 Mechanical Power Generation

The earliest windmills recorded were vertical axis mills. This windmills can be described as simple drag devices. From Persia and Middle East, the horizontal axis windmill spread across the Mediterranean countries and Central Europe. The first horizontal axis windmill appeared in England around 1150, in France 1180 and in Denmark in 1259. In Europe, windmill performance was constantly improved between the twelfth and nineteenth centuries. By the end of the nineteenth century, the typical European windmill used a rotor of 25 meters in diameter, and the stocks reached up to 30 meters [3].

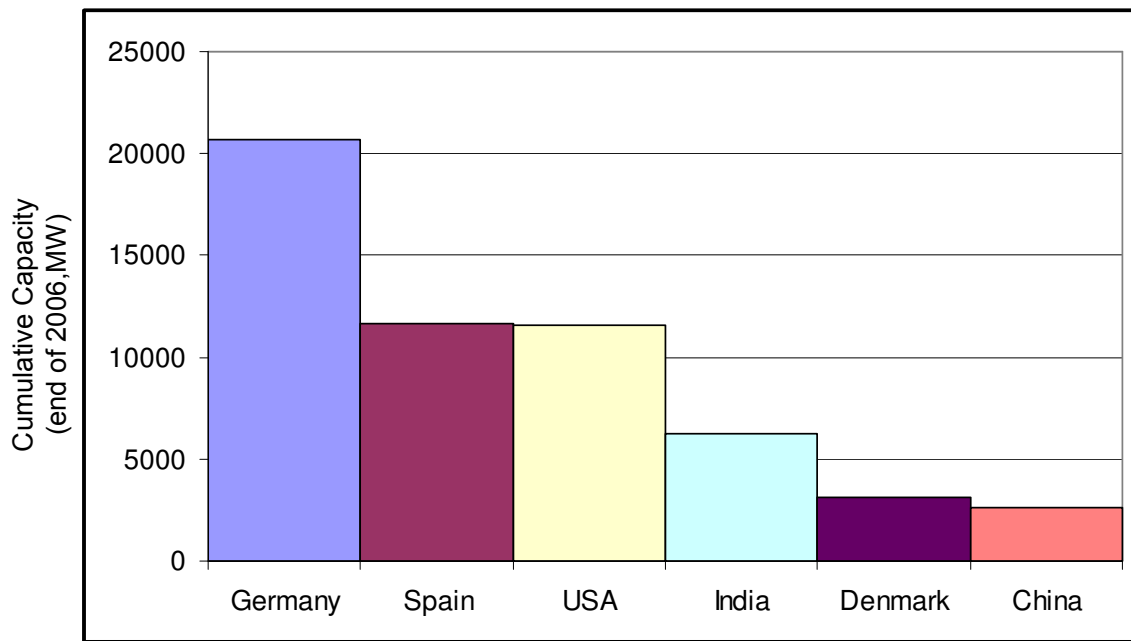
2.1.1 Electrical Power Generation

In 1891, the Dane Poul LaCour was the first to build a wind turbine that generated electricity. Danish Engineers improved the technology during World Wars 1 and 2 and used the technology to overcome energy shortages. The wind turbines by the Danish

company F.L.Smidth built in 1941-42 can be considered forrunners of modern wind turbine generators. The Smidth turbines were the first to use modern airfoils, based on the advancing knowledge of aerodynamics at this time [3].

2.2 Current status of wind power worldwide

The wind power industry is in an era of substantial growth in Europe, the USA and in fact globally. The rush to wind continues apace, as global installed capacity of wind turbines reached 74 GW by the end of 2006, after additions of 14,985 MW during the year. It has been forecast that installed capacity of wind power will double to 142 GW by 2010 and will grow further. The five leading wind power markets are Germany, Spain, the USA, India and Denmark. China is about to join to the top table. The following figure shows the comparison among these wind power leaders [4].



International ranking of Wind Power Capacity

Fig.2.1 International ranking of Wind Power Capacity

In addition, it has been reported that, GE wind the dominant manufacturer of wind turbines supplying the US market during 2006, with 47% of domestic

installations. Semens and Vestas also had significant contributions among dominant manufacturer.

2.3 Wind properties

Wind is air in motion relative to the surface of the earth. For purposes of wind turbine design, the wind vector is considered to be composed of a *steady wind* plus *fluctuations about the steady wind*. The primary cause of air motion is uneven heating of the earth by solar radiation. The air is not heated directly, but solar radiation is first absorbed by the earth's surface and is then transferred in various forms back into the overlying atmosphere. Since the surface of the earth is not homogeneous, the amount of energy that is absorbed varies both in space and time. This creates differences in atmospheric temperature, density and pressure, which in turn create forces that move air from one place to another. For example, land and water along a coastline absorb radiation differently, as do valleys and mountains, and this creates breezes.

The basic unit of measurement for this resource is 'wind power density', or power per unit of area normal to the wind 'azimuth' (the direction from which the wind is blowing), calculated as follows:

$$p_w = \frac{d}{dt}(q_d x) = 0.5\rho U^2 \frac{dx}{dt} = 0.5\rho U^3$$

where

p_w = wind power density (W/m^2)

q_d = dynamic pressure of the wind (N/m^2)

x = run of wind past a given point (m)

ρ = air - density (kg/m^3)

U = horizontal component of the mean - free stream wind velocity (m/s)

2.4 Wind Power Turbine

The wind turbine is a device for conversion of kinetic energy in the wind into electricity. Wind turbine produces electricity by using the natural power of the wind to drive a generator. The wind is a clean sustainable fuel source, it doesn't create emissions and will never run out as it is constantly replenished by energy from the sun. Although there are many different configurations of wind turbine systems they all work in the same way. The available power originates from the mass flow of the moving air, referred to as the wind speed. The transformation to mechanical torque is done by aerodynamical forces acting on the rotor blades, the actuator disc. The wind turbine shaft then transports the power to the generator which is connected to the electrical grid. Usually there is a gear box between the slowly rotating turbine shaft and the more rapidly rotating generator shaft [5].

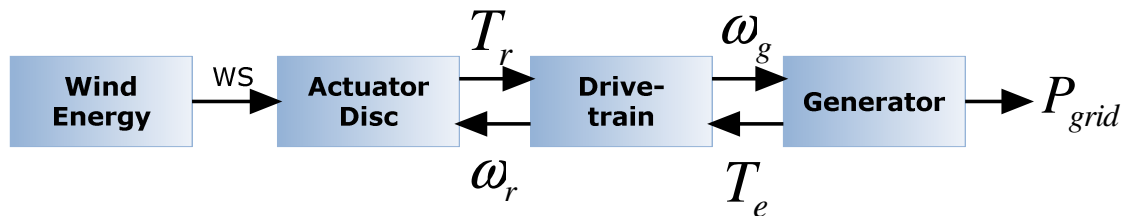


Figure 2.2 Power from the Wind

Most wind turbines start generating electricity at wind speeds of around 3-4 meters per second (m/s), generate maximum 'rated' power at around 15 m/s and shut down to prevent storm damage at 25 m/s or above.

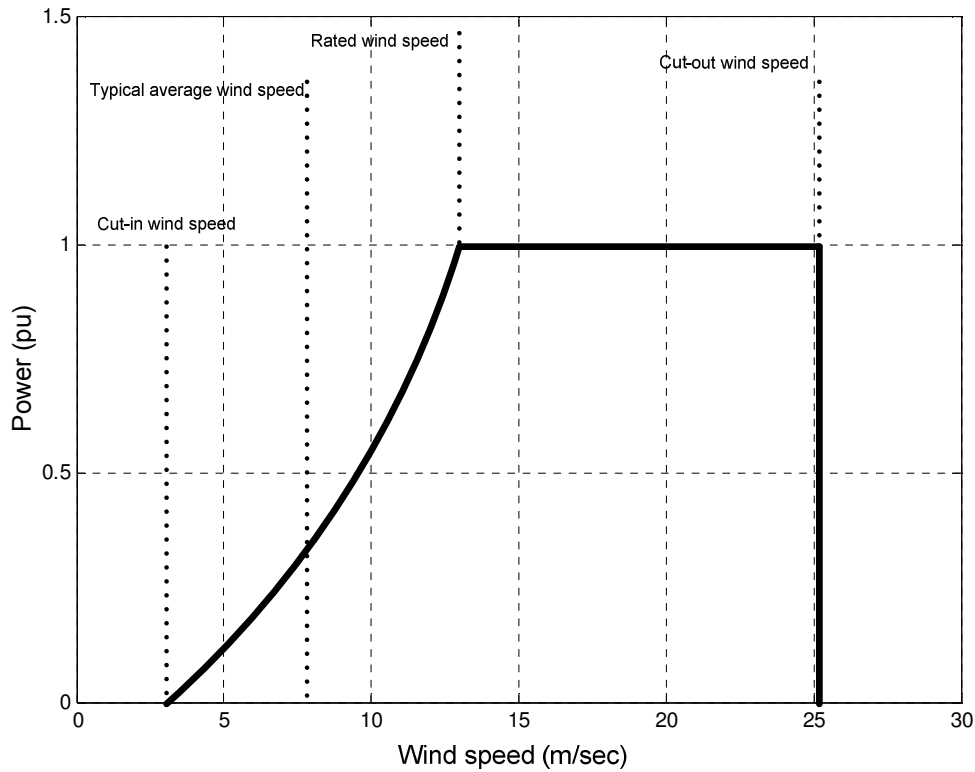


Figure 2.3 Typical power curve of a wind turbine

2.4.1 Power output from a wind turbine

From a physical point of view, the static characteristics of a wind turbine rotor can be described by the relationships between the total power in the wind and the mechanical power of the wind turbine. These relationships are readily described starting with the incoming wind in the rotor swept area. It can be shown that the kinetic energy of a cylinder of air of radius R travelling with wind speed v_{wind} corresponds to a total wind power P_{wind} within the rotor swept area of the wind turbine. This power, P_{wind} , can be expressed by:[3]

$$P_{wind} = \left(\frac{1}{2} \rho_{air} \right) \times (\pi R^2) \times v_{wind}^3$$

where

ρ_{air} = air density (1.225 kg/m³)

R = rotor radius (m)

v_{wind} = wind speed (m/s)

It is not possible to extract all the kinetic energy of the wind, since this would mean that the air would stand still directly behind the wind turbine. The wind speed is only reduced by the wind turbine, which thus extracts a fraction of the power in the wind. This fraction is determined by the power efficiency co-efficient, C_p , of the wind turbine. The mechanical power, P_{mech} , of the wind turbine is therefore, by the definition of C_p , given by the total power in the wind, P_{wind} using the following equation:

$$P_{mech} = C_p \times P_{wind}$$

However, it is theoretically possible to extract approximately 59% of the kinetic energy of the wind. This is known as Beltz's limit. Optimum C_p value lies between 0.52-0.55 for modern three-bladed wind turbines when measured at the hub of the turbine [3].

It is clear from a physical point of view that the power, P_{mech} , that is extracted from the wind will depend on rotational speed, wind speed and blade angle, β . Therefore, P_{mech} and hence also C_p must be expected to be functions of these quantities. That is,

$$P_{mech} = f_{P_{mech}}(\omega_{turb}, v_{wind}, \beta)$$

From the simple geometric considerations, which ignore the wind turbulence created by the blade tip show that the angle of incidence φ is determined by the incoming wind speed v_{wind} and the speed of the blade. The blade tip is moving with speed v_{tip} , equal to $\omega_{turb}R$. This is illustrated in Fig.2.4.

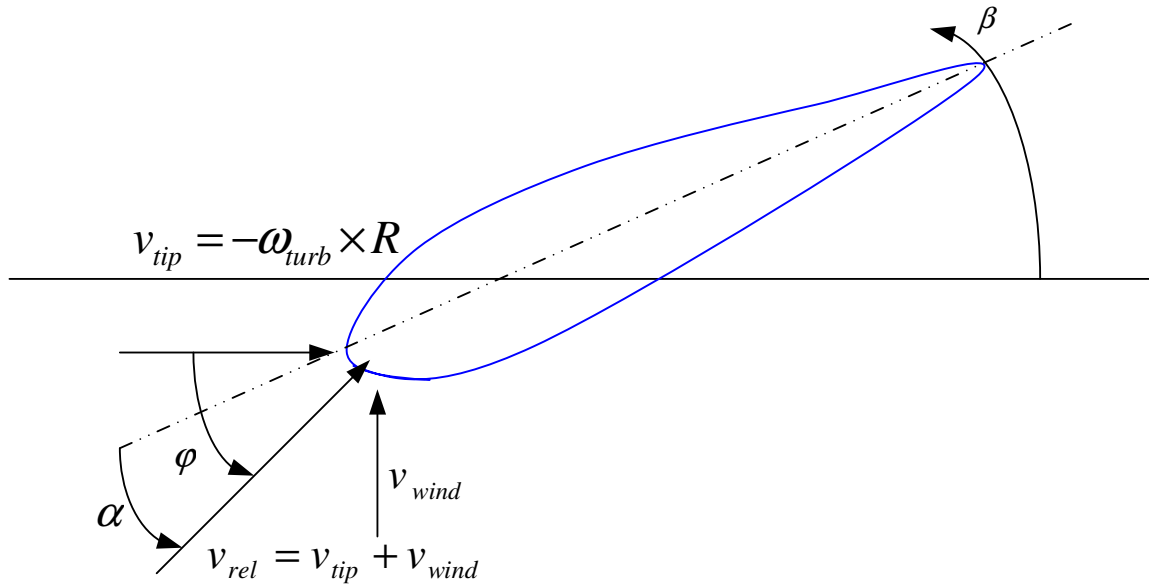


Figure 2.4 Illustration of wind conditions around the moving blade

Another commonly used term in the aerodynamics of the wind turbines is the tip-speed ratio, λ , which is defined by:

$$\lambda = \frac{\omega_{turb} R}{v_{wind}}$$

The highest values of C_p are typically obtained for λ values in the range around 8-9. This means that the angle between the relative air speed-as seen from the blade tip-and the most rotor plane is rather a sharp angle. Therefore, the angle of incidence ϕ can be calculated as:

$$\phi = \tan^{-1}\left(\frac{1}{\lambda}\right) = \tan^{-1}\left(\frac{v_{wind}}{\omega_{turb} R}\right)$$

It is possible to adjust the pitch angle β of the entire blade through a servo mechanism. If the blade is turned, the angle of attack α between the blade and relative wind v_{rel} will be changed accordingly. So the energy extraction will depend on the angle of attack α between the moving rotor blades and the relative wind speed v_{rel} as seen from the moving blades. It follows that, C_p can be expressed as a function of λ and β .

$$C_p = f_{C_p}(\lambda, \beta)$$

C_p is a highly non-linear power function of λ and β . Now, if the $C_p - \lambda$ curve is known for a specific wind turbine with a turbine rotor radius R it is easy to construct the curve of C_p against the rotational speed for any wind speed, v_{wind} . Therefore, the optimal operational point of the wind turbine at a given wind speed v_{wind} is determined by tracking the rotor speed to the point λ_{opt} . The optimal turbine rotor speed is then:

$$\omega_{turb,opt} = \frac{\lambda_{opt} v_{wind}}{R}$$

A typical $C_p - \lambda$ curve for different pitch angle is shown in Fig.2.5.

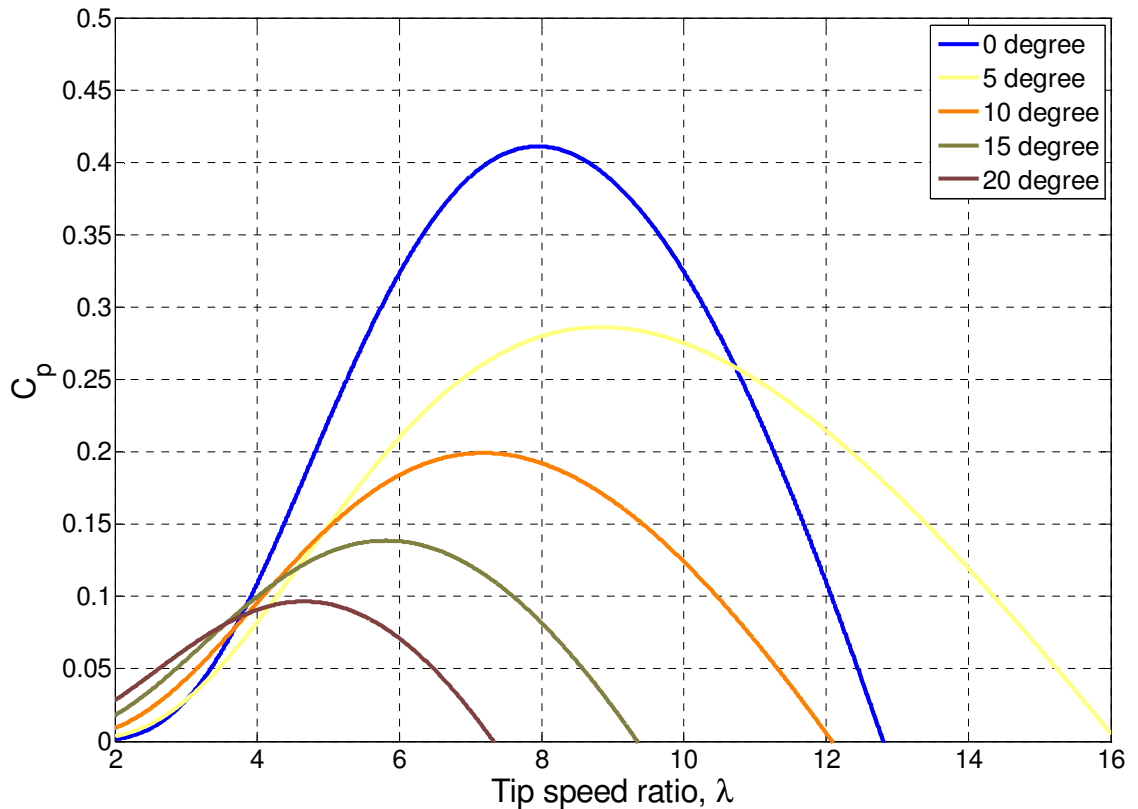


Figure 2.5 A typical λ - C_p curve for different pitch angle (from 0^0 to 20^0)

The optimal rotational speed for a specific wind speed also depends on the turbine radius, R , which increases with the rated power of the turbine. Therefore, the large the rated power of the wind turbine the lower the optimal rotational speed.

These basic aerodynamic equations of the wind turbines provide an understanding that fixed-speed wind turbines have to be designed in order for the rotational speed to match the most likely wind speed in the area of installation.

In the case of variable-speed wind turbines, the rotational speed of the wind turbine is adjusted over a wide range of wind speeds so that the tip-speed ratio λ is maintained at λ_{opt} . Therefore, C_p reaches its maximum and consequently, the mechanical power output from a variable-speed wind turbine will be higher than that of a similar fixed-speed wind turbine over a wider range of wind speeds. At higher wind speeds, the mechanical power

is kept at the rated level of the wind turbine by pitching the turbine blades. There are two possibilities for doing this-either out of the wind or up against the wind:

- If the blades are turned out of the wind, The lift on the blades is gradually reduced. This is called pitch control and requires a relatively large change in pitch angle to reduce power significantly.
- If the blades are turned up against the wind, the turbine blades will stall and thus automatically reduce the lift on the turbine blades. This effect is obtained with a relatively small change in pitch angle. This is called stall control and requires a more accurate control of the pitch angle because of the high angular sensitivity.

2.5 Aerodynamic power control

At high wind speeds it is necessary to limit the input power to the turbine, i.e., aerodynamic power control. There are three major ways of performing the aerodynamic power control, i.e. by stall, pitch or active stall control. Stall control implies that the blades are designed to stall in high wind speeds and no pitch mechanism is thus required.

Pitch control is the most common method of controlling the aerodynamic power generated by a turbine rotor, for newer large wind turbines. Pitch control is used by almost all variable-speed wind turbines. Below rated wind speed the turbine should produce as much power as possible, i.e., using a pitch angle that maximizes the energy capture. Above rated wind speed the pitch angle is controlled in such a way that the aerodynamic power is at its rated. In order to limit aerodynamic power, at high wind speeds, the pitch angle is controlled to decrease the angle of attack. It is possible to increase the angle of attack towards stall in order to limit the aerodynamic power. This method can be used to fine tune the power level at high wind speeds for fixed-speed turbines. This control method is known as active stall or combi stall [6].

2.5.1 Stall control

When no blade pitching mechanism is available i.e. when the pitch angle of the blade is constant, stall control is used to limit the power extraction. When wind speed approaches the value at which the generator reaches its rated power, further torque developed should be avoided [7]. Wind speed exceeding rated value causes higher angle of attack and thus to stalling. When the turbine is under full load and the wind speed increases to the range beyond, this results in a lower rotor torque and a lower performance coefficient. The main advantage with stall control is the fixed connection of the rotor blades to the hub. One drawback, however, is the maximization of the power production at a certain wind speed which is determined by the geometry of the rotor blade.

2.5.2 Active stall control

During high wind speed situations when the angle of attack is higher, increasing the pitch angle during those situations will reduce the angle of attack i.e. the stall point should be pushed into a higher wind speed region. Besides the better exploitation of the wind turbine system during high wind speed situations, this pitching method makes emergency stopping and starting of the wind turbine easier. This control method is used for larger fixed-speed turbines (upto 2.4 MW).

2.5.3 Pitch control

This control method is, in principle, same as the active stall control method. But in this method, the pitch angle is varied in a wider range. During high wind speed situations, the angle of attack can be maintained to a lower value by varying the pitch angle in a wider range. The advantage of this control method is the better exploitation of the system during high wind situations, decrease the thrust force on the turbine, starting the emergency stopping of the turbine. One drawback is the need of a pitching mechanism. Another drawback is the high slope of the power curve at high wind speeds which will cause a large output power variation for a small variation in wind speed. This control method is used for larger variable speed turbines.

2.6 Wind turbine concepts

Wind turbines can operate with either fixed speed (actually within a speed range about 1%) or variable speed. For fixed-speed wind turbines, the generator (induction generator) is directly connected to the grid. Since the speed is almost fixed to the grid frequency, and most certainly not controllable, it is not possible to store the turbulence of the wind in form of rotational energy. Therefore, for a fixed-speed system the turbulence of the wind will result in power variations, and thus affect the power quality of the grid [8]. For a variable-speed wind turbine the generator is controlled by power electronic equipment, which makes it possible to control the rotor speed. In this way the power fluctuations caused by wind variations can be more or less absorbed by changing the rotor speed [9] and thus power variations originating from the wind conversion and the drive train can be reduced. Hence the power quality impact caused by the wind turbine can be improved compared to a fixed-speed turbine [10].

The rotational speed, Ω_{rT} , of a wind turbine is fairly low and must therefore be adjusted to the electrical frequency. This can be done in two ways, i.e., with a gear box or with the number of poles, n_p , of the generator. The number of poles sets the mechanical speed, ω_m , of the generator with respect to the electrical frequency. If the gear ratio equals gr , the rotor speed of the wind turbine is adjusted to the electrical frequency as

$$\omega_{rT} = \frac{\Omega_{rT}}{n_p gr}$$

where ω_{rT} is referred to the electrical frequency of the grid. The dynamics of the drive train can be expressed as

$$J_T \frac{d\Omega_{rT}}{dt} = T_s - T_T$$
$$J \frac{d\omega_m}{dt} = T_e - T_s$$

where J_T is the wind-turbine inertia, J is the generator inertia, T_s is the shaft torque, T_T is the torque produced by the wind turbine rotor and T_e is the electromechanical torque

produced by the genertor. It is most often convenient to have the rotational speeds referred to same side of the gear box as

$$J_T \frac{d\Omega_{rT}}{dt} = \frac{J_T}{n_p g r} \frac{d\omega_{rT}}{dt} = \xi(\theta_r - \theta_{rT}) + \zeta(\omega_r - \omega_{rT}) - T_T$$

$$J \frac{d\omega_m}{dt} = \frac{J}{n_p} \frac{d\omega_r}{dt} = T_e - \xi(\theta_r - \theta_{rT}) - \zeta(\omega_r - \omega_{rT})$$

where ω_r is the rotational speed of the generator referred to the electrical frequency and the shaft torque has been set to $T_s = \xi(\theta_r - \theta_{rT}) + \zeta(\omega_r - \omega_{rT})$, where ξ is the shaft stiffness and ζ is the shaft dampening. The angles θ_{rT} and θ_r can be found from

$$\frac{d\theta_{rT}}{dt} = \omega_{rT} \quad \frac{d\theta_r}{dt} = \omega_r$$

In this section the following wind turbine concepts have been presented:

- Fixed-speed wind turbine.
- Limited variable-speed wind turbine using external rotor resistance.
- Variable speed with small scale frequency converter.
- Variable speed with full scale frequency converter.

2.6.1 Fixed speed

The rotor of a fixed speed wind turbine system operates at an almost fixed rotational speed determined by the frequency of the supply grid, the gear ratio and the generator design, regardless of the wind speed. In the fixed speed wind turbine system, the stator of the generator is directly connected to the grid, as shown in Fig.2.6. Since an induction generator always draws reactive power from the grid, a capacitor bank for reactive power compensation is used in this type of configuration. The output power is limited by the aerodynamic design of rotor blades in the case that the stall control method is used. In order to increase the power production, the generator of some fixed-speed wind turbines has two sets of stator windings. One is used at low wind speeds and the other is used at medium and high wind speeds.

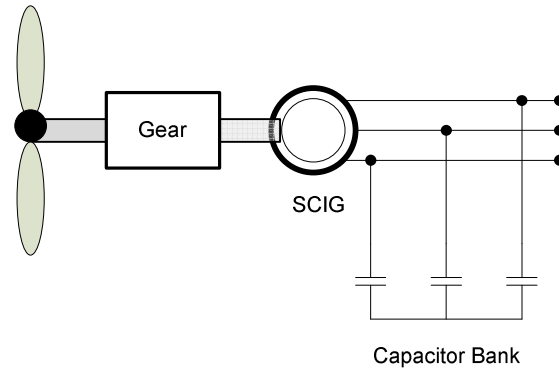


Figure 2.6 Fixed-speed wind turbine. SCIG= squirrel cage induction genertor

As the rotor speed is constant, the mechanical power on the genertor shaft can not be kept constant due to the variation in the wind speed. The mechanical power fluctuation due to the wind variation will be transmitted into the electric output power. A variable speed system on the other hand, keeps the generator torque fairly constant by changing the generator speed in response to variations in the wind speed. Variations in the incoming wind power are absorbed by rotor speed changes. The aerodynamic power control method almost exclusively used with a variable speed system is the pitch control method [11].

2.6.2 Limited variable speed using external rotor resistance

The configuration uses a wound rotor induction generator (WRIG)(Fig.2.7) and has been produced by the Danish manufacturer Vestas since the mid-1990s. The generator is directly connected to the grid and the capacitor bank provides reactive power compensation in exactly the same way as for a standard fixed speed system. The unique feature of this configuration is that it has a variable additional rotor resistance which can be changed by an optically controlled converter mounted on the rotor shaft.This gives a small variable speed range. Typically the speed range is 0-10% above synchronous speed [11].

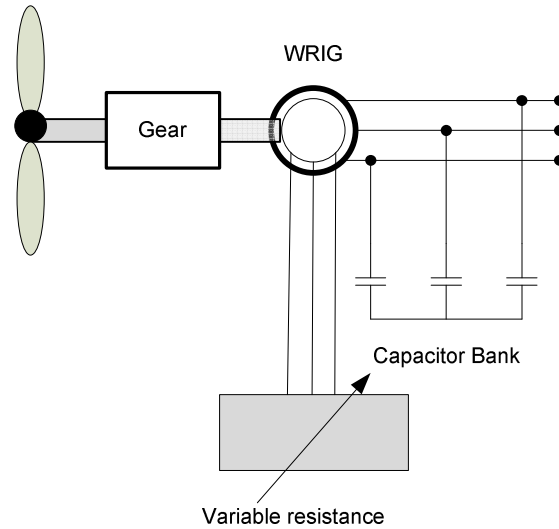


Figure 2.7 Limited variable-speed wind turbine. WRIG= wound rotor induction genertor

2.6.3 Variable speed with small scale frequency converter

Fig.2.8 shows the variable speed wind turbine with a small scale frequency converter located in the rotor circuit, which is known as the DFIG (Doubly-Fed Induction Genertor) system. In this type of configuration the stator is directly connected to the grid while the rotor windings are connected via slip rings to the converter. The frequency converter is rated at approximately 30% of the generator power. Typically the variable speed range is -40% to +30% of the synchronous speed [3]. The converter also allows for control of the reactive power [11].

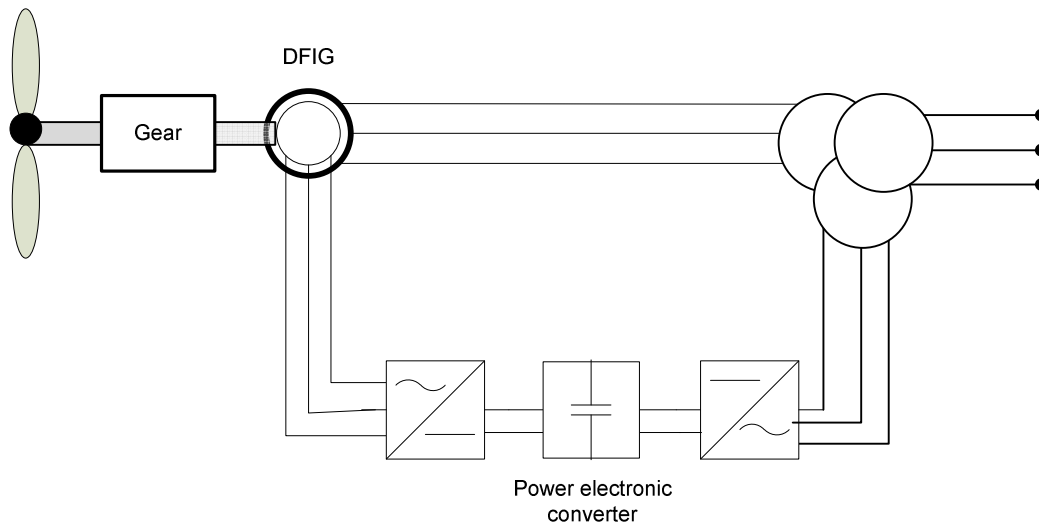


Figure 2.8 Variable-speed wind turbine with a doubly-fed induction generator (DFIG) and a partial scale frequency converter

2.6.4 Variable speed with full scale frequency converter

This type of wind turbine concept has a full variable speed range, with the generator connected to the grid through a full scale power converter, as shown in Fig.2.9. The generator can either be an induction machine or a synchronous machine. In case the generator is of synchronous type, it can be excited either by electrically or by permanent magnets. The gearbox is designed so that the maximum rotor speed corresponds to the rated speed of the generator. Some full scale power converter variable speed wind turbine systems have no gearbox. In those cases, a direct driven multiple pole generator with a large diameter is used. The German wind turbine manufacturer Enercon is successfully manufacturing this type of wind turbine [11].

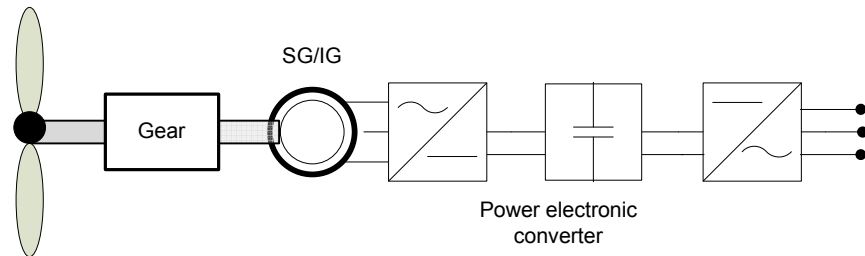


Figure 2.9 Variable-speed wind turbine with a full scale frequency converter. SG= synchronous generator, IG= induction generator

Chapter 3

Power System Requirements for WTG

The power system requirements for wind power depend mainly on the power system configuration, the installed wind power capacity and how the wind power production varies. Wind resources vary on every time scale: seconds, minutes, hours, days, months and years. On all these time scales, the varying wind resources affect the power system. An analysis of this impact will be based on the geographical area that is of interest.

3.1 Grid operation of wind turbine

When operating wind turbines in the rigid combined grid, it is usually assumed that the output provided by the turbine, upto the generator capacity, can always be directly transferred to the grid. A high degree of energy utilization can be achieved in this manner. In order to protect the drive train, generator and grid connection from overload, it is sufficient to limit the output to the design-dependent nominal or maximum value. Offshore wind power holds the promise of very large- in Denmark figures upto 1800 MW are mentioned-geographically concentrated wind power installations placed at great distances from the nearest point where it can be connected to the electric transmission system. For large onshore wind farms, i.e. 100-200 MW, high voltage overhead lines above 100 kV are normally used in this situation. For offshore wind farms however this option is not available as a large part of the distance to the connection point necessarily must be covered by a submarine cable. The distances can be considerable, depending on local conditions, water depth and bottom conditions in particular. Too deep water increases the cost for foundations and too shallow water makes construction makes construction difficult [12].

The priciple layout of a grid connection scheme for an offshore wind farm follows very much the same lines as for a large onshore installation as the basic functional requirements are the same to transmit the energy produced to a point where the electric transmission grid is strong enough to absorb it. In a typical layout for such a scheme clusters of WT are each connected to a medium voltage ring. This principle deviates from

normal onshore practice where the WT are connected to a number of radial cables from the medium voltage switchgear in the transformer station. The reason for this is the vulnerability of the submarine cables to anchors and fishing activities. It must be anticipated that sections of the ring may be out of service for repair or exchange for long periods if weather conditions makes repair work impossible. With a ring connection, production can continue upheld in the repair periods thus-at a small extra cost-reducing the economic consequences of a cable fault. The choice of voltage level within the wind farm is purely a matter of economy. Each WT is equipped with a transformer stepping up from the generator voltage-typically low voltage, i.e. below 1 kV- to a medium voltage below 36 kV. The following table showing transmittable power and connection of wind turbines to different levels of the electrical network:

Voltage system	Size of WT or wind farm	Transmittable power
Low voltage system	For small to medium turbines	Upto~300 kW
Feeder of the medium voltage system	For medium to large wind turbines and small wind farms	Upto~2-5 MW
Medium voltage system, at transformer substation to high voltage	For medium to large onshore windfarms	Upto~10-40 MW
High voltage system	Clusters of large onshore windfarms	Upto~100 MW
Extra high voltage system	Large offshore wind farms	>0.5 GW

Table:3.1 Transmittable power and connection of wind turbines to different levels of the electrical network [12]

3.2 Interaction with the Electricity Network

The modern electricity supply network is a complex system. The somewhat vague term “power quality” is to describe the interaction between traditional producers operating

fossil fired, nuclear or hydro power plants and consumers. The latter may be large or small consumers. In the last 10 years, a steadily increasing numbers of renewable energy sources such as wind powered generating systems have been added to the systems. A distinctive feature of electricity is that it can not be stored as such-there must at any instant be balance between production and demand. All renewable sources produce when the source is available-for wind power, as the wind blows. This characteristic is of little if any importance when the amount of wind power is modest compared to the total installed (and spinning) capacity of controllable power plants, but it changes into a major technical obstacle as the renewable part (termed penetration) grows to cover a large fraction of the total demand for electric energy in the system. On the local level, voltage variations are the main problem associated with wind power. Normal static tolerances on voltage levels are $\pm 10\%$. However, fast variations become a nuisance at levels as low as 0.3% and in weak grids- as is often found in remote areas where the wind conditions are best. This can be the limiting factor on the amount of wind power which can be installed. In the following, a short introduction is given to each of the electrical parameters which taken together are used to characterise power quality-or more correct, voltage quality-in a given point in the electricity supply system [12].

3.2.1 Short-circuit power level

The short circuit power level in a given point in the electrical network is a measure of its strength and, while not directly a parameter in the voltage quality, has a heavy influence. The ability of the grid to absorb disturbances is directly related to the short circuit power level of the point in question. Depending on the type of electrical equipment in the WT they can sometimes be operated successfully under weak conditions. Care should always be taken, for single or few WT in particular, as they tend to be relatively more disturbing than installations with many units. Short circuits take on a variety of forms in a network and are by far the most common. In severity they range from the one phase earth fault caused by trees growing up into an overhead transmission line, over a two phase fault to the three phase short circuit and with low impedance in the short circuit itself. Many of these faults are cleared by the relay protection of the transmission system either by disconnection and fast reclosure, or by disconnection of the equipment in question after a

few hundred milliseconds. In all situations the result is a short period with low or no voltage followed by a period where the voltage returns. A large-off shore- wind farm in the vicinity will see this event and disconnect from the grid immediately if only equipped with the proper protection. This is equivalent to the situation “loss of production capacity” and disconnection of the wind farm will further aggravate the situation. Up to now, no utility has put forward requirement to dynamic stability of WT during grid faults. The situation in Denmark today, and the visions for the future, have changed the situation and for wind farms connected to the transmission grid, that is at voltages above 100 kV, this will be required [12].

3.2.2 Voltage variations and flicker

Voltage variations caused by fluctuating loads and/or production is the most common cause of complaints over the voltage quality. Very large disturbances may be caused by arc-welding machines and frequent starting of large motors. Slow voltage variations within the normal-10+6% tolerance band are not disturbing and neither are infrequent (a few times per day) step changes of up to 3%, though visible to the naked eye. Fast and small variations are called flicker. Flicker evaluation is based on IEC 1000-3-7 which gives guidelines for emission limits for fluctuating loads in medium voltage (MV, i.e. voltages between 1 and 36 kV) and high voltage (HV, i.e. voltages between 36 and 230 kV) networks. Determination of flicker emission is always based on measurement. IEC 61000-4-15 specifies a flickermeter which can be caused to measure flicker directly. As flicker in the general situation is the result of flicker already present on the grid and the emissions to be measured, a direct measurement requires a undisturbed constant impedance power supply and this is not the feasible for WTGs due to their size [12].

3.2.3 Harmonics

Harmonics are a phenomenon associated with the distortion of the fundamental sinewave of the grid voltages, which is purely sinusoidal in the ideal situation. The concept stems back to the French mathematician Josef Fourier who in the early 1800 found that any periodical function can be expressed as a sum of sinusoidal curves with different frequencies ranging from the fundamental frequency- the first harmonic- and integer

multiple thereof where the integer designates the harmonic number. Harmonic disturbances are produced by many types of electrical equipment. Depending on their harmonic order they may cause different types of electrical equipment. All harmonic causes increased currents and possible destructive overheating in capacitors as the impedance of a capacitor goes down in proportion to the increase in frequency. As harmonics with order 3 and odd higher multiples of 3 are in phase in a three phase balanced network, they cannot cancel out between the phases and cause circulating currents in the delta windings of transformers, again with possible overheating as the result. The higher harmonics may further give rise to increased noise in analogue telephone circuits. Highly distorting loads are older unfiltered frequency converters based on thyristor technology and similar types of equipment. It is characteristic for this type that it switches one time in each half period and it may generate large amounts of the lower harmonic orders. Newer transistor based designs are used in most VSWT today. The method is referred to as Pulse Width Modulation (PWM). It switches many times in each period and typically starts producing harmonics where the older types stop, that is around 2 kHz. Their magnitude is smaller and they are easier to remove by filtering than the harmonics of lower order [12].

3.2.4 Frequency

The electrical supply and distribution systems used world-wide today are based on alternating voltages and currents (AC systems). That is, the voltage constantly changes between positive and negative polarity and the current its direction. The number of changes per second is designated the frequency of the system with the unit Hz. In Europe the frequency is 50 Hz whereas it is 60 Hz in many other places in the world. The frequency of the system is proportional to the rotating speed of the synchronous generators operating in the system and they are part from an integer even factor depending on machine design-essentially running at the same speed: They are synchronised. Increasing the electrical load in the system tends to brake the generators and the frequency falls. The frequency control of the system then increases the torque on some of the generators until equilibrium is resored and the frequency is 50 Hz again. The requirements for frequency control in the West European grid are laid down in the

UCPTE (Union for the Co-ordination of Production and Transmission of Electricity) rules. The area is divided in a number of control zones each with its own primary and secondary control. The primary control acts on fast frequency deviations, with the purpose of keeping equilibrium between instantaneous power consumption and production for the whole area. The secondary control aims at keeping the balance between production and demand within the individual zones and keeping up the agreed exchange of power with other zones. The power required for primary control is 3000 MW distributed throughout the control zones whereas the frequency control related to keeping the time for electric grid controlled watches is accomplished by operating the system at slightly deviating frequencies in a diurnal pattern so that the frequency on an average is 50 Hz. In the Scandinavian grid a similar scheme is operated in the NORDEL system [12].

3.2.5 Reactive power

Reactive power is a concept associated with oscillating exchange of energy stored in capacitive and inductive components in a power system. Reactive power is produced in capacitive components (e.g. capacitors, cables) and consumed in inductive components (e.g. transformers, motors, fluorescent tubes). The synchronous generator is special in this context as it can either produce reactive power (the normal situation) when overmagnetised. Voltage control is effected by controlling the magnetising level results in high voltage and production of reactive power. As the current associated with the flow of reactive power is perpendicular to the current associated with active power and the voltage on the terminals of the equipment the only energy lost in the process is the resistive losses in lines and components. The losses are proportional to the total current squared. Since the active and reactive currents are perpendicular to each other, the total resulting current is the root of the squared sum of the two currents and the reactive currents hence contribute as much to the system losses as do the active currents. To minimise the losses it is necessary to keep the reactive currents as low as possible and this is accomplished by compensating reactive consumption by installing capacitors at or close to the consuming inductive loads. Furthermore, large reactive currents flowing to inductive loads is one of the major causes of voltage instability in the network due to

associated voltage drops in the transmission lines. Locally installed capacitor banks mitigates this tendency and increases the voltage stability in area. Many WT are equipped with induction generators. The induction generator is basically an induction motor, and as such a consumer of reactive power, in contrast to the synchronous generator which can produce reactive power. At no load, the consumption of reactive power is in the order of 35-40% of the rated active power increasing to around 60% at rated power. In any given local area with WT, the total reactive power demand will be the sum of the demand of the loads and the demand of WT. To minimise losses and to increase voltage stability, the WT are compensated to level between their no-load reactive demand and their full-load demand, depending on the requirements of the local utility or distribution company. Thus the power factor of WT, which is the ratio between active power and apparent power, is in general in the range above 0.96. For WT with PWM inverter systems the reactive power can be controlled by the inverter. Thus these WT can have a power factor of 1.00. But these inverter systems also give the possibility to control voltage by controlling the reactive power (generation or consumption of reactive power) [12].

Chapter 4

Model and Case Studies

Simulation tool used during the calculations and simulations of this thesis will first be mentioned in this chapter. A short description of investigated model and modelling will follow later. Different cases that have been investigated in this thesis will be mentioned.

4.1 Simulation tool used

Computer simulation is a very valuable tool in many different contexts. It makes it possible to investigate a multitude of properties in the design and construction phase as well as in the application phase. For wind turbines, the time and costs of development can be reduced considerably, and prototype wind turbines can be tested without exposing physical prototype wind turbines to the influence of destructive full-scale tests, for instance. Thus, computer simulations are a very cost-effective way to perform very thorough investigations before a prototype is exposed to real, full-scale, tests. Simulations and calculations presented in this thesis are done using Matlab® and Simulink®.

4.2 The GE® WTG

The WT model and parameters used in this thesis are based on [13], [14]. The WTG generator is unusual from a system simulation perspective. Physically the machine is a relatively conventional wound-rotor induction machine. The machine is of DFIG type and the AC excitation system is supplied through an solid-state voltage-source converter. The overall model structure is shown in Fig.4.1.

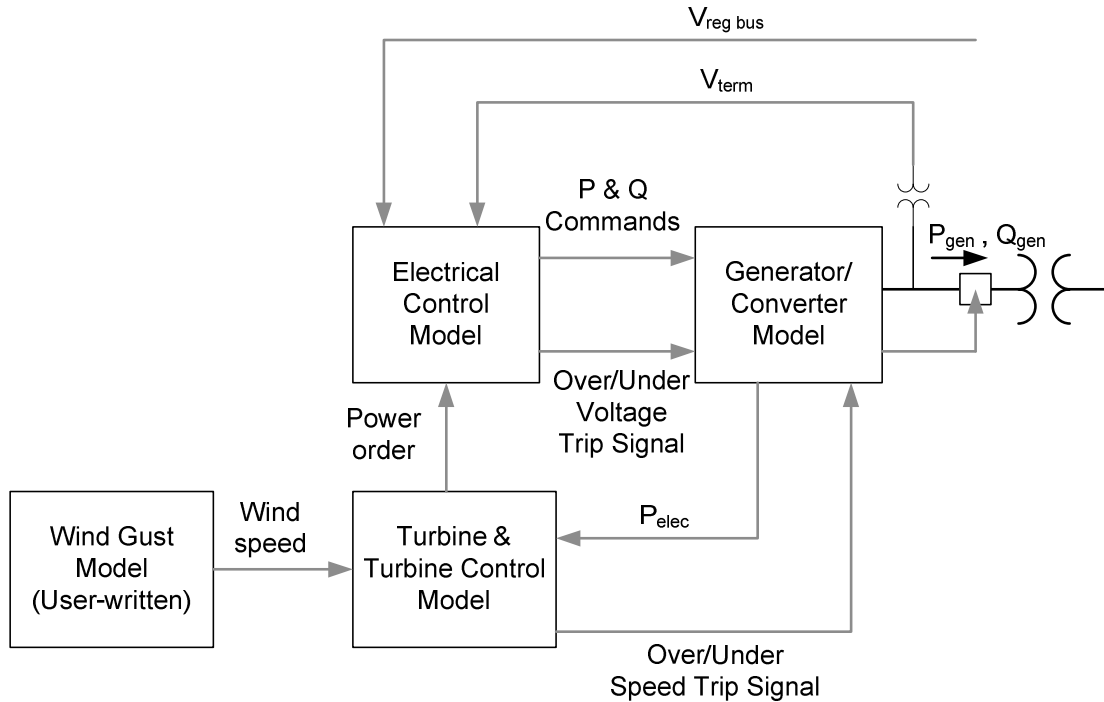


Fig.4.1 GE WTG Dynamic models and data connectivity from [13], [14]

- Generator/converter model : Interfaces with network and models several hardware related constraints.
- Electrical control model: Includes closed and open loop reactive power controls and provides for other system level features, e.g. governor function, for future applications.
- Turbine and turbine control model: Mechanical controls, including blade pitch control and power order to converter; over/under speed trips; rotor inertia equation; wind power as a function of wind speed, blade pitch, and rotor speed.
- Wind-gust model: This user written model can input input wind speed vs time sequences.

The wind turbine model provides a simplified representation of a very complex electromechanical system. The block diagram for the model is shown in Fig.4.2. In simple terms, the function of the wind turbine is to extract as much power from the available wind as possible without exceeding the rating of the equipment. The wind turbine model represents all of the relevant controls and mechanical dynamics of the wind turbine.

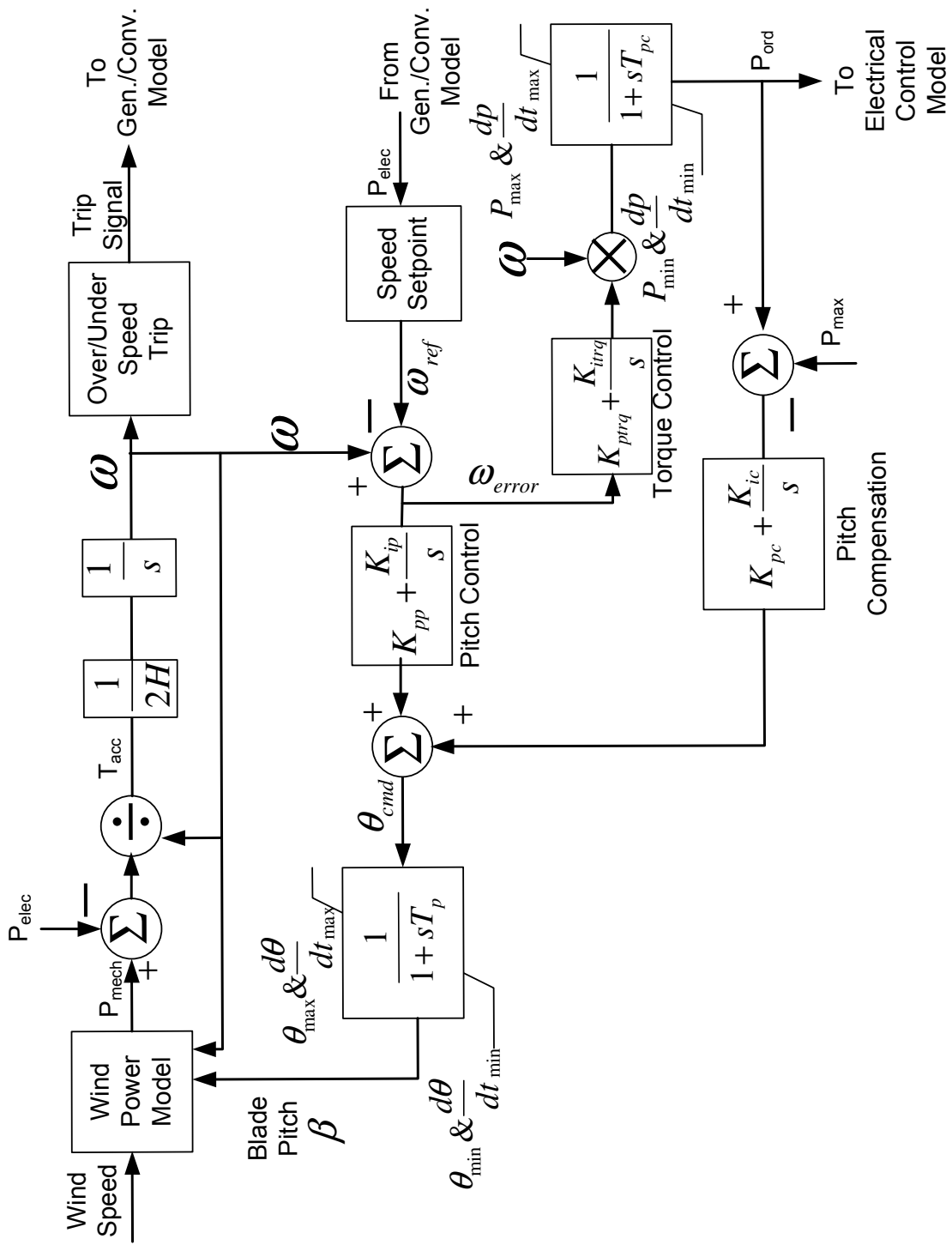


Fig.4.2 GE3.6 MW WT model block diagram [13], [14]

4.2.1 GE WTG charcateristic curves

All model parameters and calculations of GE ETG used for the investigations in this thesis have been presnted in Appendices. The following are some characteristic curves for GE 3.6 MW WTG.

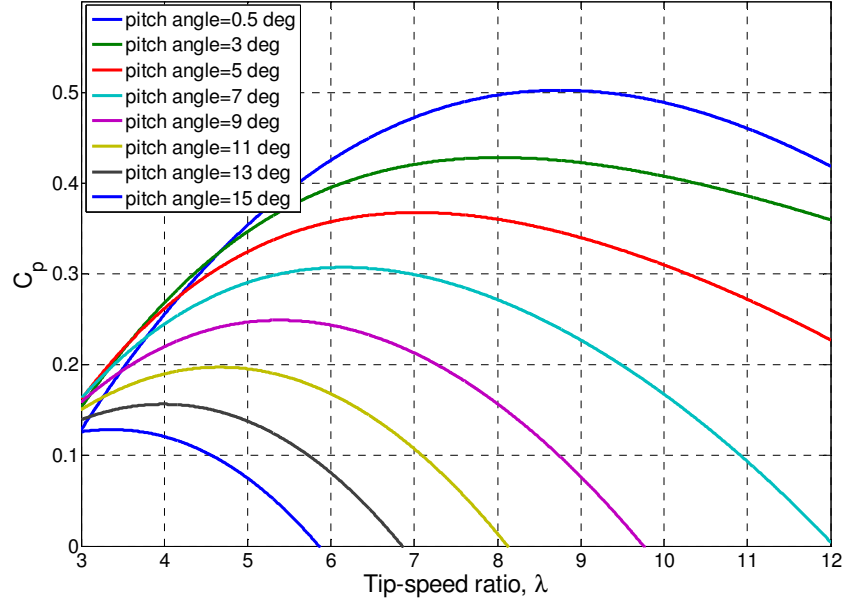


Fig.4.3 The C_p - λ curve (2D) of GE3.6 MW WT for different pitch angle (0.5^0 to 15^0)

The $C_p(\lambda, \beta)$ curves for the GE3.6 MW WT are shown in Fig.4.3. Curve fitting was performed to obtain the mathematical representation of the $C_p(\lambda, \beta)$ curves used in the model:

$$C_p(\beta, \lambda) = \sum_{i=0}^4 \sum_{j=0}^4 \alpha_{i,j} \beta^i \lambda^j$$

The coefficients $\alpha_{i,j}$ are given in Appendix. The curve fit is a good approximation for values of $2 < \lambda < 13$, values of λ outside this range represent very high and low wind speeds, respectively, that are outside the continuous rating of the machine.

From Fig.4.3 it is evident that, C_p has its optimal value of 0.5 when $\lambda_{opt} = 8.25$ and pitch angle is then its minimum position which is 0.5^0 . As pitch angle increases C_p decreases from its optimal value with new λ . A 3D representation of this $C_p(\lambda, \beta)$ characteristic curve is shown in Fig.4.4.

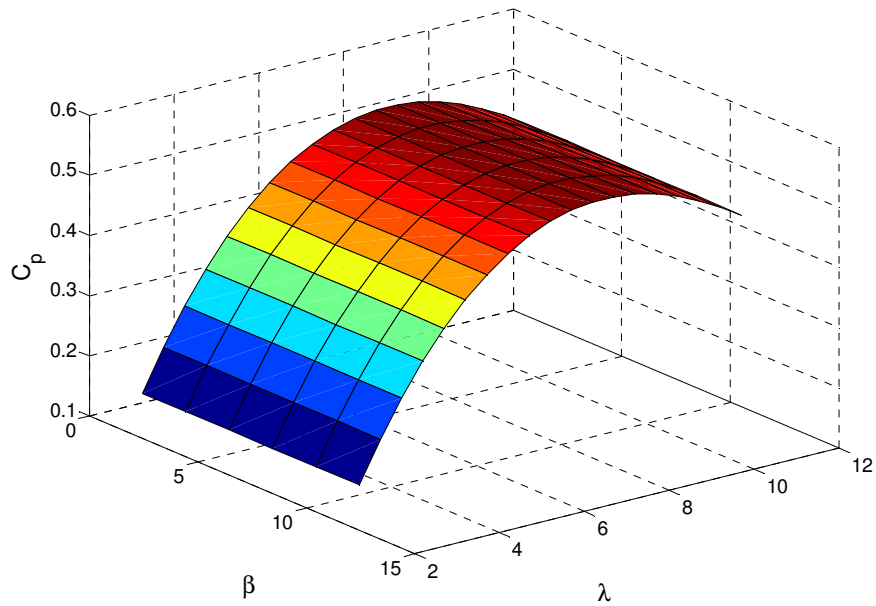


Fig.4.4 The C_p - λ curve (3D) of GE3.6 MW WT for different pitch angle

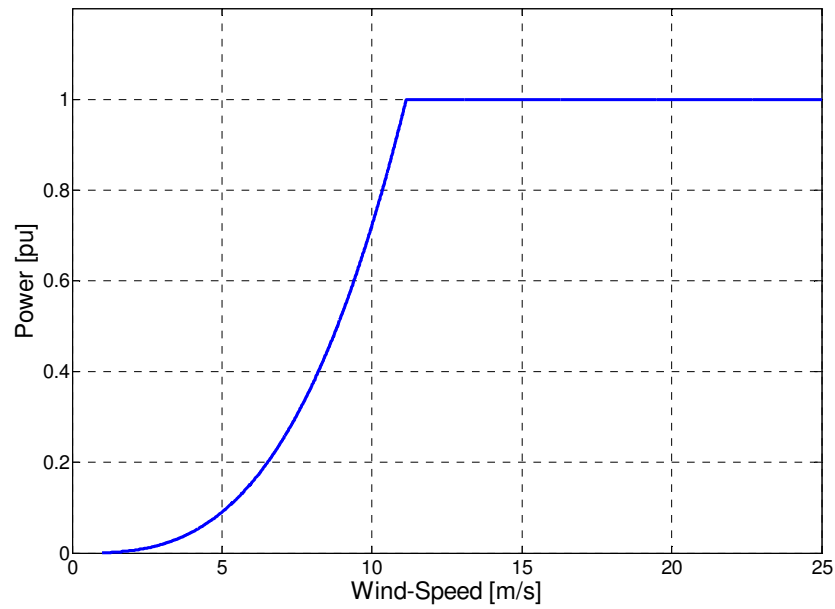


Fig.4.5 Power vs wind speed of GE3.6 MW WT

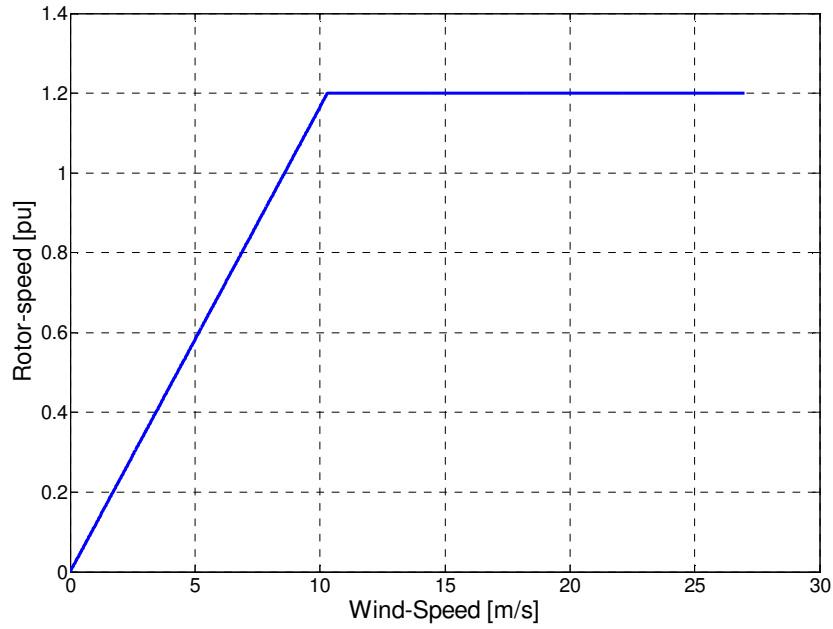


Fig.4.6 Rotor speed vs wind speed of GE3.6 MW WT

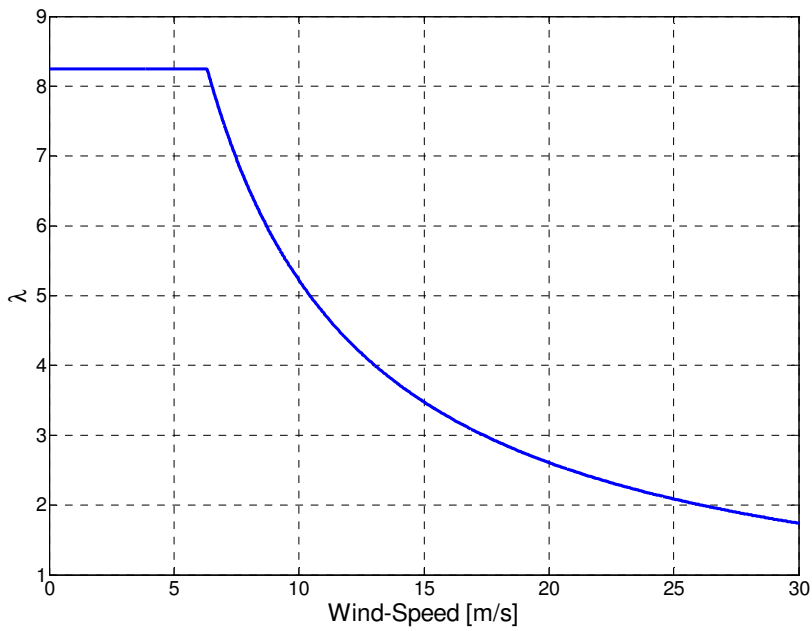


Fig.4.7 Tip-speed ratio vs wind speed of GE3.6 MW WT

Fig.4.5 shows the turbine output power vs wind speed of GE3.6 MW WT keeping pitch angle to its minimum position 0.5^0 (≈ 0). Turbine parameters are given in Appendix. It is clear from the Figure4.5 that, the turbine reaches its rated power when the wind speed is 11.2 m/sec. The cut-in wind speed for GE 3.6 MW WT is 3.5 m/sec and cut-off wind speed is 27 m/sec. The rotor reaches its rated value which is 1.2 pu, a slightly lower than the rated wind speed at which the turbine reaches its rated power, which is shown in Fig.4.6. In this connection, it is better to mention that GE 3.6 MW WT has its minimum rotor speed of 0.7 pu. Above the rated wind speed the pitch controller will be in action to keep the WT power at its rated value. Fig.4.7 is a representation of variation of tip-speed ratio from its optimal value which is 8.25 as the wind speed increases, of course the variation of tip-speed ratio as the wind speed increases, is in the decreasing mode is obvious from the basic equation relating rotor speed and wind speed with tip-speed ratio as $\lambda = \frac{\omega_{urb} R}{v_{wind}}$. As in GE 3.6 WT model rotor speed is presented in pu this equation is

something like $\lambda = K_b \frac{\omega_{urb}}{v_{wind}}$; $K_b = 69.5$, detail explanations can be found in the Appendix.

4.3 Case studies

The following cases have been studied:

- Simulation of GE model in low-wind speed region.
- Simulation of GE model for transition from low-to-high wind speed region.
- Simulation of GE model in high wind speed region.
- Grid fault simulation in both low and high wind speed region.
- Effect of C_p - λ variations in low and high wind speed region
 - Reducing C_p by 20% from optimal value
 - Shifting optimal lambda towards right by 1
 - Shifting optimal lambda towards left by 0.5

Chapter 5

Simulation Results

The whole operating range for a variable speed wind turbine may be considered into three different wind speed intervals. Below rated power, the objective is to get as much energy as possible, the turbine is then operating in the optimal power tracking mode and is referred to as ‘low-wind-speed’ region. This region usually starts from 4m/sec and ends around 9-10m/sec when the maximum rotor speed is reached but not the maximum rated power. In the ‘middle-wind-speed’ region the objective is to keep the rotor speed in a certain span, described as a speed band around the maximum rotor speed. Usually this interval starts at 9m/sec and ends when nominal generator power is reached (11-12m/sec) so in this region turbine also operate below rated power. In the ‘high-wind-speed’ region nominal generated power is reached and in this region pitch control adjust the aerodynamical power to be at or below rated. This interval is valid upto around 25m/sec where due to safety reason the turbine is disconnected and shut down.

5.1 GE® base Cases

[4] presents recommendations for dynamic modelling of the GE 1.5 and GE 3.6 WTG for use in studies related to the integration of GE wind turbines into power grids. However, in this work, GE 3.6 WTG model has been considered. All the values of the parameters of the GE3.6 MW wind turbine can be found in the Appendix. The following sections will show the simulation results which have been obtained mainly two types of disturbance namely, ‘wind-signal-step’ and ‘grid-fault’. As from the model implementation it is clear that, ‘rotor-speed error’ is the input to ‘pitch-controller’, so it is quiet interesting to see how the pitch controller reacts with the change in rotor speed not only ‘step’ disturbance but also when grid fault lasts for fractions of a second.

5.1.1 Simulation in the low-wind-speed region

These simulations have been carried-out in two ways.

- keeping 'pitch-angle controller' loop inactive and setting the fixed value of minimum pitch-angle, which is 0.5 degree.
- keeping 'pitch-angle controller' loop active.

A comparison between these two is also shown.

5.1.1.1 With pitch-angle controller loop inactive

The following simulation results have been found. Which may be referred to as the GE base case results when simulated in the low-wind speed region.

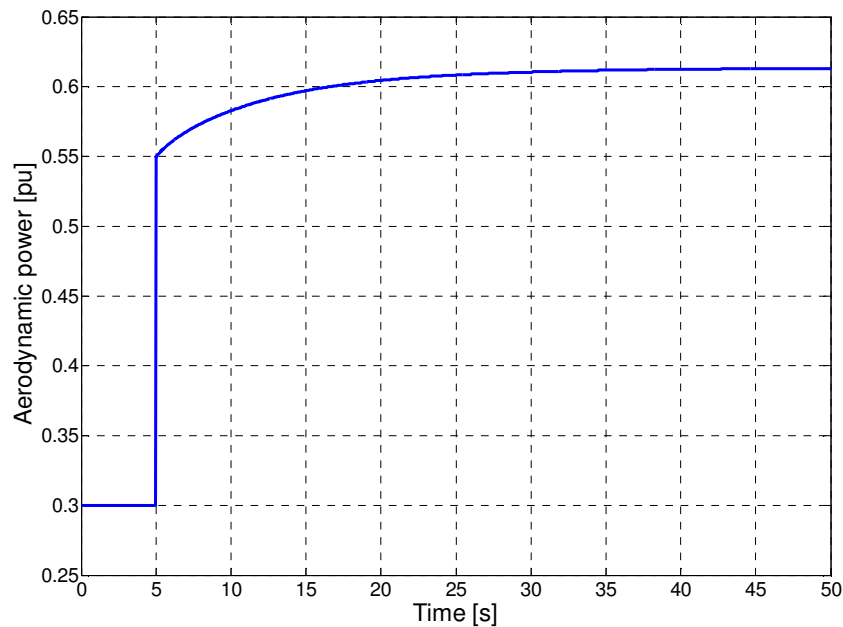


Fig.5.1 Aerodynamic power of GE3.6 MW WT when a wind-speed step is applied at 5 sec (from 7.5 m/s to 9.5 m/s)

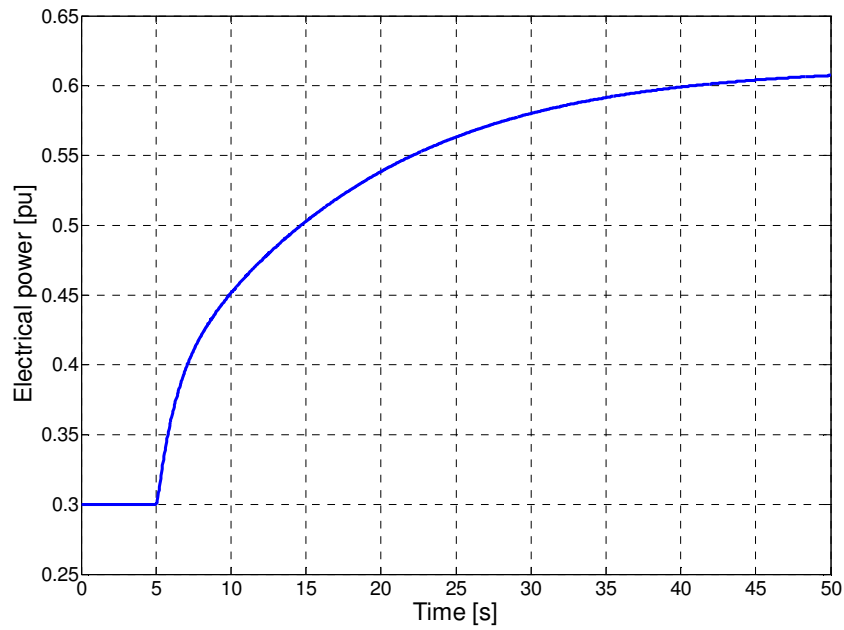


Fig.5.2 Electrical power of GE3.6 MW WT when a wind-speed step is applied at 5 sec (from 7.5 m/s to 9.5 m/s)

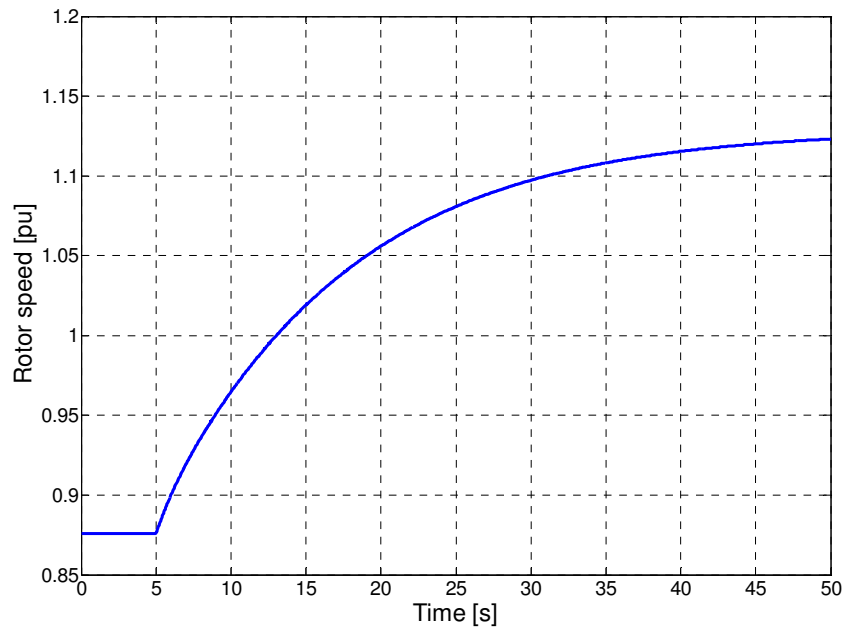


Fig.5.3 Rotor speed of GE3.6 MW WT when a wind-speed step is applied at 5 sec (from 7.5 m/s to 9.5 m/s)

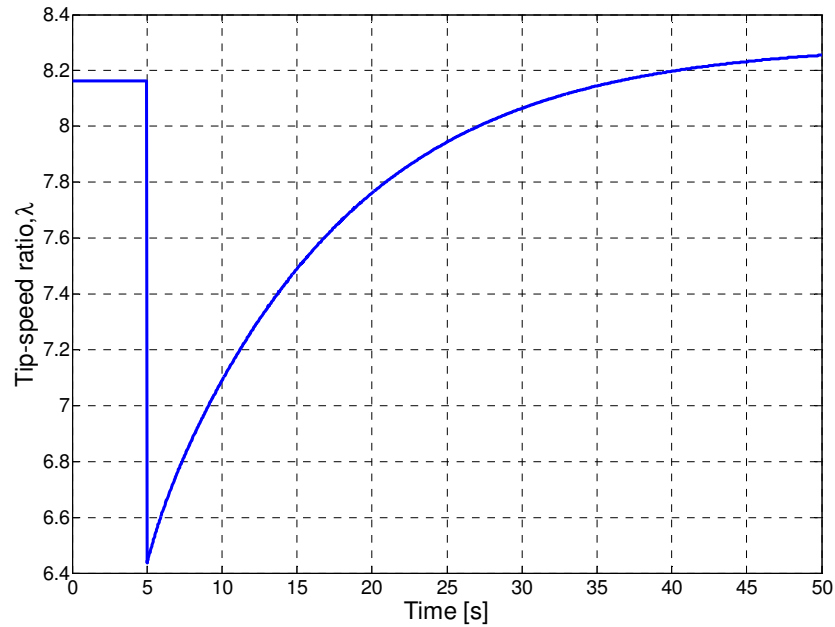


Fig.5.4 Tip-speed ratio (λ) of GE3.6 MW WT when a wind-speed step is applied at 5 sec (from 7.5 m/s to 9.5 m/s)

Fig.5.1 to Fig.5.4 shows the simulation results for low wind speed region when a wind speed step of 7.5 m/sec to 9.5 m/sec is applied at 5 sec. These simulations have been performed keeping pitch angle controller of the original model inactive and setting minimum pitch angle 0.5° artificially. In the following section, the results are combined when simulations done keeping pitch-angle controller active.

5.1.1.2 Comparison of simulations in low-wind speed region

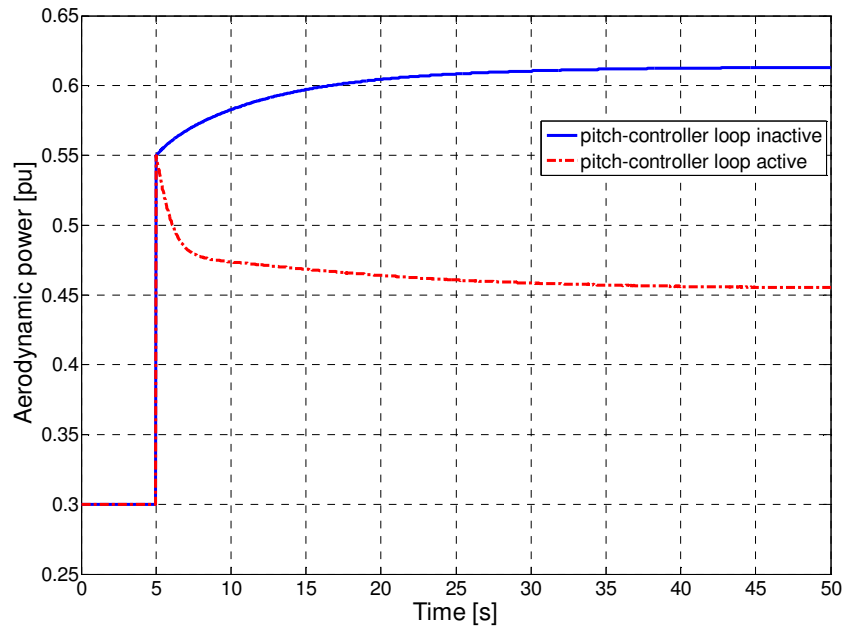


Fig.5.5 Comparison of Aerodynamic power of GE3.6 MW WT without and with pitch-controller loop active (when a wind-speed step is applied at 5 sec from 7.5 m/s to 9.5 m/s)

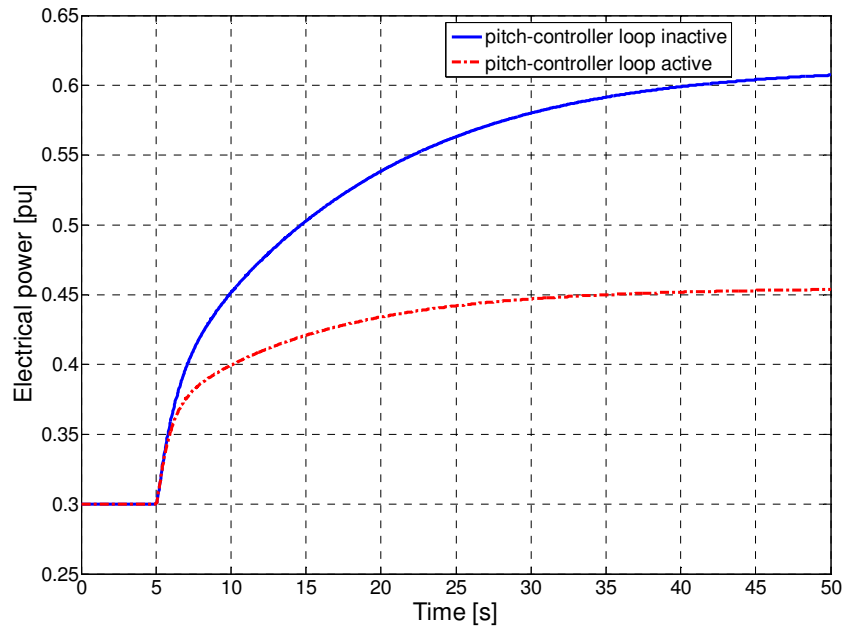


Fig.5.6 Comparison of Electrical power of GE3.6 MW WT without and with pitch-controller loop active (when a wind-speed step is applied at 5 sec from 7.5 m/s to 9.5 m/s)

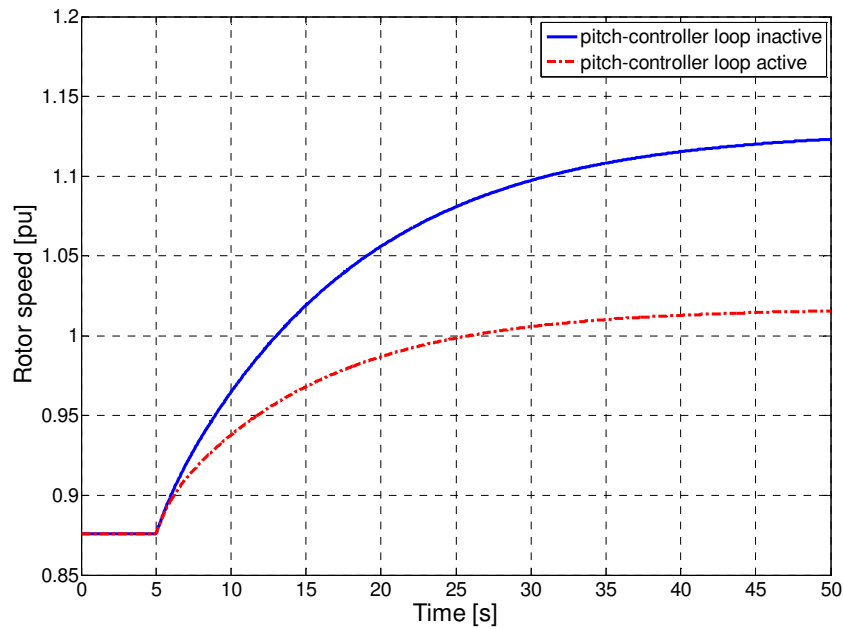


Fig.5.7 Comparison of Rotor speed of GE3.6 MW WT without and with pitch-controller loop active (when a wind-speed step is applied at 5 sec from 7.5 m/s to 9.5 m/s)

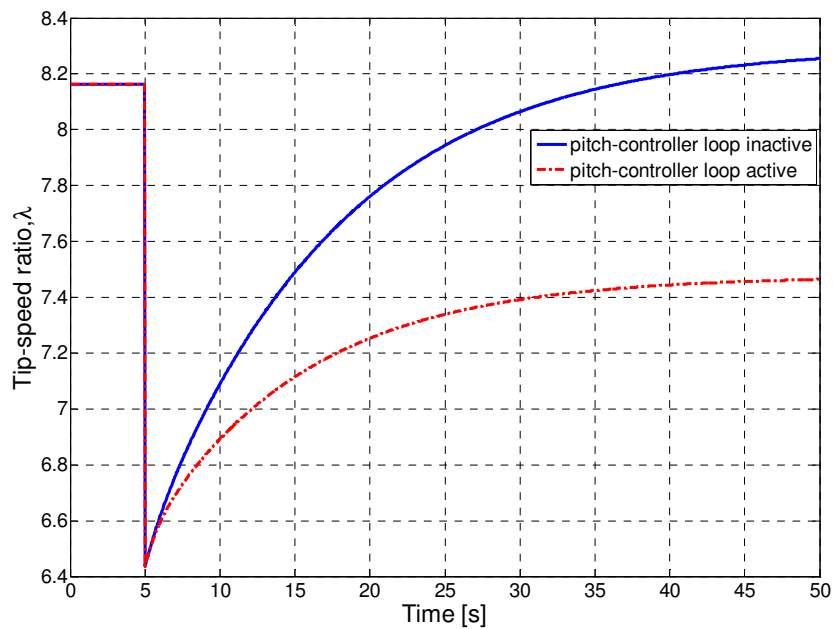


Fig.5.8 Comparison of Tip-speed ratio of GE3.6 MW WT without and with pitch-controller loop active (when a wind-speed step is applied at 5 sec from 7.5 m/s to 9.5 m/s)

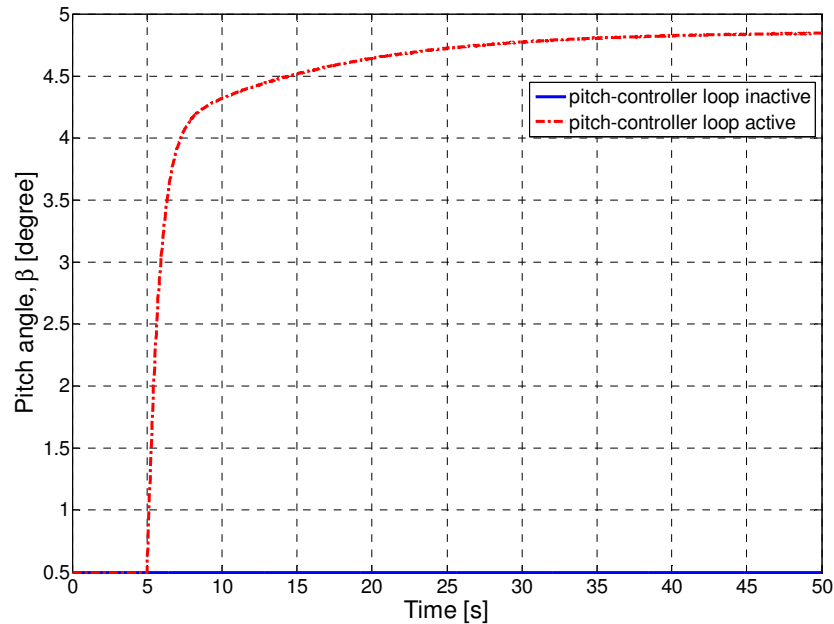


Fig.5.9 Comparison of Pitch-angle of GE3.6 MW WT without and with pitch-controller loop active (when a wind-speed step is applied at 5 sec from 7.5 m/s to 9.5 m/s)

Fig.5.5 to Fig.5.9, that is comparison when pitch-angle controller is active as of original model. The main distinctive feature is that, even simulating in low-wind speed region by applying a step at $t=5$ sec from 7.5 m/sec to 9.5 m/sec the pitch-angle is going to change when pitch-angle loop is active, but this should not be in the case of low-wind speed region. It is clear from Fig.5.9 where pitch angle settles close to 5 degree! Also Fig.5.5 tells us, different steady state values of aerodynamic power, and a sharp peak when pitch-angle loop is active. Different steady-state values for electrical power, rotor-speed and tip-speed ratio has also been observed from Fig.5.6 to Fig.5.8 as well when the pitch-angle controller loop is active.

5.1.2 Simulation for transition from low-to-high wind speed region

Now 'pitch-angle controller' loop is active and the following simulation results are obtained, when a step in wind speed is applied at 5 sec from 10.35 m/sec to 12.35 m/sec.

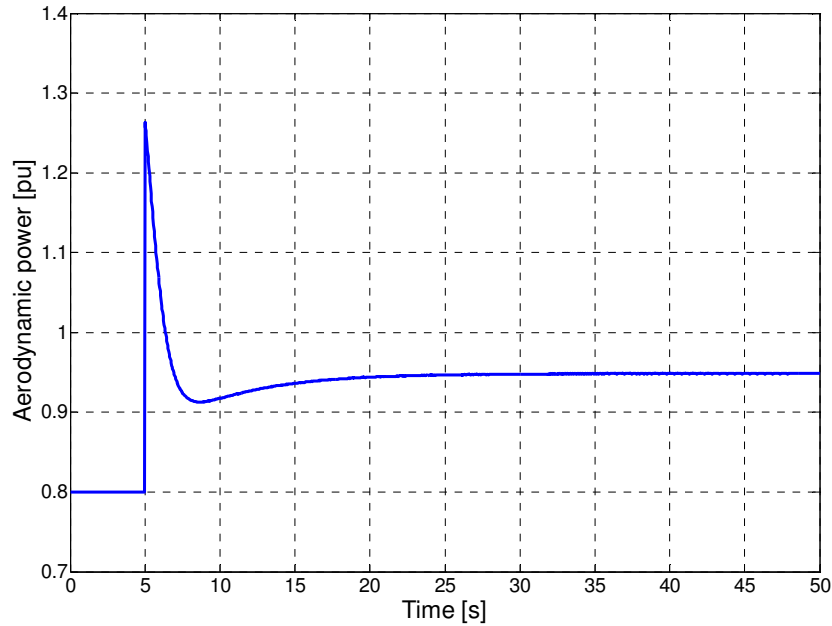


Fig.5.10 Aerodynamic power of GE3.6 MW WT when a wind-speed step is applied at 5 sec (from 10.35 m/s to 12.35 m/s)

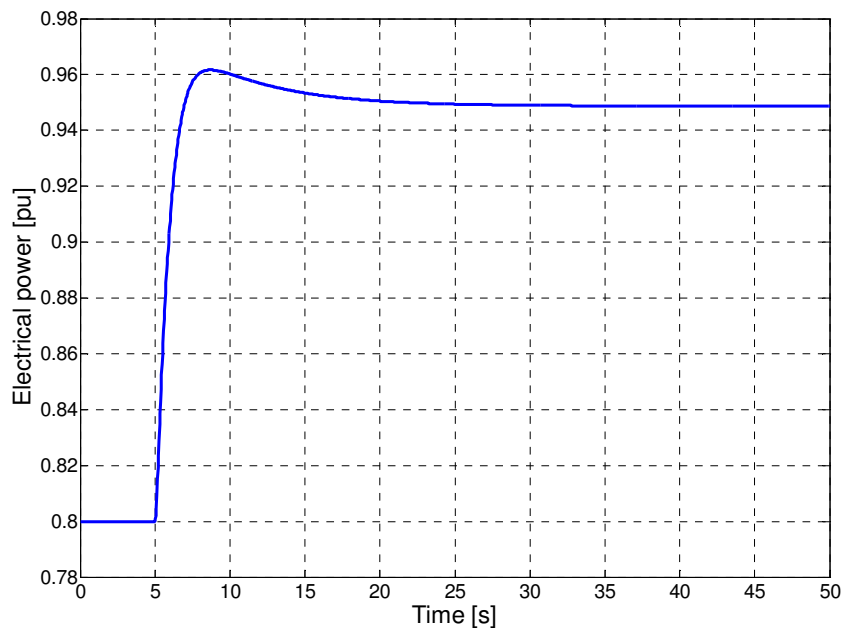


Fig.5.11 Electrical power power of GE3.6 MW WT when a wind-speed step is applied at 5 sec (from 10.35 m/s to 12.35 m/s)

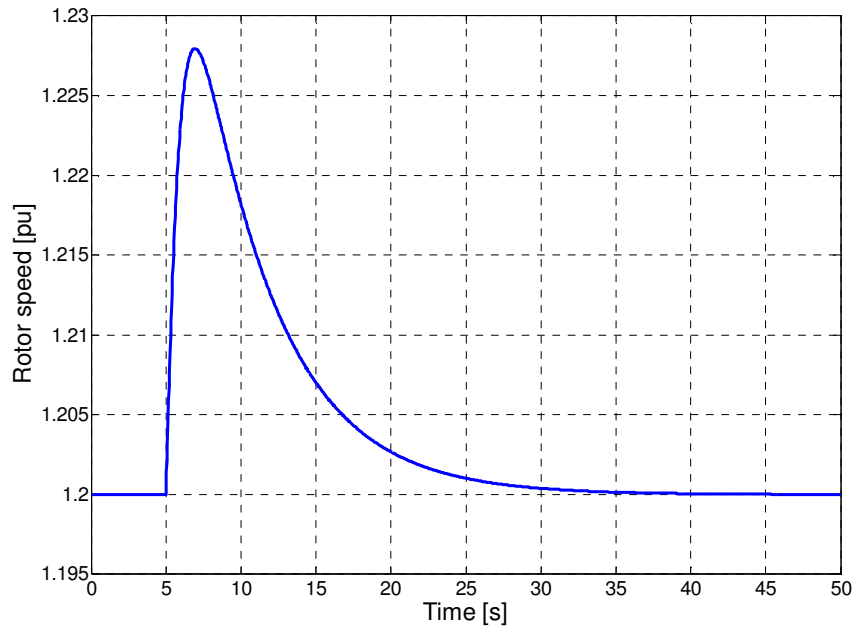


Fig.5.12 Rotor speed of GE3.6 MW WT when a wind-speed step is applied at 5 sec (from 10.35 m/s to 12.35 m/s)

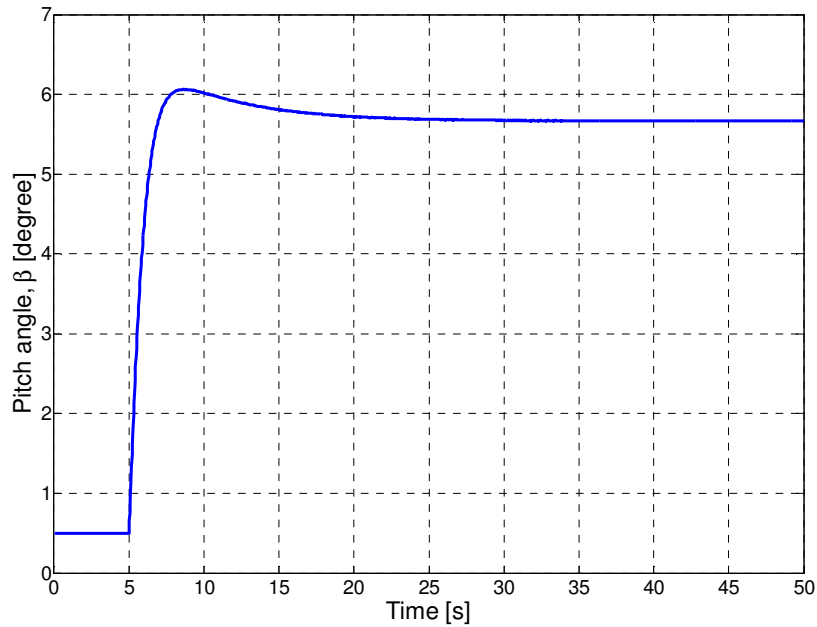


Fig.5.13 Pitch-angle (β) of GE3.6 MW WT when a wind-speed step is applied at 5 sec (from 10.35 m/s to 12.35 m/s)

From Fig.5.10 the aerodynamic power have a sharp peak to 1.25 pu before reaches to steady-state. But from Fig.5.11 electrical power has smooth variations with step as it should be for power system requirements. Fig.5.12 shows that rotor speed has long settling time when transition from low-to-high wind speed region. Pitch-variation while transition from low-to-high wind speed region is shown in Fig.5.13, varies from 0.5 degree to 5.7 degree to limit the power.

5.1.3 Simulation in the high-wind-speed region

The following simulation results are obtained.

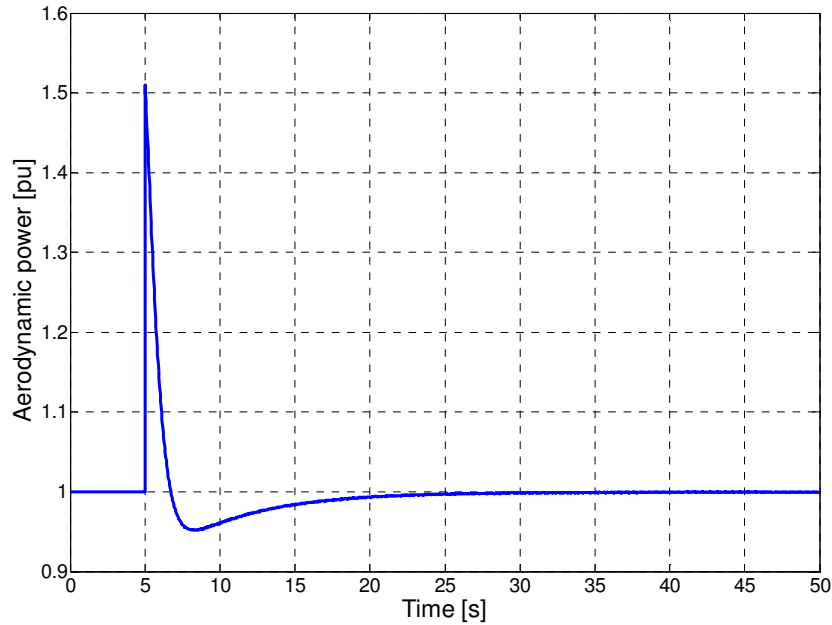


Fig.5.14 Aerodynamic power of GE3.6 MW WT when a wind-speed step is applied at 5 sec (from 12 m/s to 14 m/s)

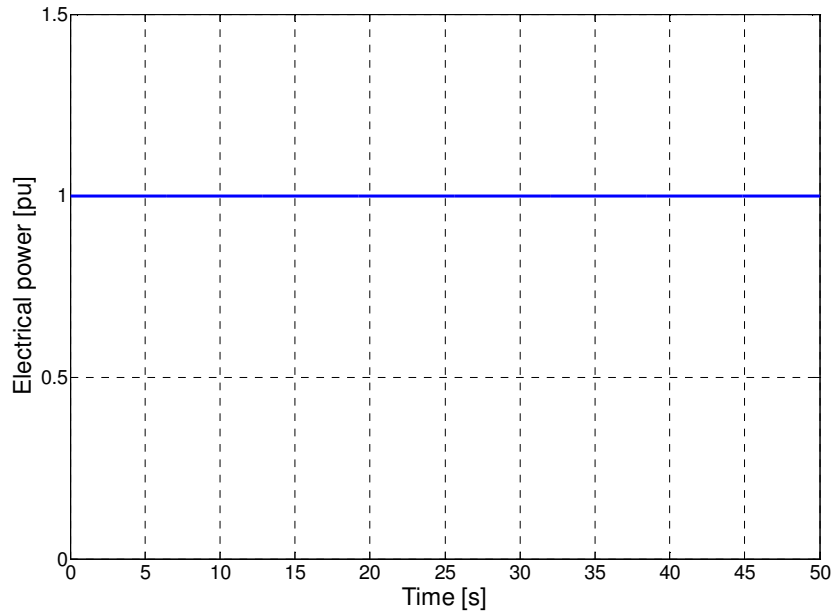


Fig.5.15 Electrical power of GE3.6 MW WT when a wind-speed step is applied at 5 sec (from 12 m/s to 14 m/s)

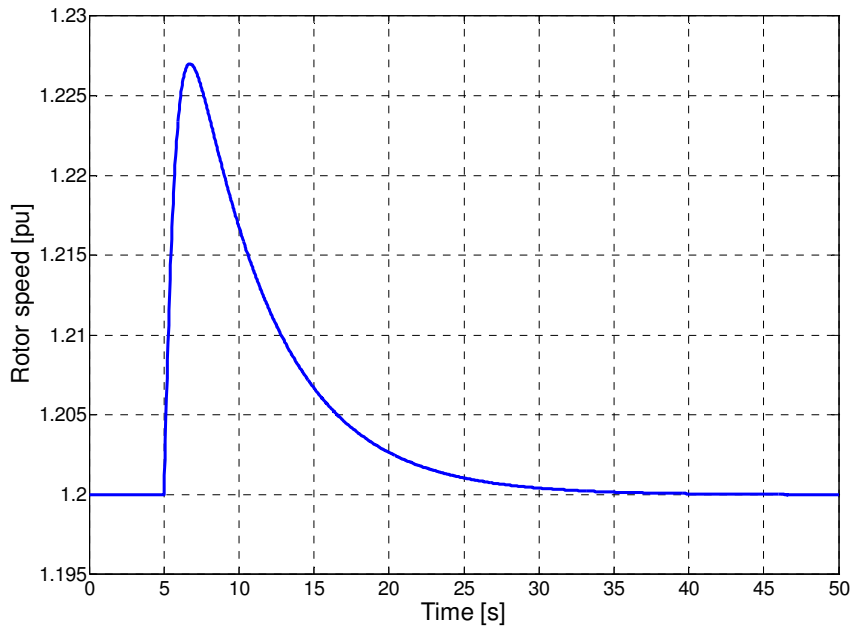


Fig.5.16 Rotor speed of GE3.6 MW WT when a wind-speed step is applied at 5 sec (from 12 m/s to 14 m/s)

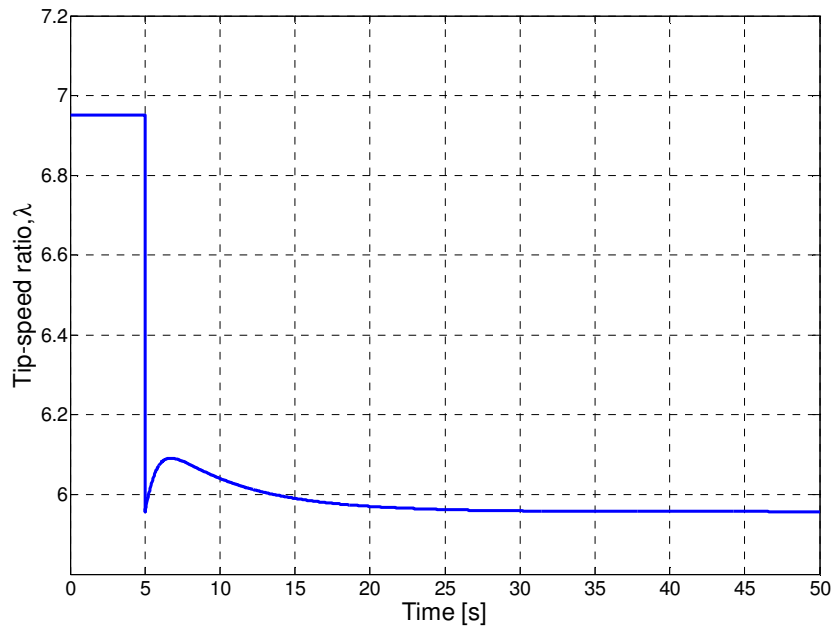


Fig.5.17 Tip-speed ratio (λ) of GE3.6 MW WT when a wind-speed step is applied at 5 sec (from 12 m/s to 14 m/s)

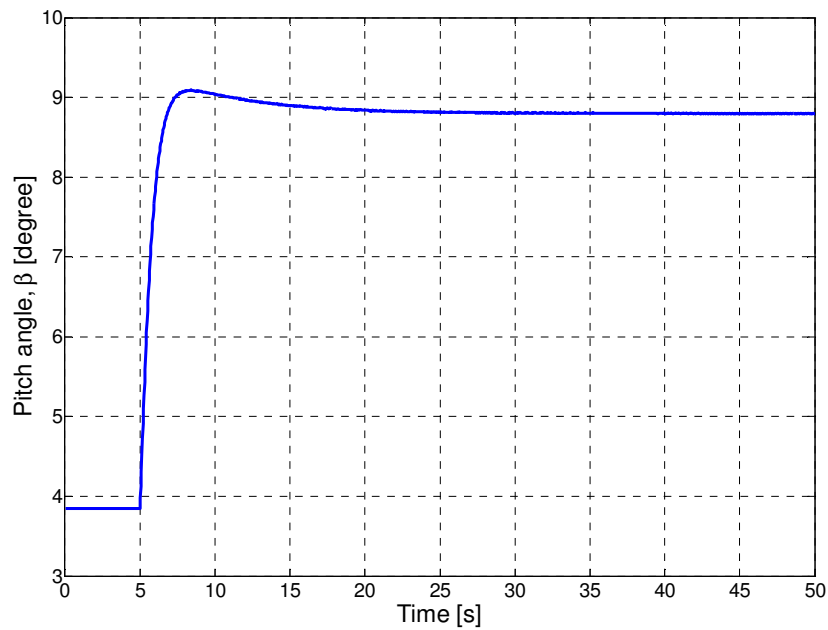


Fig.5.18 Pitch-angle (β) of GE3.6 MW WT when a wind-speed step is applied at 5 sec (from 12 m/s to 14 m/s)

Fig.5.14 shows that aerodynamic power needs more time to settle down in this high wind speed region simulation. Fig.5.15 shows electrical power as step changes, which is 1 pu. Fig.5.16 shows that rotor speed requires long time to settle as step changes. Fig.5.17 shows that tip-speed ratio has an overshoot as step changes before settling. Pitch variation in the high wind-speed region is quiet smooth as from Fig.5.18.

5.1.3 Grid-fault simulation in the low-wind-speed region

Here, grid fault occurred at $t = 5$ sec and lasts for 0.5 sec. The simulation results are obtained for the following two cases.

5.1.3.1 Pitch-angle controller loop inactive

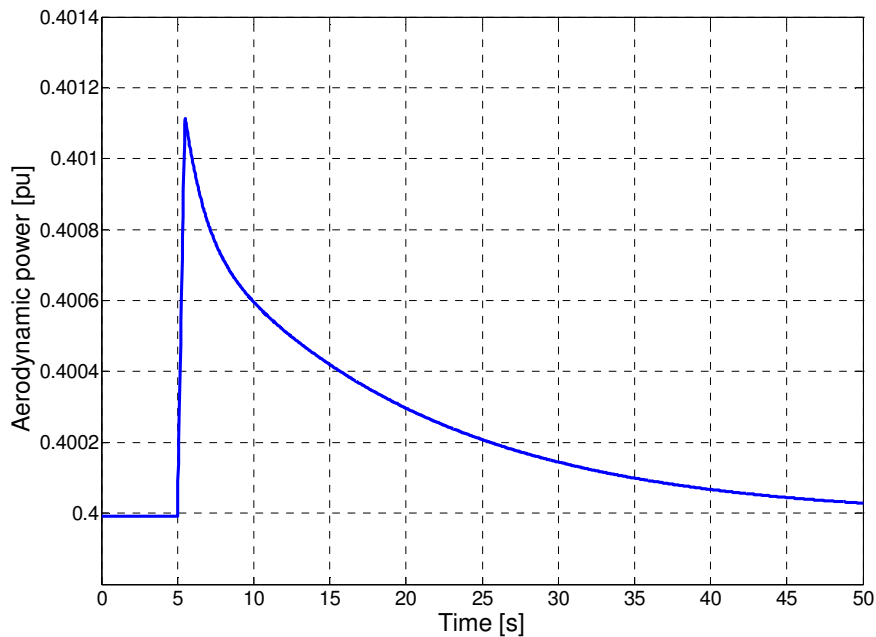


Fig.5.19 Aerodynamic power when grid-fault occurred at $t=5$ sec and lasts for 500 ms with pitch-angle loop inactive

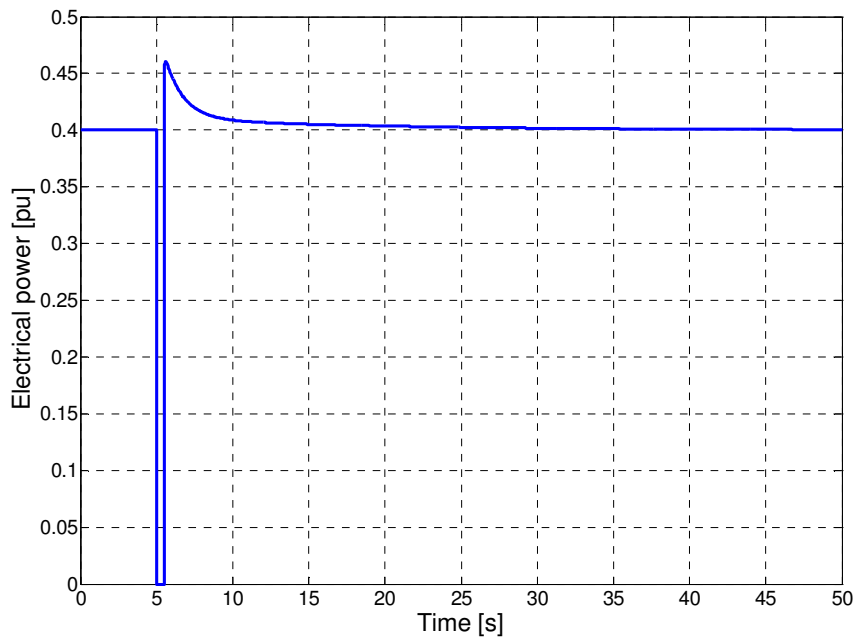


Fig.5.20 Electrical power when grid-fault occurred at $t=5$ sec and lasts for 500 ms with pitch-angle loop inactive

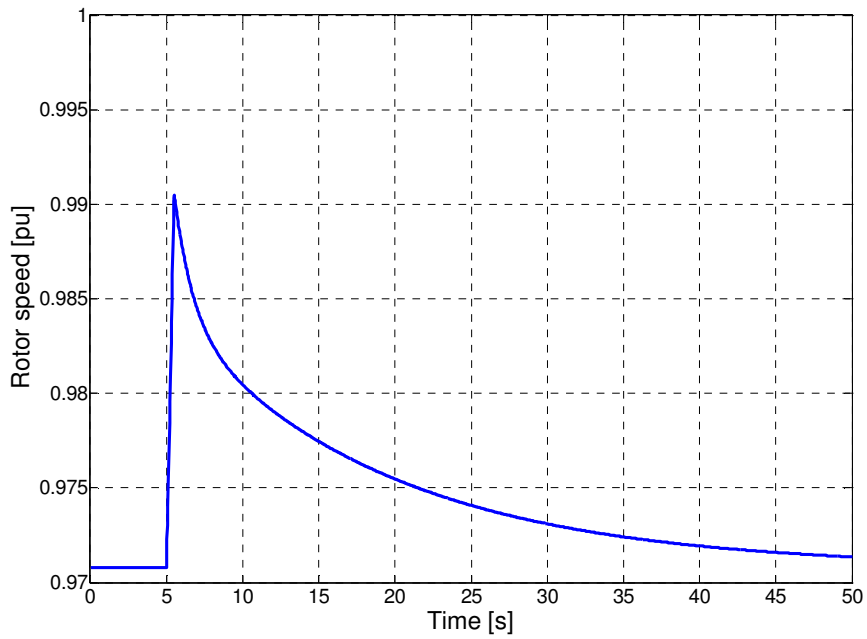


Fig.5.21 Rotor speed when grid-fault occurred at $t=5$ sec and lasts for 500 ms with pitch-angle loop inactive

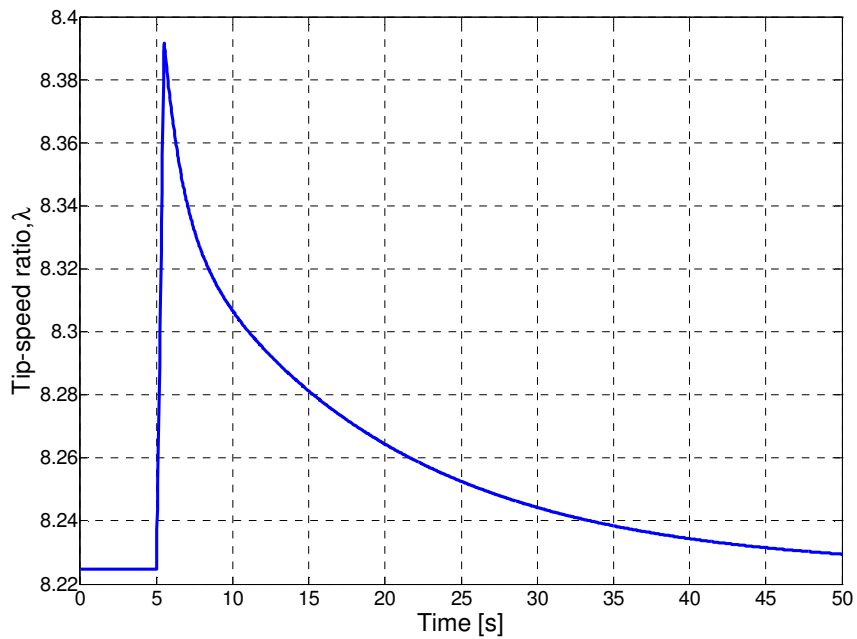


Fig.5.22 Tip-speed ratio (λ) when grid-fault occurred at t=5 sec and lasts for 500 ms with pitch-angle loop inactive

5.1.3.1 Pitch-angle controller loop active

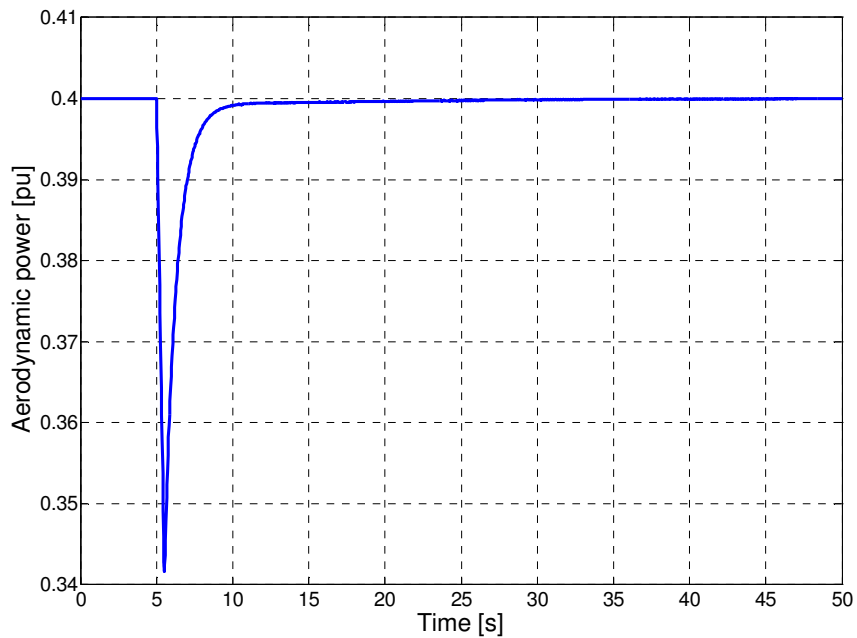


Fig.5.23 Aerodynamic power when grid-fault occurred at t=5 sec and lasts for 500 ms with pitch-angle loop active

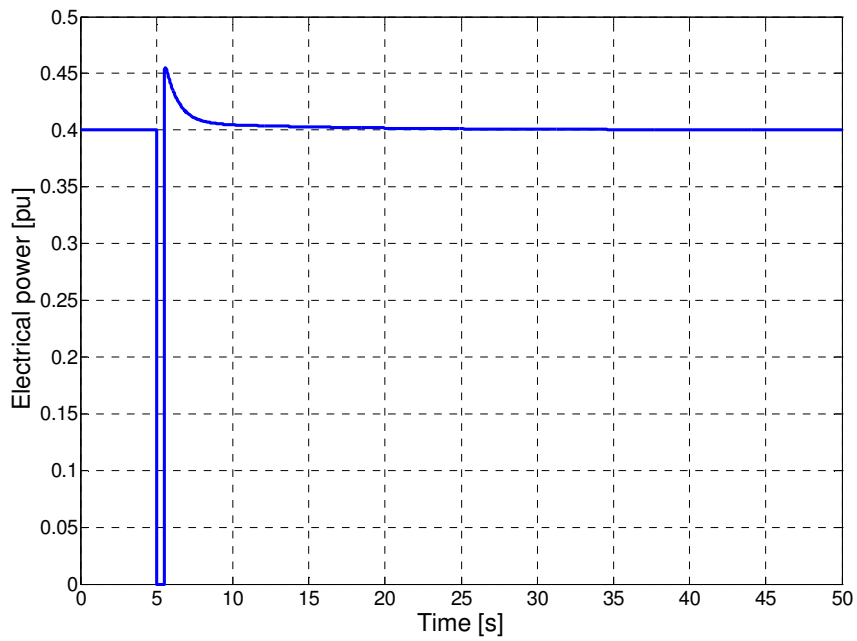


Fig.5.24 Electrical power when grid-fault occurred at t=5 sec and lasts for 500 ms with pitch-angle loop active

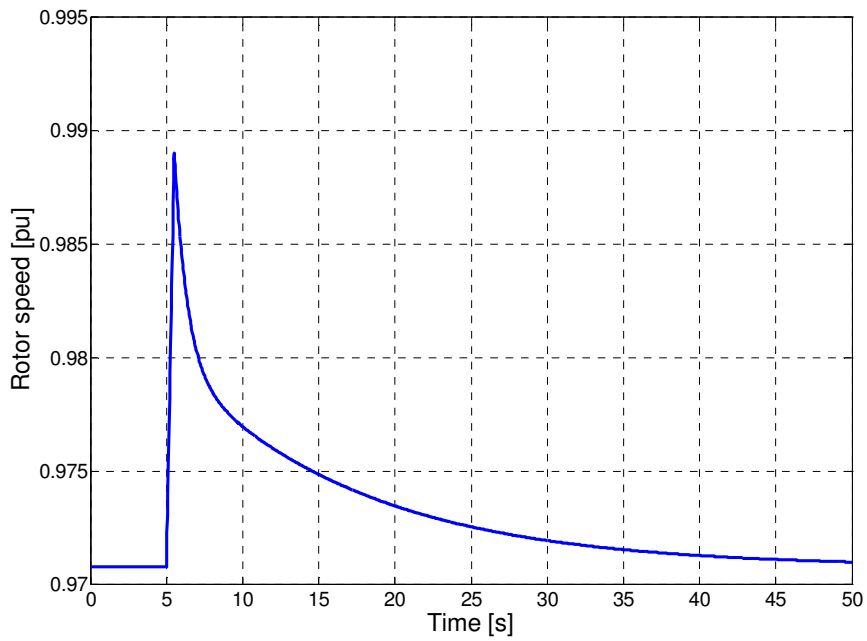


Fig.5.25 Rotor speed when grid-fault occurred at t=5 sec and lasts for 500 ms with pitch-angle loop active

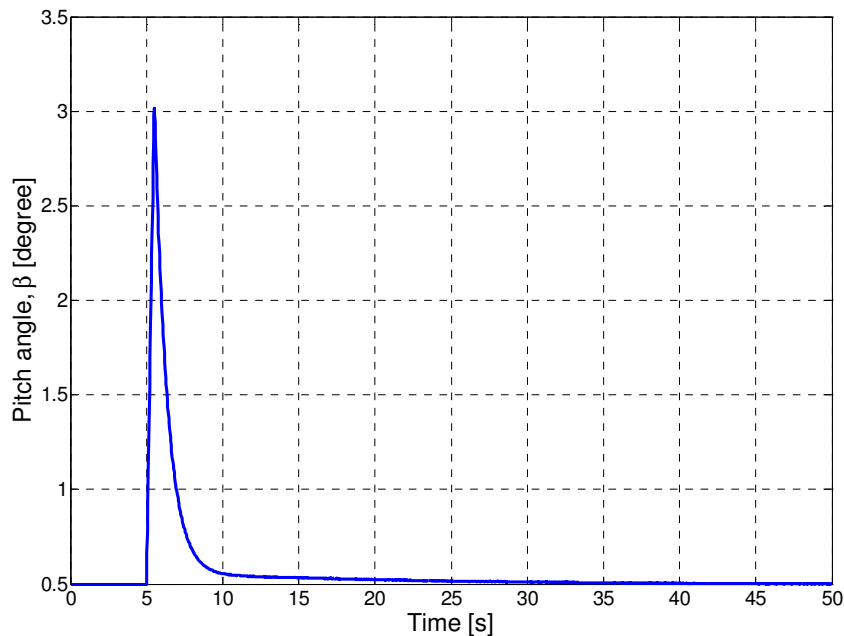


Fig.5.26 Pitch-angle (β) when grid-fault occurred at $t=5$ sec and lasts for 500 ms with pitch-angle loop active

Grid-fault simulations have been performed in low-wind-speed region with pitch-angle controller inactive and with pitch-angle controller active in the previous two sections. The results are obvious as per conclusions drawn from simulation in the low wind speed region. Only distinctive feature here in between Fig.5.19 and Fig.5.23 of aerodynamic power. If pitch-angle controller is not active for grid fault simulation there will be an overshoot in aerodynamic power. So pitch-angle controller should be active as normal case while simulating grid fault in low wind-speed region. The pitch-angle variations (Fig.5.26) in this case are due to the fact that, rotor-speed error. In model, two controllers' (torque controller and pitch-controller) input is rotor-speed error.

5.1.4 Grid-fault simulation in the high-wind-speed region

Here, grid fault occurred at $t = 5$ sec and lasts for 0.5 sec. The simulation results are obtained as follows.

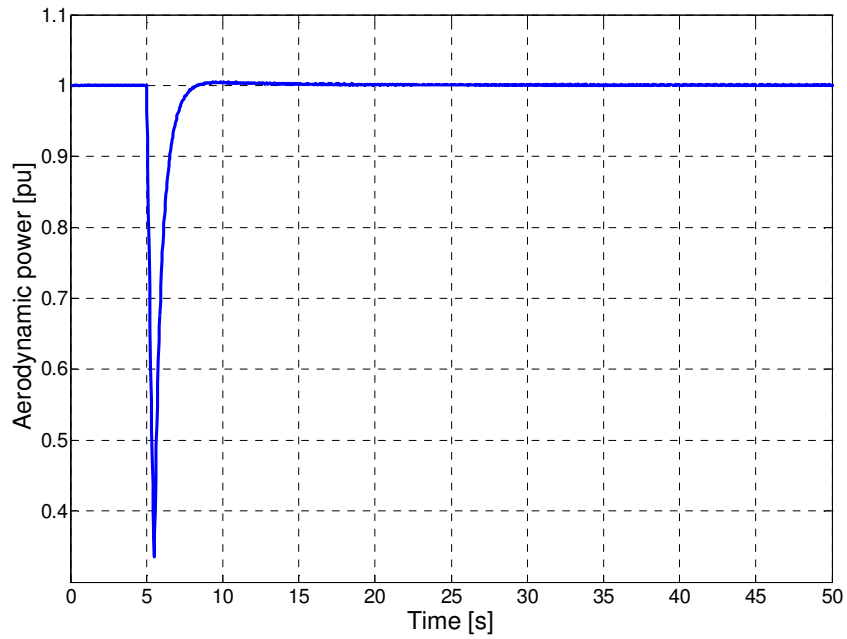


Fig.5.27 Aerodynamic power when grid-fault occurred at t=5 sec and lasts for 500 ms

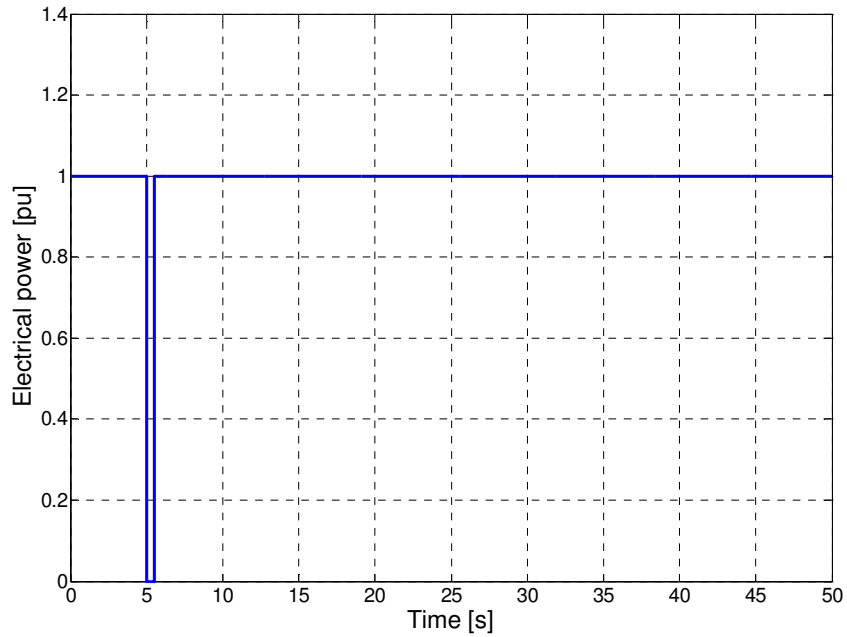


Fig.5.28 Electrical power when grid-fault occurred at t=5 sec and lasts for 500 ms

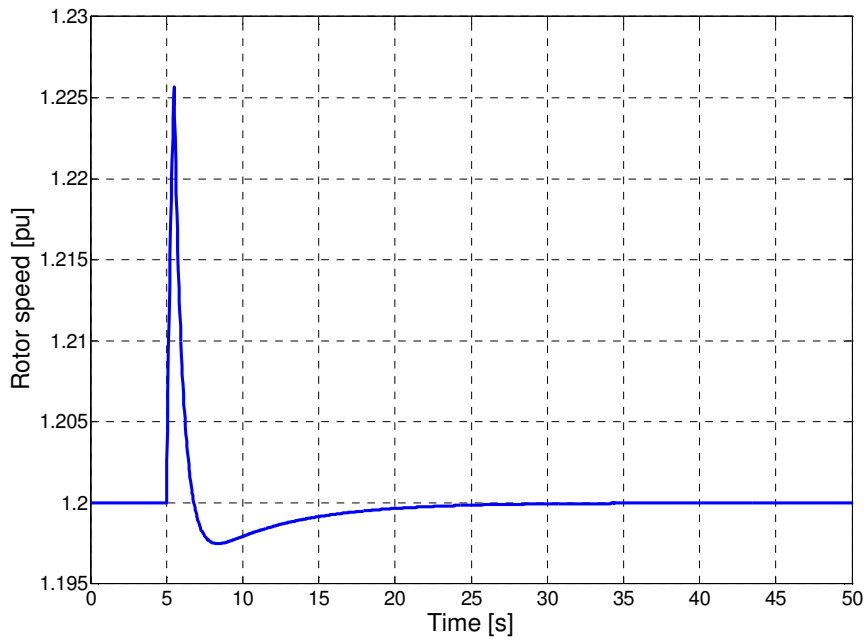


Fig.5.29 Rotor speed when grid-fault occurred at t=5 sec and lasts for 500 ms

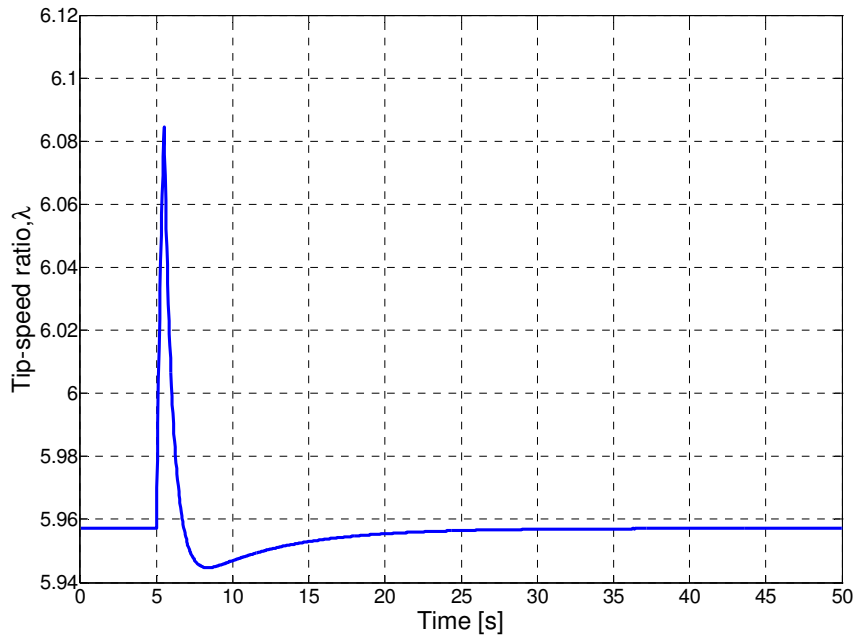


Fig.5.30 Tip-speed ratio (λ) when grid-fault occurred at t=5 sec and lasts for 500 ms

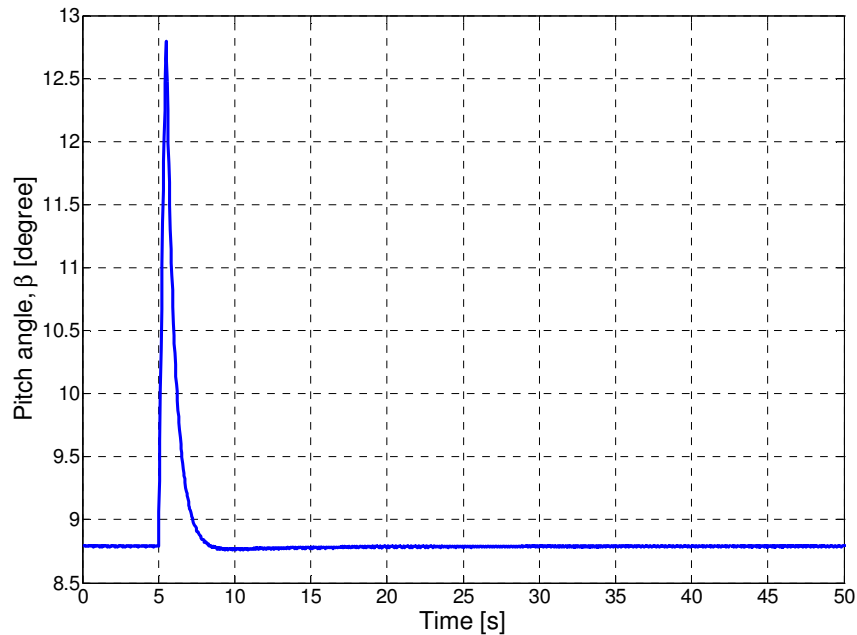


Fig.5.31 Pitch-angle (β) when grid-fault occurred at $t=5$ sec and lasts for 500 ms

Fig.5.27 to Fig.5.31 shows the grid-fault simulations in the high-wind speed region. The results are quiet normal except the noticeable things are from Fig.5.29 and Fig.5.30 where both rotor-speed and tip-speed ratio has overshoot before settling.

5.1.5 Grid-fault severity

Simulations shown here for grid-fault severity in low-wind speed region (Fig.5.32 & Fig.5.33) and high-wind speed region (Fig.5.34 & Fig.5.35). Fig.5.32 and Fig.5.33 shows the variations of rotor speed (max) and pitch-angle (max) respectively as the remaining grid-voltage increases (low-wind speed region). The worst case is when grid-voltage is equal to zero and at this time the maximum rotor speed is about 0.9885 and the maximum pitch-angle is 3 degree. Fig.5.34 and Fig.5.35 shows the variations of rotor speed (max) and pitch-angle (max) respectively as the remaining grid-voltage increases (high-wind

speed region). The worst case is when grid-voltage is equal to zero and at this time the maximum rotor speed is 1.226 and the maximum pitch-angle is about 12.55 degree.

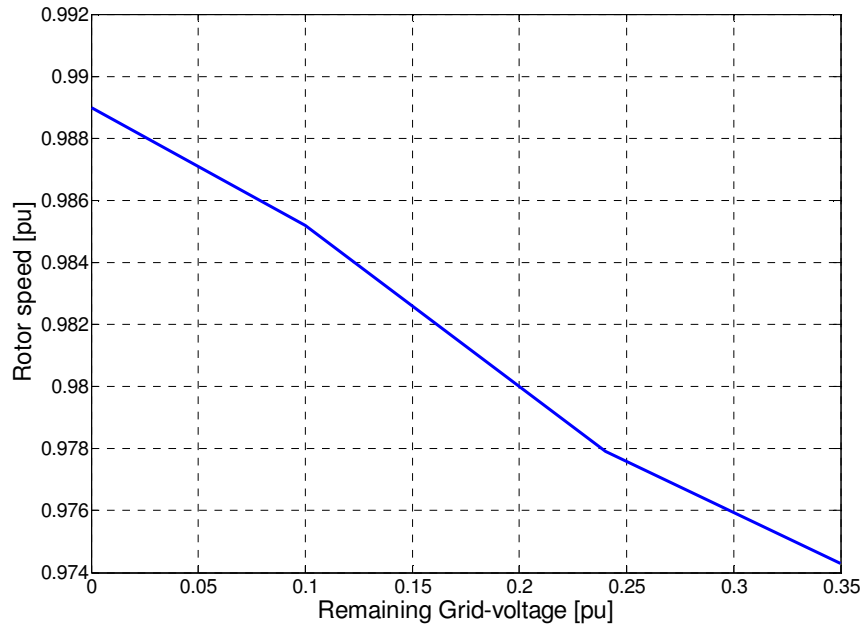


Fig.32 Grid-fault severity in low-wind speed region of GE 3.6 MW WT (Max. rotor speed vs remaining grid-voltage)

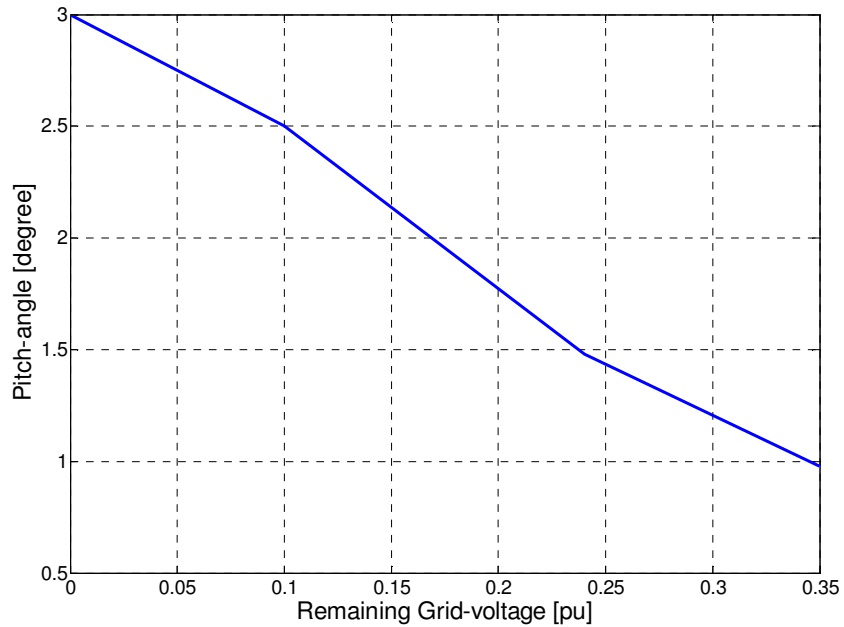


Fig.33 Grid-fault severity in low-wind speed region of GE 3.6 MW WT (Max. pitch angle vs remaining grid-voltage)

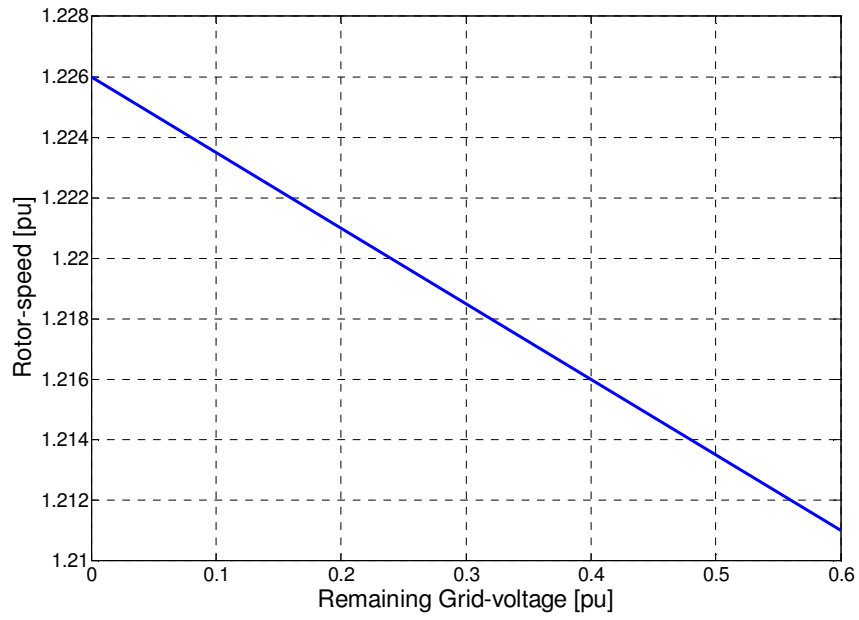


Fig.34 Grid-fault severity in high-wind speed region of GE 3.6 MW WT (Max. rotor speed vs remaining grid-voltage)

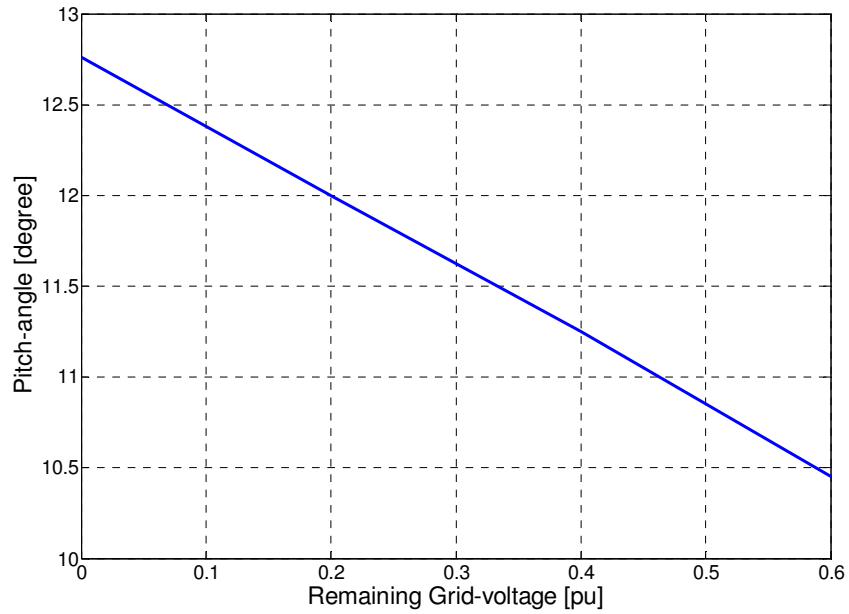


Fig.35 Grid-fault severity in high-wind speed region of GE 3.6 MW WT (Max. pitch-angle vs remaining grid-voltage)

5.2 Effect of $C_p(\lambda)$

The variable-speed wind turbines are commonly pitch controlled for better power output optimization. The most commonly used parameter describing the relative rotor speed is $\frac{\text{Tip speed}}{\text{Wind speed}} = \lambda$ (Tip - speed ratio). The aerodynamic efficiency $C_p(\lambda, \beta)$ is a function of the tip-speed ratio and the pitch angle, β . Given a pitch angle, the power efficiency coefficient, C_p has a maximum for a certain tip-speed ratio, λ . The $C_p(\lambda, \beta)$ characteristic is highly non-linear and depends on the rotor geometry for a particular wind turbine. It is thus obvious $C_p(\lambda, \beta)$ characteristic curve vary from manufacturer to manufacturer for their designed wind turbine. C_p has its optimal value as defined by Beltz's limit and λ has its optimal value not varying to a great extent for different wind turbines of the same type (e.g. pitch-controlled variable-speed wind turbine of DFIG type). Thus in order to check the functionality of a base model to be able to use it for other power system studies the investigation parameters are C_p and λ . As $C_p(\lambda, \beta)$ curve can vary from manufacturer to manufacturer, so the effect of wind turbine parameter $C_p(\lambda, \beta)$ is varied from a base case value and the calculations presented earlier are repeated to be able to generalize the findings for other turbines. The following three cases have been considered so far.

Case: 1 Reducing the maximum value of the $C_p(\lambda)$ curve

Case: 2 Shifting the $C_p(\lambda)$ curve rightward in the λ -axis

Case: 3 Shifting the $C_p(\lambda)$ curve leftward in the λ -axis

The reference speed (ω_{ref}) - measured electrical power (P_{ef}) relationship for maximum power tracking can also be expressed as [2].

$$P_{ef} = \left(\frac{1}{2} \frac{\rho A_r}{S_n} C_{p,\max} \left(\frac{\omega_0 R}{\lambda_{opt}} \right)^3 \right) \omega_{ref}^3$$

$$= K_{tub} \omega_{ref}^3$$

where

ρ = The air density, kg / m^3

A_r = The rotor swept area, m^2

$C_{p,\max}$ = The maximum value of the $C_p(\lambda)$ curve at $\beta \approx 0^\circ$

λ_{opt} = The optimal value of λ for which the value of C_p is maximum

S_n = The WT rating in MW

ω_0 = The rotor base speed, rad / sec

R = The rotor radius, m

P_{ef} = The measured electrical power, pu

ω_{ref} = The reference speed for for maximum power tracking, pu

[NB : See the appendix for the values of these parameters for the GE 3.6 MW wind turbine]

For the base case of GE 3.6 MW wind turbine, $K_{tub} = 0.4341$

For,

Case: 1 $K_{tub} = 0.3472$ (When $C_{p,\max}$ is reduced by 20% from the base case)

Case: 2 $K_{tub} = 0.30798$ (λ_{opt} is shifted to 9.25)

Case: 3 $K_{tub} = 0.5211$ (λ_{opt} is shifted to 7.75)

The effect of these changes on the corresponding $P_{ef}(\omega_{ref})$ curves are shown in Fig.5.36

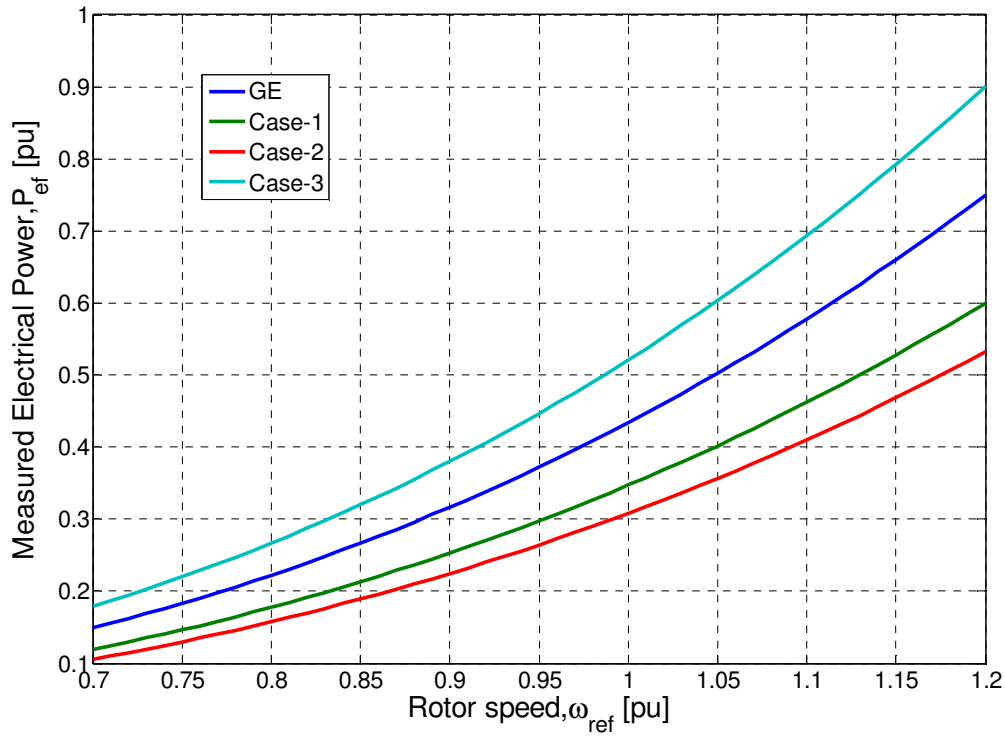


Fig.5.36 Optimal rotor speed- power curves for maximum power tracking with changes Case-1 and Case-2 and Case-3 together with the GE case

5.2.1 Case-1: Reducing the maximum value of C_p

Here $C_{p,max}$ is reduced by 20% from the base case, which was 0.5. Simulations have been performed by applying a grid-fault disturbance at $t = 5$ sec for 0.5 sec and compared with the base cases.

5.2.1.1 Simulation in the low-wind-speed region

The following simulation results are found.

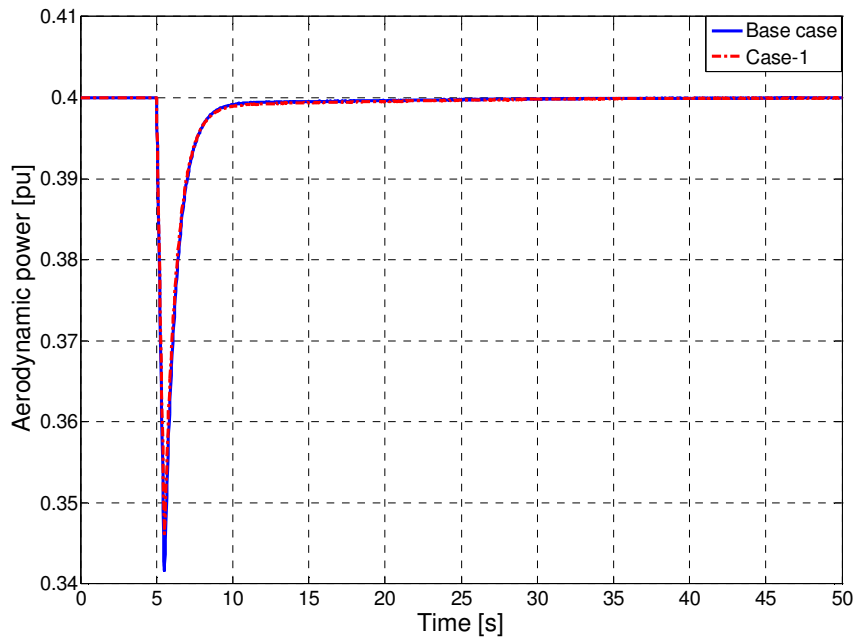


Fig.5.37 Aerodynamic power when C_p is reduced by 20% from GE case of 0.5 (low-wind speed region) when a grid-fault occurs at $t=5\text{sec}$ and lasts for 500 ms

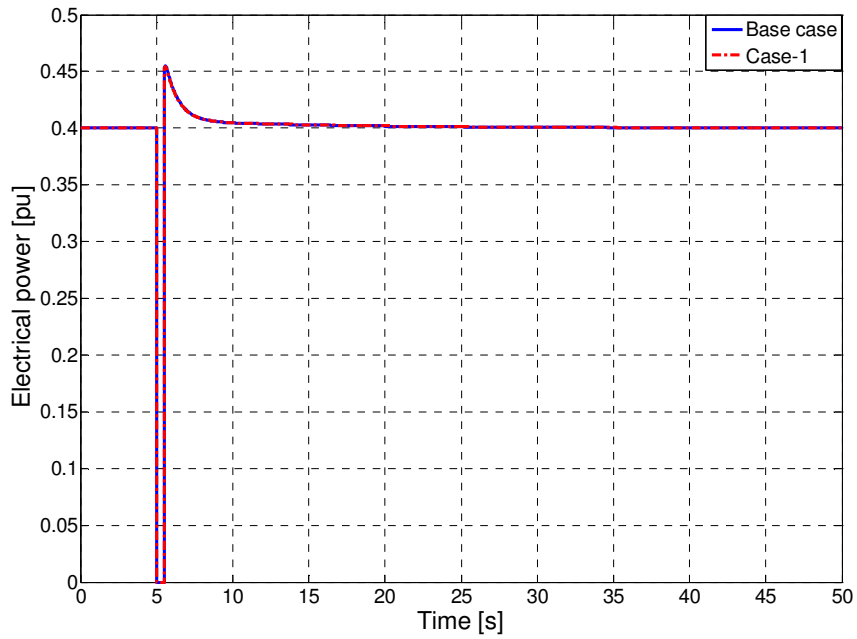


Fig.5.38 Electrical power when C_p is reduced by 20% from GE case of 0.5 (low-wind speed region) when a grid-fault occurs at $t=5\text{sec}$ and lasts for 500 ms

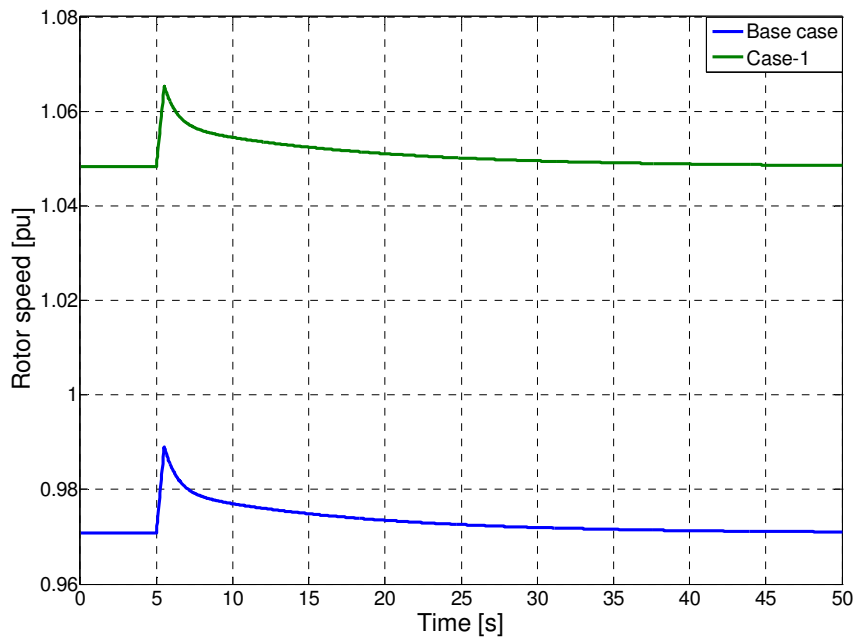


Fig.5.39 Rotor speed when C_p is reduced by 20% from GE case of 0.5 (low-wind speed region) when a grid-fault occurs at $t=5$ sec and lasts for 500 ms

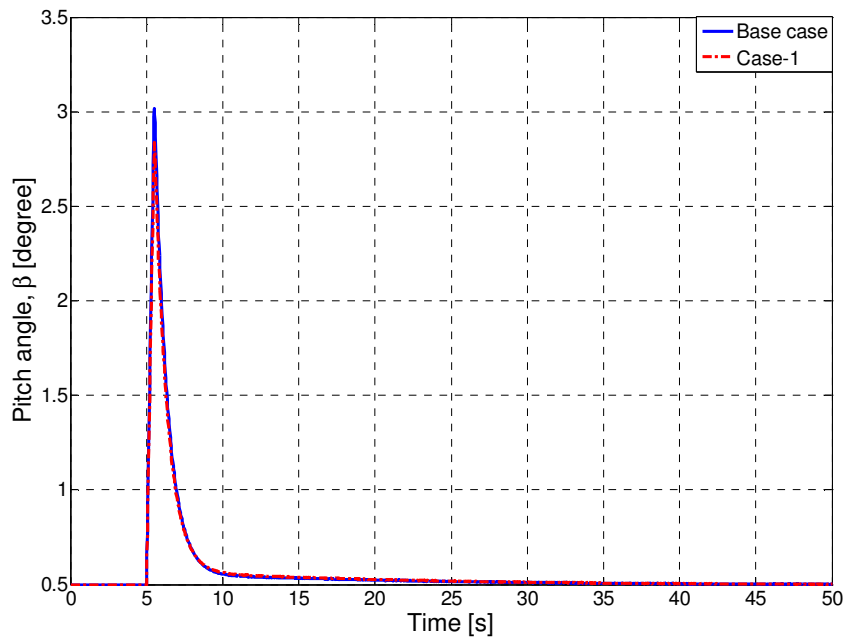


Fig.5.40 Pitch-angle (β) when C_p is reduced by 20% from GE case of 0.5 (low-wind speed region) when a grid-fault occurs at $t=5$ sec and lasts for 500 ms

These simulations have been performed for grid-fault disturbance at 5 sec, in the low-wind speed region, when C_p is reduced by 20% from GE case, which was 0.5. For simulation results found from Fig.5.37 to Fig.5.40, we can conclude that, both aerodynamic power and pitch-angle have lower overshoot than base case. Higher overshoot than base case has been observed in case of rotor speed. Electrical power follows exactly the same as base case. Different levels of steady-states of rotor-speed is due to change in wind-speed.

5.2.1.1 Simulation in the high-wind-speed region

The following simulation results are found.

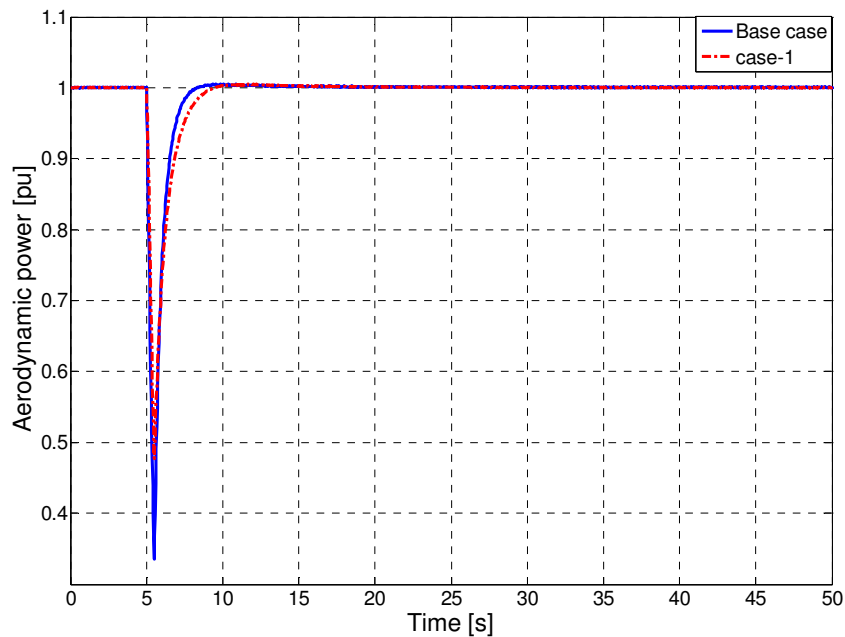


Fig.5.41 Aerodynamic power when C_p reduced by 20% from GE case of 0.5 (high-wind speed region) when a grid-fault occurs at $t=5$ sec and lasts for 500 ms

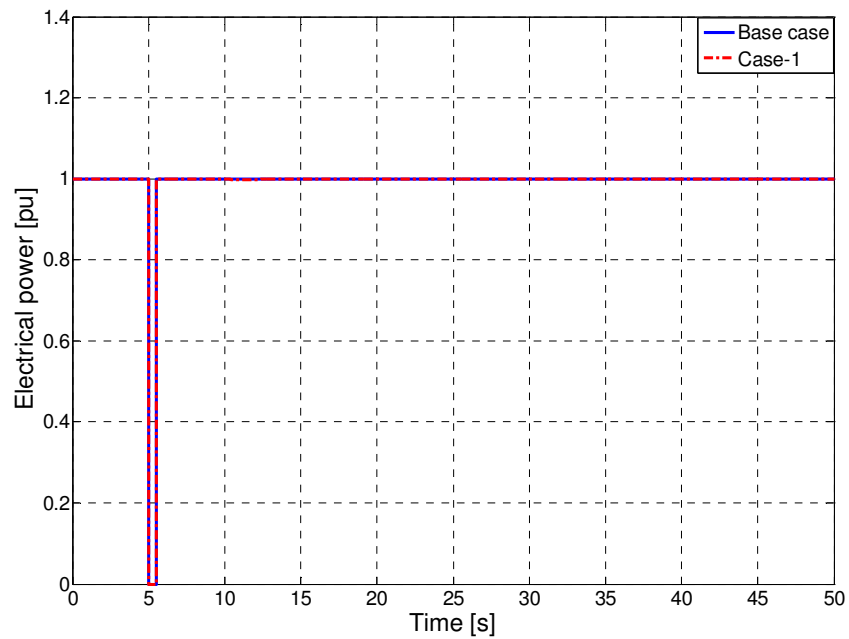


Fig.5.42 Electrical power when C_p reduced by 20% from GE case of 0.5 (high-wind speed region) when a grid-fault occurs at $t=5\text{sec}$ and lasts for 500 ms

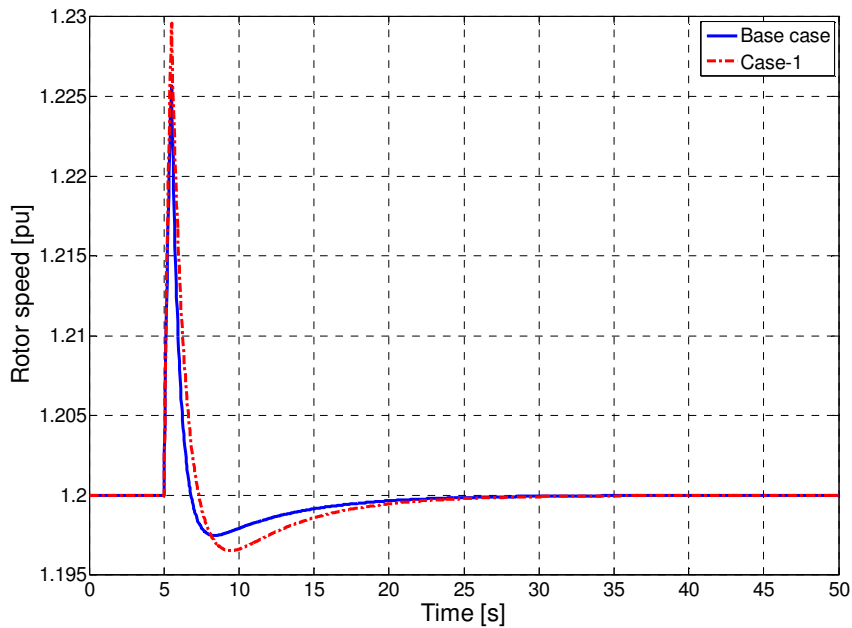


Fig.5.43 Rotor speed when C_p reduced by 20% from GE case of 0.5 (high-wind speed region) when a grid-fault occurs at $t=5\text{sec}$ and lasts for 500 ms

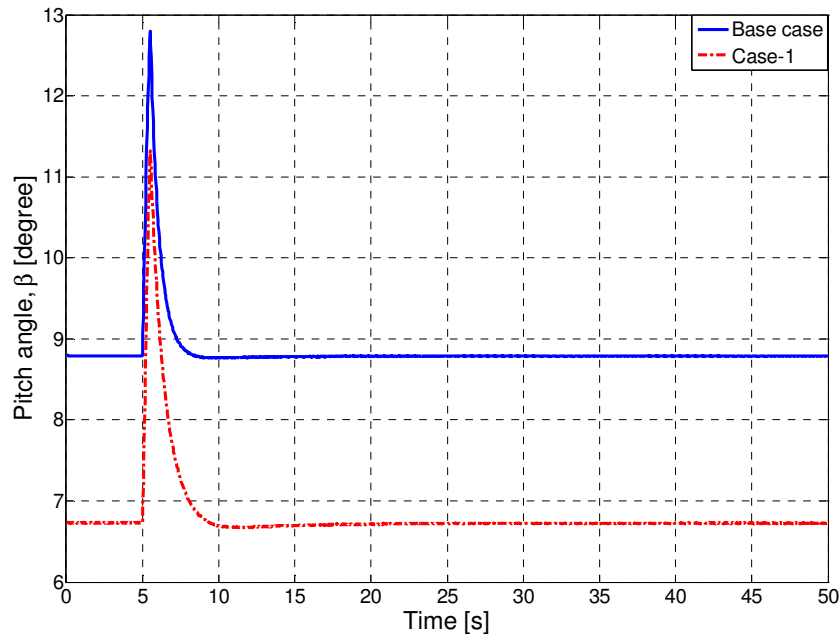


Fig.5.44 Pitch-angle (β) when C_p reduced by 20% from GE case of 0.5 (high-wind speed region) when a grid-fault occurs at $t=5$ sec and lasts for 500 ms

These simulations have been performed for grid-fault disturbance at 5 sec, in the high-wind speed region, when C_p is reduced by 20% from GE case, which was 0.5. For simulation results found from Fig.5.41 to Fig.5.44, we can conclude that, only the electrical power follows the same results as found for GE case. The aerodynamic power requires higher settling time, but lower overshoot as compared to base case. The pitch-angle variation with higher overshoot than base case is found. The rotor speed has higher overshoot and higher settling time as compared to base case results in slow steady-state response. Different levels of steady-states of pitch-angle is due to change in wind-speed.

5.2.2 Case-2: Shifting the $C_p(\lambda)$ curve rightward along the λ -axis

For, GE λ_{opt} is 8.25. But here λ_{opt} is shifted to 9.25. Simulations have been performed by applying a grid-fault disturbance at $t = 5$ sec for 0.5sec and compared with the base cases.

5.2.2.1 Simulation in the low-wind-speed region

The following simulation results are found.

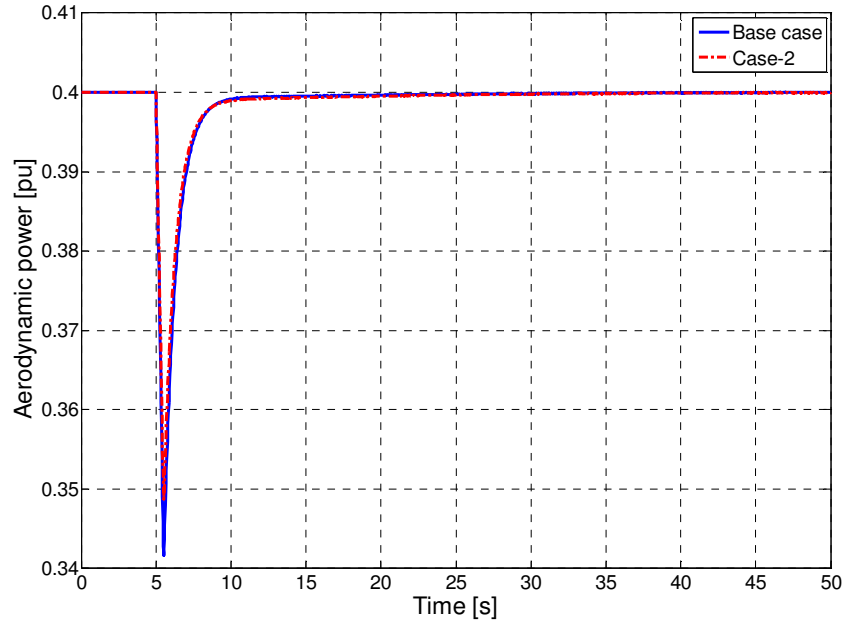


Fig.5.45 Aerodynamic power when λ shifted to 9.25 from GE case of 8.25 (low-wind speed region) when a grid-fault occurs at t=5sec and lasts for 500 ms

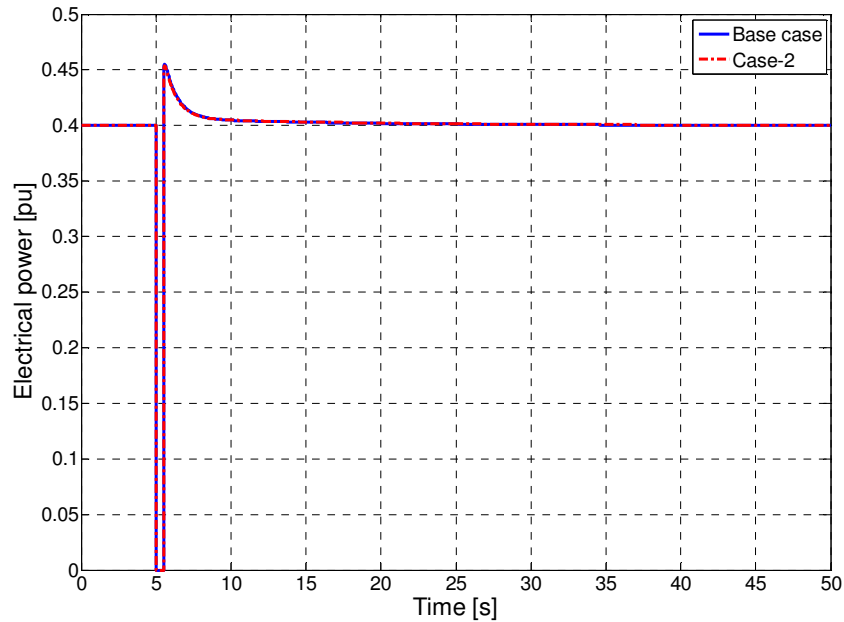


Fig.5.46 Electrical power when λ shifted to 9.25 from GE case of 8.25 (low-wind speed region) when a grid-fault occurs at t=5sec and lasts for 500 ms

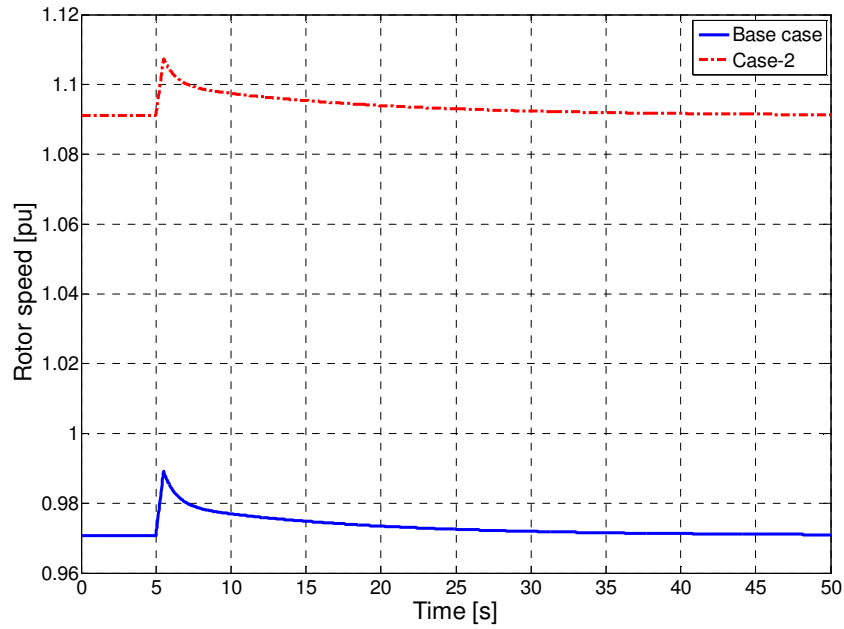


Fig.5.47 Rotor speed when λ shifted to 9.25 from GE case of 8.25 (low-wind speed region) when a grid-fault occurs at t=5sec and lasts for 500 ms

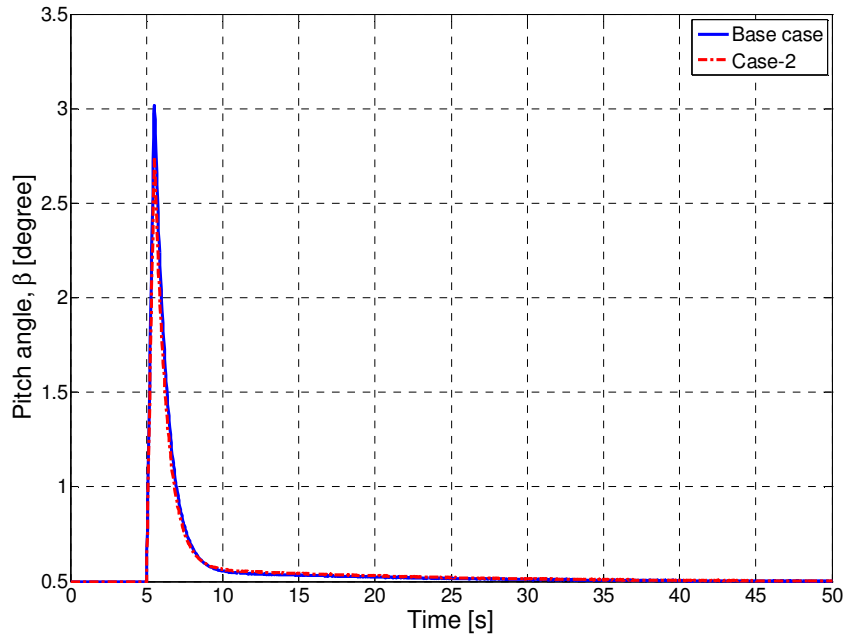


Fig.5.48 Pitch-angle(β) when λ shifted to 9.25 from GE case of 8.25 (low-wind speed region) when a grid-fault occurs at t=5sec and lasts for 500 ms

These simulations have been performed in low-wind speed region when λ shifted to 9.25 from base case and a grid-fault disturbance is applied at 5 sec. For simulation results found from Fig.5.45 to Fig.5.48, we can conclude that, both the aerodynamic power and pitch-angle has lower overshoot than base case. Rotor speed has higher overshoot as compared to base case. The electrical power follows the same results as found for GE base case.

5.2.2.2 Simulation in the high-wind-speed region

The following simulation results are found.

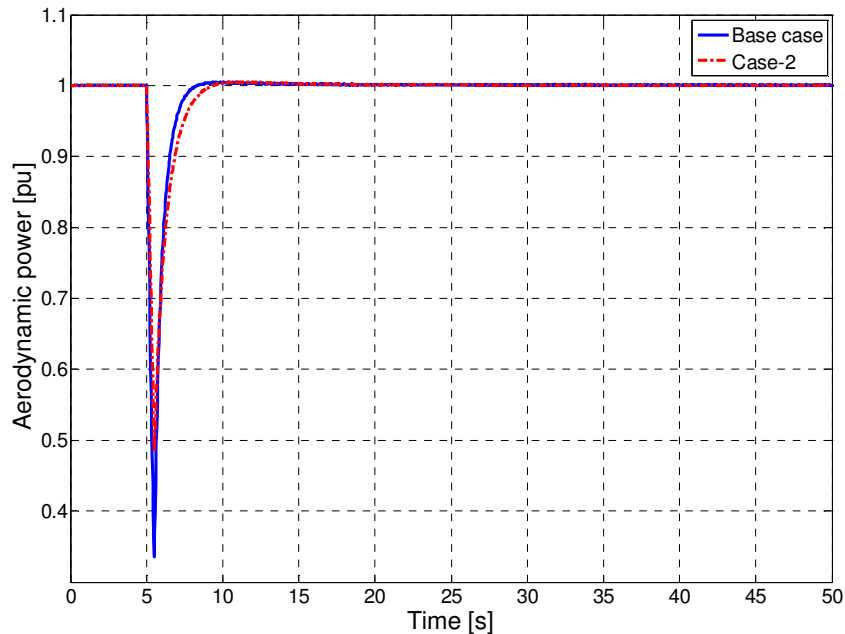


Fig.5.49 Aerodynamic power when λ shifted to 9.25 from GE case of 8.25 (high-wind speed region) when a grid-fault occurs at t=5sec and lasts for 500 ms

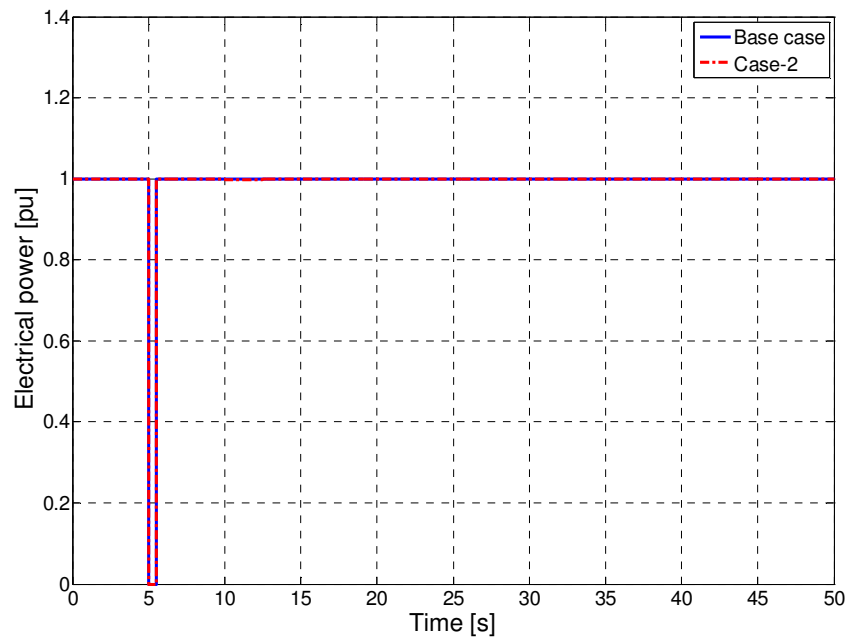


Fig.5.50 Electrical power when λ shifted to 9.25 from GE case of 8.25 (high-wind speed region) when a grid-fault occurs at t=5sec and lasts for 500 ms

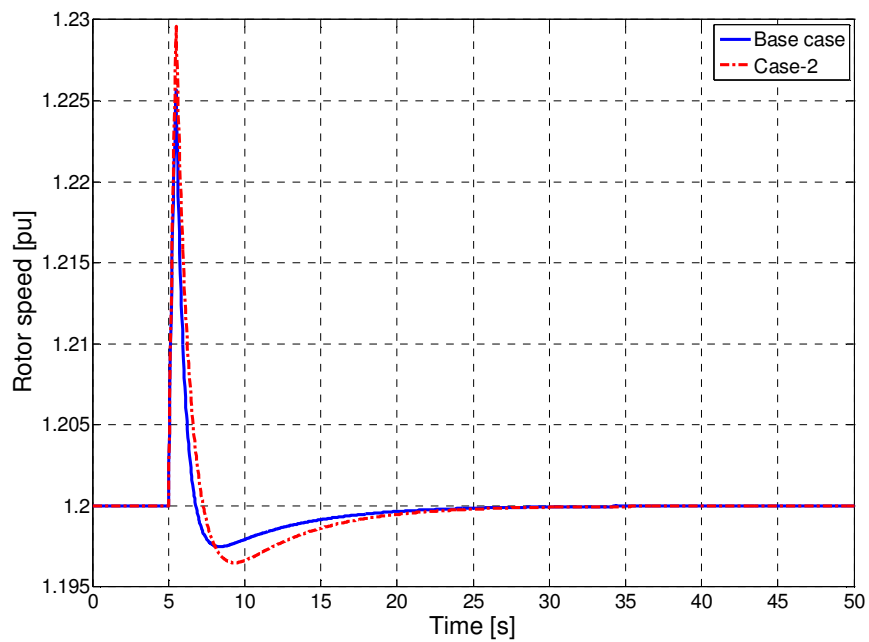


Fig.5.51 Rotor speed when λ shifted to 9.25 from GE case of 8.25 (high-wind speed region) when a grid-fault occurs at t=5sec and lasts for 500 ms

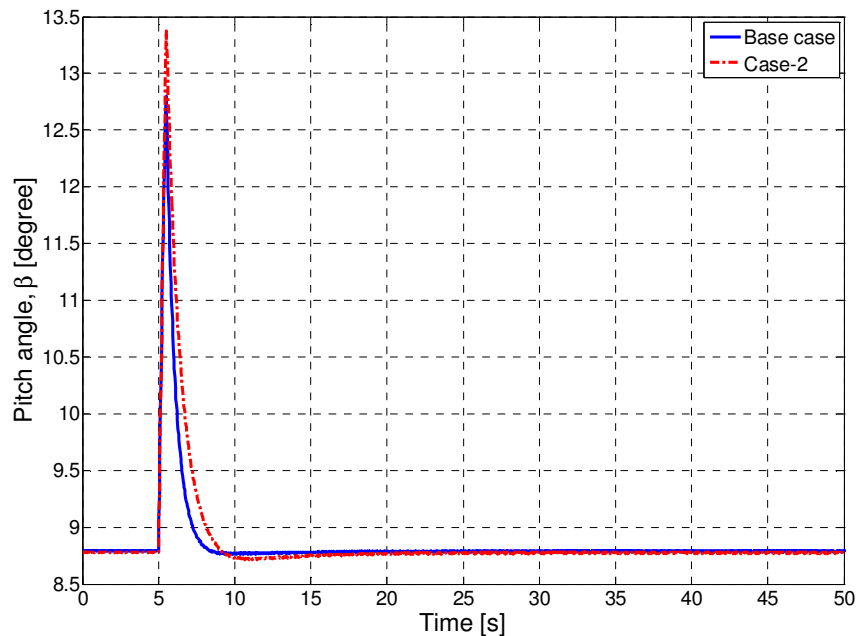


Fig.5.52 Pitch-angle (β) when λ shifted to 9.25 from GE case of 8.25 (high-wind speed region) when a grid-fault occurs at $t=5$ sec and lasts for 500 ms

These simulations have been performed in high-wind speed region when λ shifted to 9.25 from base case and a grid-fault disturbance is applied at 5 sec. For simulation results found from Fig.5.49 to Fig.5.52, we can conclude that, only the electrical power follows the same results as found for GE base case. Both the rotor speed and pitch-angle requires higher settling time, results in a slower response, and higher overshoot. The aerodynamic power with lower overshoot higher settling time is found as compared to GE base case.

5.2.3 Case-3: Shifting the $C_p(\lambda)$ curve leftward along the λ -axis

For, GE λ_{opt} is 8.25. But here λ_{opt} is shifted to 7.75. Simulations have been performed by applying a grid-fault disturbance at $t = 5$ sec for 0.5 sec and compared with the base cases.

5.2.3.1 Simulation in the low-wind-speed region

The following simulation results are found.

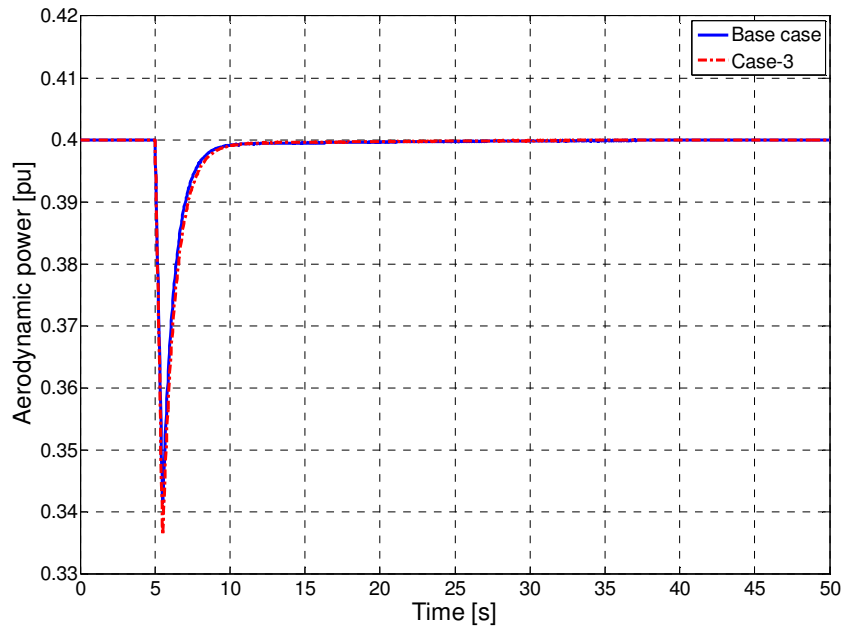


Fig.5.53 Aerodynamic power when λ shifted to 7.75 from GE case of 8.25 (low-wind speed region) when a grid-fault occurs at t=5sec and lasts for 500 ms

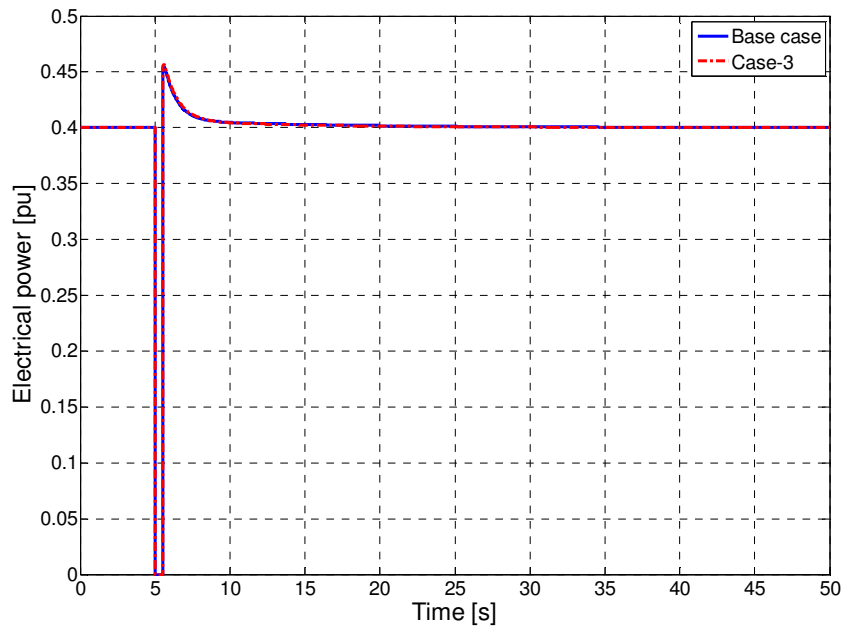


Fig.5.54 Electrical power when λ shifted to 7.75 from GE case of 8.25 (low-wind speed region) when a grid-fault occurs at t=5sec and lasts for 500 ms

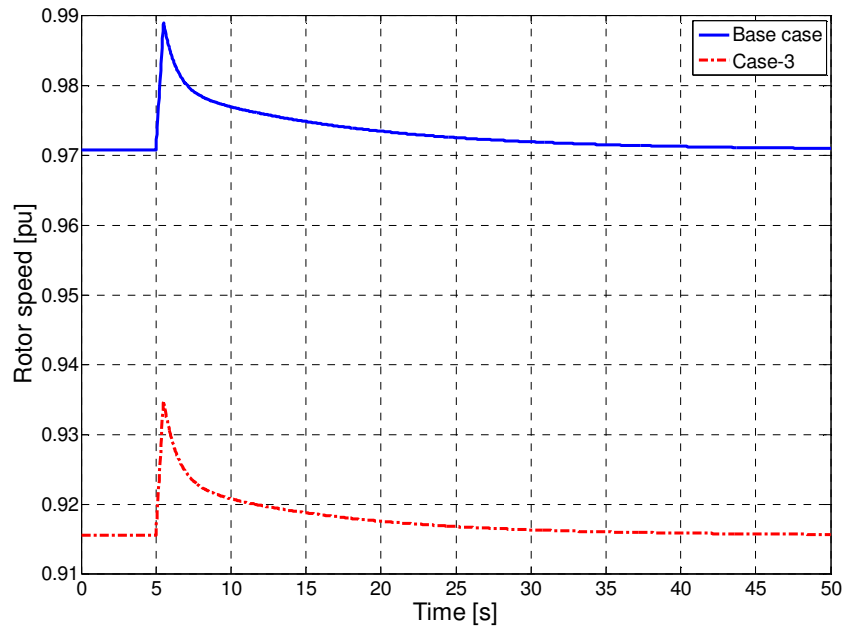


Fig.5.55 Rotor speed when λ shifted to 7.75 from GE case of 8.25 (low-wind speed region) when a grid-fault occurs at t=5sec and lasts for 500 ms

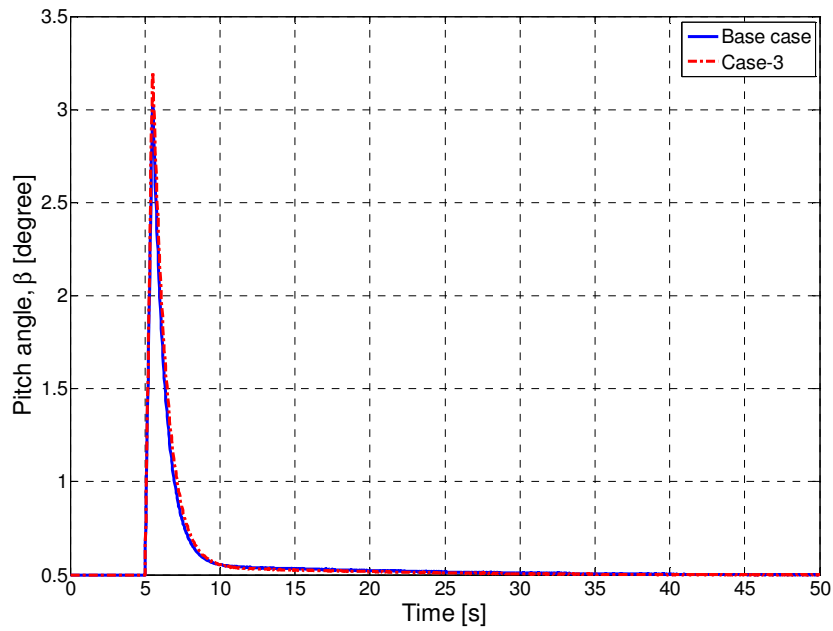


Fig.5.56 Pitch-angle(β) when λ shifted to 7.75 from GE case of 8.25 (low-wind speed region) when a grid-fault occurs at t=5sec and lasts for 500 ms

These simulations have been performed in low-wind speed region when λ shifted to 7.75 from base case and a grid-fault disturbance is applied at 5 sec. For simulation results found from Fig.5.53 to Fig.5.56, we can conclude that, the aerodynamic power has higher overshoot and a little bit higher settling time as compared to GE base case. Very small increased overshoot for rotor-speed and higher overshoot for pitch-angle are found as compared to GE base case. The electrical power follows the same results as found for GE base case.

5.2.3.2 Simulation in the high-wind-speed region

The following simulation results are found.

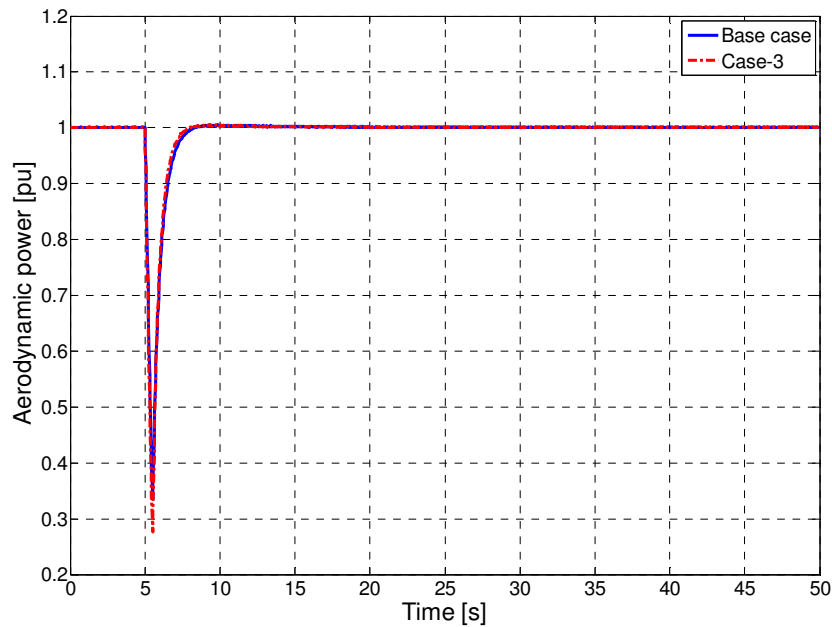


Fig.5.57 Aerodynamic power when λ shifted to 7.75 from GE case of 8.25 (high-wind speed region) when a grid-fault occurs at t=5sec and lasts for 500 ms

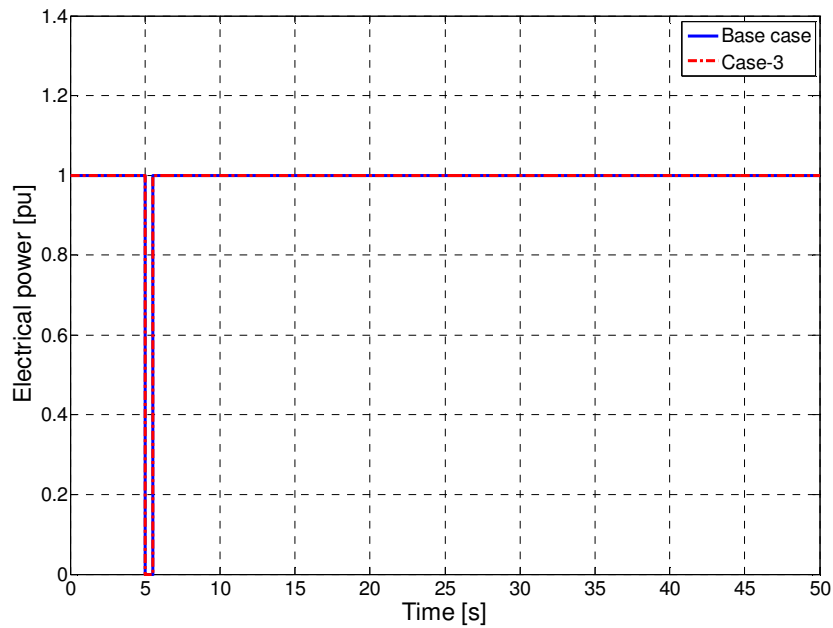


Fig.5.58 Electrical power when λ shifted to 7.75 from GE case of 8.25 (high-wind speed region) when a grid-fault occurs at t=5sec and lasts for 500 ms

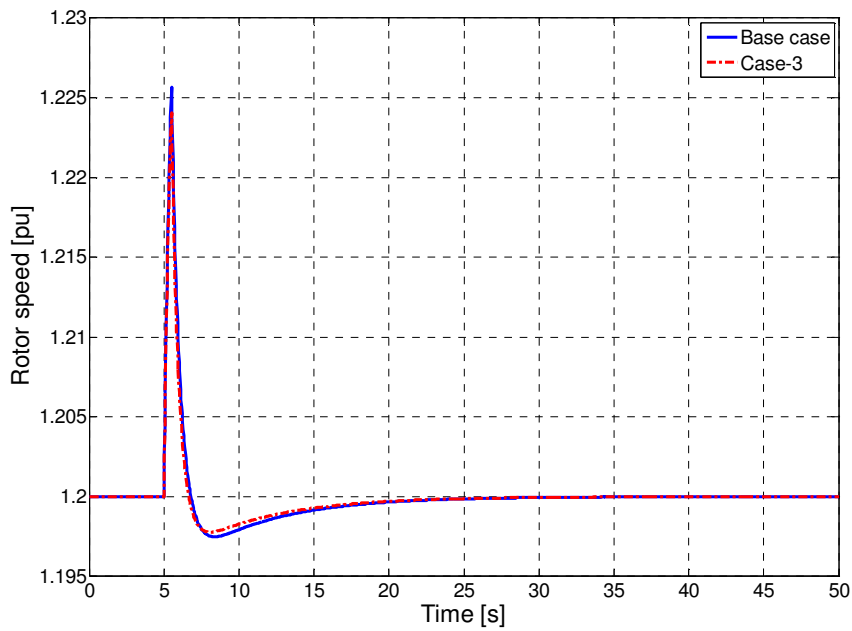


Fig.5.59 Rotor speed when λ shifted to 7.75 from GE case of 8.25 (high-wind speed region) when a grid-fault occurs at t=5sec and lasts for 500 ms

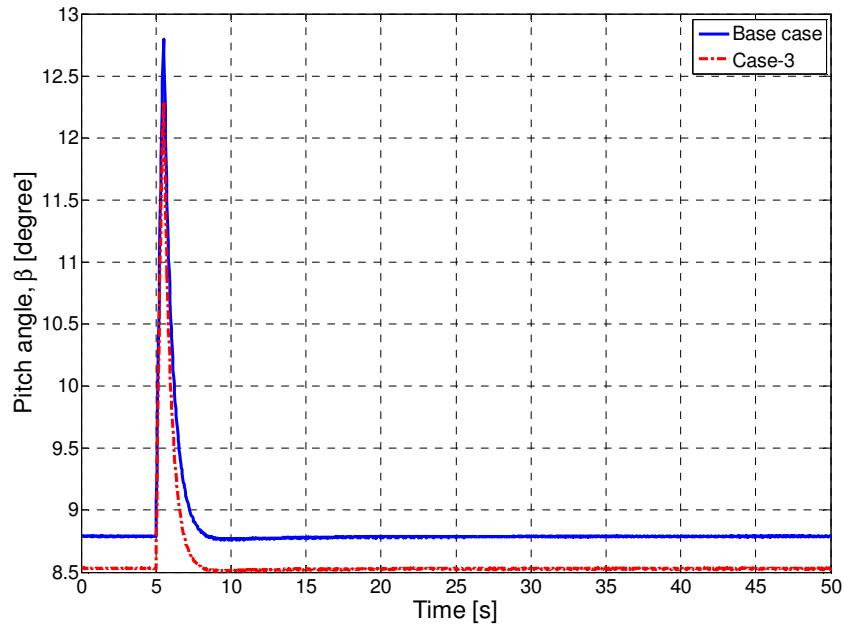


Fig.5.60 Pitch-angle(β)when λ shifted to 7.75 from GE case of 8.25 (high-wind speed region) when a grid-fault occurs at $t=5$ sec and lasts for 500 ms

These simulations have been performed in high-wind speed region when λ shifted to 7.75 from base case and a grid-fault disturbance is applied at 5 sec. For simulation results found from Fig.5.57 to Fig.5.60, we can conclude that, the electrical power and rotor speed follows the same results as found for GE base case. The aerodynamic power with higher overshoot and pitch-angle with lower overshoot are found as compared to GE base case.

5.2.4 Comparison table

The Table.5.1 shows the comparison results as found for the stated three cases with respect to GE cases.

Cases	Grid-fault simulation (Low wind-speed region)				Grid-fault simulation (High wind-speed region)			
	P_m	P_e	ω	β	P_m	P_e	ω	β
Case-1	Lower overshoot	Exactly same	Higher overshoot	Lower overshoot	Lower overshoot, higher settling time	Exactly same	Higher overshoot, higher settling time	Higher overshoot
Case-2	Lower overshoot	Exactly same	Higher overshoot	Lower overshoot	Smaller overshoot	Exactly same	Higher overshoot, higher settling time	Higher overshoot, higher settling time
Case-3	Higher overshoot, slightly higher settling time	Exactly same	Slightly higher overshoot	Higher overshoot	Higher overshoot	Exactly same	Exactly same	Lower overshoot

Table.5.1 Comparison chart of simulation results of Case-1 and Case-2 and Case-3 as compared to GE base case

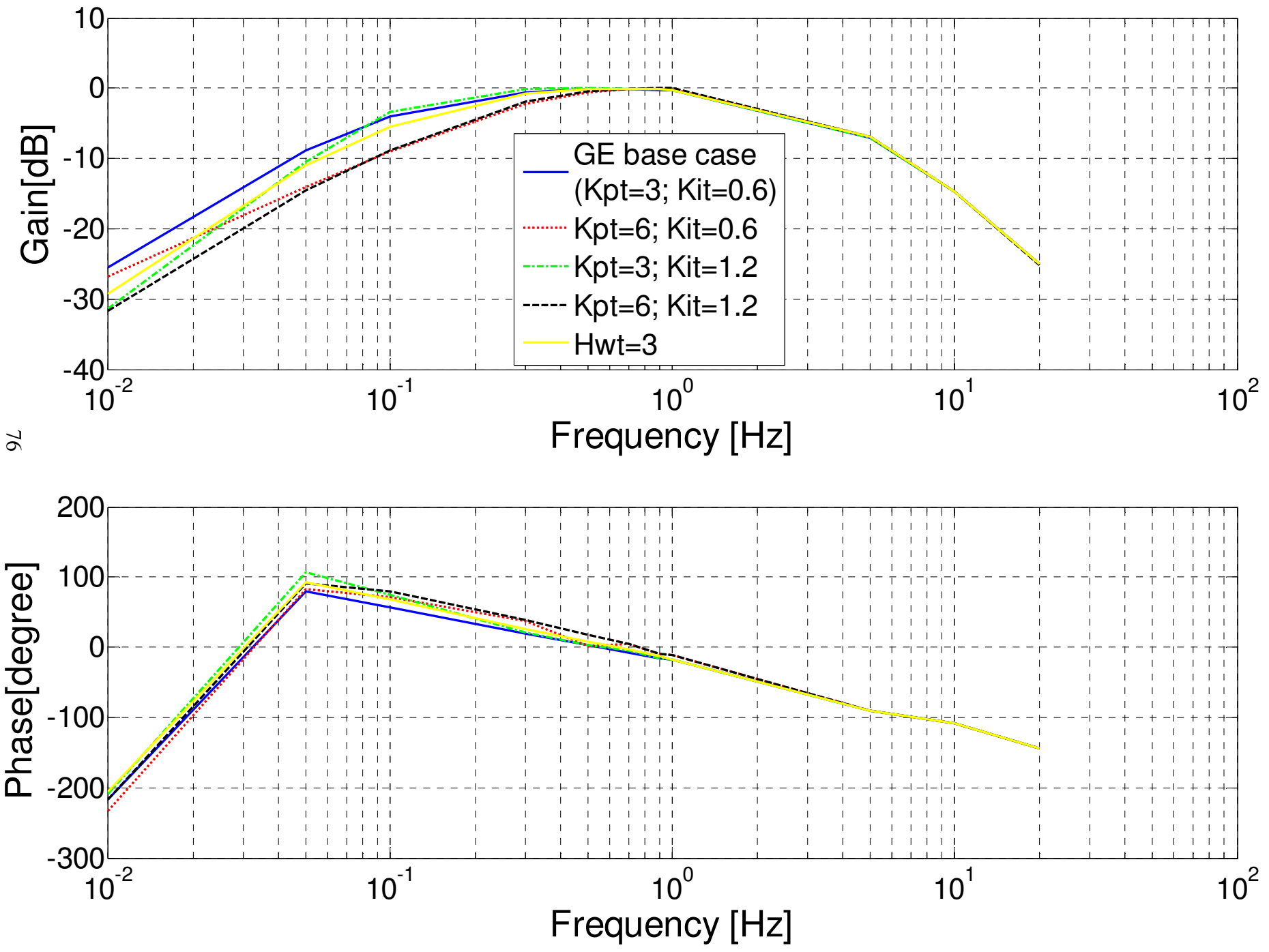
5.3 Frequency response in low-wind speed region

Fig.5.61 shows the frequency responses in low-wind speed region for GE base case and varying the parameters of speed controller and inertia of rotor-generator.

It is found that, an external signal added with the torque controller output, in the frequency range of 0.4~1 Hz, can be reflected unaffected on the electrical power output of the investigated WT. When the gain of the torque controller is increased from the base case, the above mentioned frequency range changed to 0.6~1 Hz.

From Fig.5.61, it is found that gain reduced for both low and high frequency region. For the low frequency gain reduction, we can say that, disturbance frequency is too low, but controller is too fast to follow, so output ripple is low. But in the case of high frequency gain reduction, frequency of disturbance is too high, and is filtered by two low-pass filters in series, one of them is converter (See the sample Simulink® model in Appendix). Phase difference follows the same in the high-frequency region irrespective of cases considered so far, but some differences have been observed in the low-frequency region.

Fig.5.61 Frequency response in low-wind speed region when a disturbance is applied at the output of torque controller and output is measured at electrical power output



Chapter 6

Conclusions and Future Work

6.1 Conclusions

In this thesis the functionality of the GE 3.6 MW wind turbine model exposed to a wind step and frequency disturbance implemented in Matlab® and Simulink® have been investigated.

Robustness of the WT is tested by varying the aerodynamic parameters $C_{p,max}$ and λ_{opt} .

Results from these investigations of the functionality and robustness influenced by wind step and grid-fault were presented in Chapter 5.

It is found that, the implemented model function as expected in different wind speed region under different disturbances, e.g. wind step, grid-fault. However, while simulating in the low-wind speed region, it is found that, the pitch controller does not work according to the expected behaviour. For instance, in low-wind speed operation when a wind step is applied at 5 sec from 7.5 m/sec to 9.5 m/sec, simulation shows that the pitch-angle changes from 0.5 degree to 4.57 degree, although it should not be the case for low-wind speed operation.

For robustness investigations, a grid-fault at 5 sec of 500 ms duration was applied instead of wind step. The results were summerized in Table:5.1. No significant abnormalities were found, except some variations in overshoot and settling time. Electrical power output was same as of base case for both low-wind speed and high-wind speed operation.

The frequency response in the low-wind speed region of the investigated WT shows that an external signal added with the torque controller output in the frequency range of 0.4~1 Hz can be reflected unaffected on the electrical power output and when the gain of the torque controller is increased from the base case, the above mentioned frequency range changed to 0.6~1 Hz.

6.2 Future work

There are some subjects worthy of further power system study and investigations, such as frequency control, power oscillation damping.

References

- [1] Gary L. Johnson, *Wind Energy Systems*. Englewood Cliffs, New Jersey: Prentice-Hall INC., 1985.
- [2] Nayeem Rahamat Ullah, Torbjörn Thiringer, Daniel Karlsson, “Temporary Primary Frequency Control Support by Variable Speed Wind Turbines-Potential and Applications,” *IEEE Transactions on Power Systems*, paper no.TPWRS-00427.2007.
- [3] T. Ackermann, Ed., *Wind Power in Power Systems*. West Sussex: John Wiley and Sons Ltd., 2005.
- [4] U.S. Department of Energy, Energy Efficiency and Renewable Energy, “Annual Report on U.S. Wind Power Installation, Cost and Performance Trends: 2006”, May 2007.
- [5] Mika Rasila, “Torque and Speed control of a pitch-regulated Wind Turbine”, Masters thesis, Chalmers University of Technology, Göteborg, Sweden, 2003.
- [6] T.Burton, D.Sharpe, N.Jenkins, and E. Bossanyi, *Wind Energy Handbook*. West Sussex: John Wiley and Sons Ltd., 2001.
- [7] Siegfried Heier, *Grid Integration of Wind Energy Conversion System*. West Sussex: John Wiley and Sons Ltd., 1998.
- [8] M.P.Papadopoulos, S.A. Papathanassiou, N.G.Boulaxis, and S.T.Tentzerakis, “Voltage quality change by grid-connected wind turbines”, In *European Wind Energy Conference*, pp.783-785, Nice, France, 1999.
- [9] T.Petru and T. Thiringer, “Active filter reduction from a sea-based 2.5 MW wind park connected to a weak grid”, In *2000 IEEE Nordic Workshop on Power and Industrial Electronics (NORPIE/2000)*, pp.7-11, Aalborg, Denmark, 2000.
- [10] Å.Larsson, P.Sorensen, and F. Santjer, “Grid impact of variable speed wind turbines”, In *European Wind Energy Conference and Exhibition (EWEC 99)*, Nice, France, 1999.
- [11] Nayeem Rahamat Ullah, “Grid Reinforcing Wind Generation”, Licentiate thesis, Chalmers University of Technology, Göteborg, Sweden, 2006.
- [12] Deutsches Windenergie-Institut Techwise A/S DM Energy. *Wind turbine grid connection and interaction*.
- [13] Nicholas W.Miller, William W. Price, Juan J.sanchez-Gasca, “Dynamic modeling of GE 1.5 and 3.6 wind-turbine generators,” GE- Power System Energy Consulting, U.S.A., Tech. Rep. Version 3.0, October 2003.
- [14] Nicholas W.Miller, William W. Price, Juan J.sanchez-Gasca and Robert W.Delmerico, “Dynamic modeling of GE1.5 and 3.6MW wind turbine-generators for stability simulations,” in *IEEE PES general meeting*, July 2003, pp.1977-1983.

Appendix

GE parameters

For the rigid shaft representation used in GE model, the relationship between blade tip speed and generator rotor speed, ω , is a fixed constant, K_b . The calculation of λ becomes:

$$\lambda = K_b \left(\frac{\omega}{v_{wind}} \right)$$

GE WTG's wind power co-efficients are listed in Table:1.

	GE 1.5	GE 3.6
$\frac{1}{2} \rho A_r$	0.00159	0.00145
$K_b (= \omega_0 R)$	56.6	69.5

Table:1 Wind Power Coefficients

C_p is a characteristic of the wind turbine and is usually provided as a set of curves relating to C_p to λ , with β as a parameter. The C_p curves for the GE 3.6 WTG are shown in Fig.1. Curve fitting was performed to obtain the mathematical representation of the C_p curves used in the model:

$$C_p(\lambda, \beta) = \sum_{i=0}^4 \sum_{j=0}^4 \alpha_{i,j} \beta^i \lambda^j$$

The co-efficients $\alpha_{i,j}$ are given in Table: 2.

i	j	$\alpha_{i,j}$
4	4	4.9686e-010
4	3	-7.1535e-008
4	2	1.6167e-006
4	1	-9.4839e-006
4	0	1.4787e-005
3	4	-8.9194e-008
3	3	5.9924e-006
3	2	-1.0479e-004
3	1	5.7051e-004
3	0	-8.6018e-004
2	4	2.7937e-006
2	3	-1.4855e-004
2	2	2.1495e-003
2	1	-1.0996e-002
2	0	1.5727e-002
1	4	-2.3895e-005
1	3	1.0683e-003
1	2	-1.3934e-002
1	1	6.0405e-002
1	0	-6.7606e-002
0	4	1.1524e-005
0	3	-1.3365e-004
0	2	-1.2406e-002
0	1	2.1808e-001
0	0	-4.1909e-001

Table:2 Cp Coefficients $\alpha_{i,j}$

Table:3 shows the WT physical parameters:

Parameter Name	Recommended Value
H_{WT}	5.19s
$\frac{0.5\rho A_r}{S_n}$	0.00145
$C_{p,max}$	0.5023
λ_{opt}	8.25
ω_0	1.335 rad/sec
R	52m

Table:3 WT Physical Parameters

Table:4 shows the turbine control parameters:

Parameter Name	Recommended Value
K_{pp}	150
K_{ip}	25
T_p (second)	0.01
θ_{max} (degrees)	27
θ_{min} (degrees)	0.0
$d\theta/dt$ max (degrees/sec)	10.0
$d\theta/dt$ min (degrees/sec)	-10.0
P_{max} (pu)	1.0
P_{min} (pu)	0.1
dP/dt max (pu/sec)	0.45
dP/dt min (pu/sec)	-0.45
K_{ptrq}	3.0
K_{itrq}	0.6

Table:4 Turbine Control Parameters

Sample Matlab® program

```
clc
close all
clear

tic
pm=1;
wind_speed_user=12;
windstep=2;

#####
Hwt=5.19;

if pm<1

xyz=-0.67*pm^2+1.42*pm+0.51;

if xyz<1.2
    ini_1=xyz;
else
    ini_1=1.2;
end

theta=0.5;
vw= [6:.00001:30];

lambda=(69.5*ini_1)./vw;

kk=.00145*vw.^3;

ppp=kk.* ((-4.1909e-1) * theta^0 * lambda.^0 ...
+         (2.1808e-1) * theta^0 * lambda.^1 ...
+         (-1.2406e-2) * theta^0 * lambda.^2 ...
+         (-1.3365e-4) * theta^0 * lambda.^3 ...
+         (1.1524e-5) * theta^0 * lambda.^4 ...
...
+         (-6.7606e-2) * theta^1 * lambda.^0 ...
+         (6.0405e-2) * theta^1 * lambda.^1 ...
+         (-1.3934e-2) * theta^1 * lambda.^2 ...
+         (1.0683e-3) * theta^1 * lambda.^3 ...
+         (-2.3895e-5) * theta^1 * lambda.^4 ...
...
+         (1.5727e-2) * theta^2 * lambda.^0 ...
+         (-1.0996e-2) * theta^2 * lambda.^1 ...
+         (2.1495e-3) * theta^2 * lambda.^2 ...
```

```

+          (-1.4855e-4) * theta^2 * lambda.^3 ...
+          (2.7937e-6) * theta^2 * lambda.^4 ...
...
+          (-8.6018e-4) * theta^3 * lambda.^0 ...
+          (5.7051e-4) * theta^3 * lambda.^1 ...
+          (-1.0479e-4) * theta^3 * lambda.^2 ...
+          (5.9924e-6) * theta^3 * lambda.^3 ...
+          (-8.9194e-8) * theta^3 * lambda.^4 ...
...
+          (1.4787e-5) * theta^4 * lambda.^0 ...
+          (-9.4839e-6) * theta^4 * lambda.^1 ...
+          (1.6167e-6) * theta^4 * lambda.^2 ...
+          (-7.1535e-8) * theta^4 * lambda.^3 ...
+          (4.9686e-10) * theta^4 * lambda.^4 );

```

```
L_opt=lambda.*(abs(pm-ppp)<0.00001);
```

```

disp(max(L_opt))
wind_speed=(69.5*(ini_1))/max(L_opt);
disp(wind_speed)

```

```
theta_ini=theta;
```

```
else
```

```
xyz=-0.67*pm^2+1.42*pm+0.51;
```

```

if xyz<1.2
    ini_1=xyz;
else
    ini_1=1.2;
end

```

```
theta=[0.5:.00001:27];
```

```
vw= wind_speed_user;
```

```

lambda=(69.5*ini_1)/vw;
disp(lambda)
kk=.00145*vw^3;

```

```

ppp=kk.* ((-4.1909e-1) * theta.^0 * lambda^0 ...
+          (2.1808e-1) * theta.^0 * lambda^1 ...
+          (-1.2406e-2) * theta.^0 * lambda^2 ...
+          (-1.3365e-4) * theta.^0 * lambda^3 ...

```

```

+      (1.1524e-5) * theta.^0 * lambda^4 ...
...
+      (-6.7606e-2) * theta.^1 * lambda^0 ...
+      (6.0405e-2) * theta.^1 * lambda^1 ...
+      (-1.3934e-2) * theta.^1 * lambda^2 ...
+      (1.0683e-3) * theta.^1 * lambda^3 ...
+      (-2.3895e-5) * theta.^1 * lambda^4 ...
...
+      (1.5727e-2) * theta.^2 * lambda^0 ...
+      (-1.0996e-2) * theta.^2 * lambda^1 ...
+      (2.1495e-3) * theta.^2 * lambda^2 ...
+      (-1.4855e-4) * theta.^2 * lambda^3 ...
+      (2.7937e-6) * theta.^2 * lambda^4 ...
...
+      (-8.6018e-4) * theta.^3 * lambda^0 ...
+      (5.7051e-4) * theta.^3 * lambda^1 ...
+      (-1.0479e-4) * theta.^3 * lambda^2 ...
+      (5.9924e-6) * theta.^3 * lambda^3 ...
+      (-8.9194e-8) * theta.^3 * lambda^4 ...
...
+      (1.4787e-5) * theta.^4 * lambda^0 ...
+      (-9.4839e-6) * theta.^4 * lambda^1 ...
+      (1.6167e-6) * theta.^4 * lambda^2 ...
+      (-7.1535e-8) * theta.^4 * lambda^3 ...
+      (4.9686e-10) * theta.^4 * lambda^4 );

```

```

theta_opt=theta.*(abs(pm-ppp)<0.00001);
disp(max(theta_opt))

```

```

wind_speed=wind_speed_user;

```

```

theta_ini=max(theta_opt);

```

```

end

```

```

sim high_wind_speed_ge

```

```

toc

```

Sample Simulink® model

